Interleukin 6 trans-signaling in normal and malignant stem and progenitor cells

Dissertation

zur Erlangung des Doktorgrades der Naturwissenschaften (Dr. rer. nat.)
der Fakultät für Biologie und Vorklinische Medizin der
Universität Regensburg

vorgelegt von

Milan MS Obradović

aus Belgrad, Serbien

2013

Das Promotionsgesuch wurde eingereicht am 05. Februar 2013

Die Arbeit wurde angeleitet von Herrn Prof. Dr. Christoph A. Klein

Prüfungsausschuss:

Vorsitzender: Prof. Dr. Richard Warth

1. Gutachter: Prof. Dr. Ralph Witzgall

2. Gutachter: Prof. Dr. Christoph Klein

3. Prüfer: Prof. Dr. Gunter Meister

Milan MS Obradović

Dedicated to my parents, Miroslav and Smilja Obradović.

All I can do is mention your names with all the gratitude for your endless love.

Table of contents

1. Introduction

1.1. Cellular composition and physiology of human mammary gland

The mammary gland is positioned between the pectoralis major muscle and the nipple (Henrikson et al., 1997). The mammary gland is a paired, tubuloalveolar, exocrine gland which produces milk in females (Henrikson et al., 1997; Linzell and Peaker, 1971). The produced milk is collected in the nipple sinus and excreted in a response of infant's suckling (Linzell and Peaker, 1971). The nipples are surrounded with sebaceous glands rich areola and represent the convergent point of mammary lobes, functional units of the adult mammary gland. It has been suggested that sebaceous glands positioned within the nipple areola and/or sweet glands might represent the evolutionary origin of the mammary glands (Oftedal, 2002). In human, primitive sebaceous glands and/or sweet glands evolved in 15-20 epithelial lobes which produce milk (Henrikson et al., 1997; Oftedal, 2002). During the course of mammary gland ontogeny, the mammary lobes arise from a primitive anlage, which undergoes series of morphological changes mainly postnatal (Radisky and Hartmann, 2009). The mammary gland reaches functional maturity at pregnancy during the process known as lactation when the mammary gland is composed of secretory epithelia (Borellini and Oka, 1989).

The adult mammary gland is an inhomogeneous organ composed of epithelial derived ducts surrounded by connective tissue and immersed in the adipose tissue lobes (Figure 1 a) (Sheffield, 1988). Although the milk production and excretion in the mammary gland is accomplished by epithelial derived cells, various biological processes (i.e. mammary gland development, hypertrophy, involution) in the adult and developing mammary gland are regulated trough inter -cellular and -tissue interactions (Maller et al., 2010).

The ratio between mammary cells of the epithelial and stromal origin is changing during the life time due to the continuous cycles of proliferation, differentiation,

lactation and regression of mammary gland epithelial component (Parmar and Cunha, 2004). During the puberty, the first changes occur in the growth of the stromal tissue. It has been suggested that stromal proliferation serves to inhibit the growth of the epithelial compartment (Howard and Gusterson, 2000). While the mammary fat-pad of non-pregnant females is largely assembled of the adipose tissue, the adipose compartment is gradually substituted by epithelial tissue, blood vessel and connective tissue during the pregnancy (Borellini and Oka, 1989; Russo and Russo, 2004) .

Moreover, the adult mammary gland is well-vascularized organ and supplied with wide lymph drainage, which is relevant to oncology because the breast cancer metastases develop on the distant sites due to the dissemination of cancer cells via blood and lymph vessels (Howard and Gusterson 2000; Eccles, Paon et al. 2007; Andres and Djonov 2010; Vermeulen, van Golen et al. 2010).

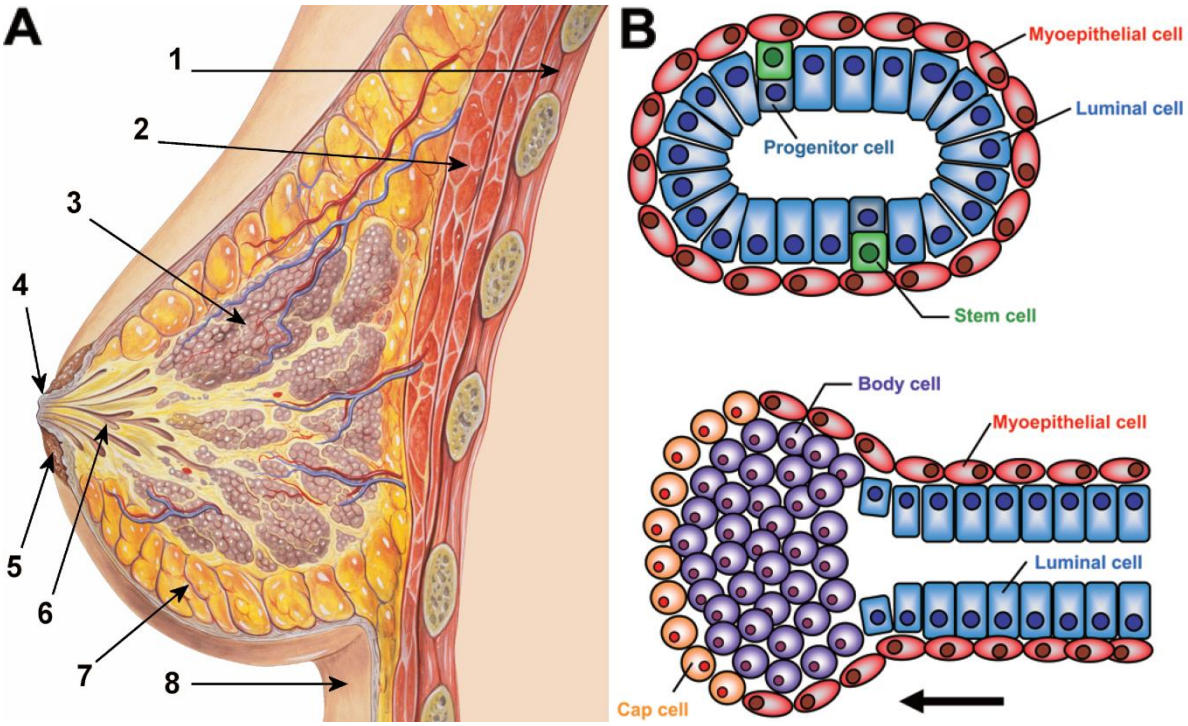

Figure 1. Human breast anatomy and the cellular organization of a TDLU. (A) Human breast is a complex organ composed of tissue of diverse origin. 1) Chest wall; 2) Pectoralis muscles; 3) Mammary gland ducts and lobules; 4) Nipple; 5) Areola mammae; 6) Lactiferous duct; 7) Adipose tissue; 8) Skin. (B) Mammary gland duct is composed of myoepithelial cells, luminal cells, secreting (cap) cells and mammary stem and progenitor cells. Picture modified from (Tiede and Kang, 2011; Wikipedia, 2012).

Deregulation of the both stromal and epithelial cell growth may cause breast hypertrophy, which is manifested in the abnormal breast sizes (macromastia or gigantomastia). The hypertrophy usually develops during puberty or at menopause (Dancey et al., 2008; Dehner et al., 1999). Following the medical care policy, the patients diagnosed with macromastia or gigantomastia undergo breast reduction surgery due to the physical, aesthetic or psychophysical difficulties (Nguyen et al., 2008). Tissue specimens of patients experiencing breast reduction can be used for the experimental purposes (Dontu et al., 2003a).

Mammary lobes of an adult gland consist of a collection of acini arising from terminal ducts embedded in intralobular stromal tissue (Parmar and Cunha, 2004). Terminal duct lobular units (TDLU) are considered as the functional units of the mammary gland. Each duct is composed of the two major cell types: myoepithelial and luminal cells (Figure 1 b). A layer of myoepithelial cells is found positioned directly below the basal membrane. Myoepithelial cells are characterized by the expression of the alpha smooth muscular actin and cytokeratins 5 and 14 (Stingl et al., 2005). Contractions of the myoepithelal cells enable milk excretion. Above the myoepithelal cell layer towards the lumen is the inner layer of luminal cells subdivided into ductal luminal cells, which line inside of the ducts, and alveolar luminal cells, which arise during the pregnancy and secrete milk (Visvader and Lindeman, 2011). The majority of the cells (>90%) found within the mammary ducts are differentiated luminal and myoepithelial cells (Chepko and Smith, 1997; Stingl et al., 2005).

1.2. The mammary gland development

The mammary gland development occurs in three distinct and differentially regulated stages: embryonic, pubertal and adult (Gjorevski and Nelson, 2011; Howard and Gusterson, 2000). Embryonic development and extensive proliferation and differentiation during each pregnancy cycle are enabled by the presence of mammary stem cells (Dontu et al., 2005; Van Keymeulen et al., 2011). Moreover, the regulation of developmental and differentiation processes involve an ample variety of hormones and growth factors such as estrogen, progesterone, and prolactin that drive primitive mammary stem cells towards differentiated functional cells (Henrikson et al., 1997; Stingl, 2011; Tiede and Kang, 2011).

Development of the human mammary gland begins at week 5 of the embryonic development. The first developmental sign is the formation of the milk streak, thickening in the ectoderm, extending from the axilla to the groin. During week 6 and 7 the milk streak develops to the mammary crest which later develops into the epithelial bud (Gusterson and Stein, 2012; Howard and Gusterson, 2000). Cells expressing some of the myoepithelial cell markers are observed in this period of embryonic development (Van Keymeulen et al., 2011). Embryonic development ends with a formation of a series of blind-ended tubes, with bulbous tips, well defined lobules and terminal duct lobular units, similar to those observed in the adult mammary gland. Shortly after birth, the mammary gland undergoes involution similar to the observed process in the post-menopausal breast (Anbazhagan et al., 1991; Gusterson and Stein, 2012).
The infant's mammary gland development after involution process at birth follows the overall body development until puberty when the swift development in females starts. Nevertheless, while the knowledge about the embryonic human mammary gland development is still incomplete due to the lack of tissue specimens, the developmental stages and processes in the animal models increase significantly our knowledge during the last decade pinpointing key steps of early development and involved signaling networks (Hens and Wysolmerski, 2005; Van Keymeulen et al., 2011).

The mammary gland development in human is hormonally regulated as many other processes of the pubertal maturation (Sternlicht et al., 2006; Stingl, 2011). The hormonal regulation starts before the first menstrual cycle when estrogen receptors are detectable in the low percent of the luminal cells (Gusterson and Stein, 2012; Sternlicht et al., 2006). Development of the TDLU is characterized by the development of the end buds and lateral buds (Russo and Russo, 2004). Unfortunately, the knowledge about the mammary gland development during pre-pubertal and pubertal age is not yet sufficient to prove any of the proposed models due to the low number of the analyzed samples. Moreover, little is known about the molecular mechanism of the stromal influence during development while it has become clear that stromal cells actively influence and shape many of the mammary

gland abnormalities related to the developmental processes (Bonafe et al., 2012; Cirri and Chiarugi, 2012).

1.3. Cellular hierarchy in the normal mammary gland

The majority of cells found within adult mammary ducts are differentiated luminal and myoepithelial cells (Chepko and Smith, 1997; Stingl et al., 2005). Myoepithelial cells are in direct contact with the basal membrane and they are cells responsible for the ductal contraction and milk circulation in a response to oxytocin (Sternlicht et al., 2006). Luminal cells are orientated towards lumen and build TDLU. During lactation, a sub-type of luminal cells located in the alveoli and hence named alveolar cells produce milk. In addition to these differentiated cell types, the adult mammary gland contains stem cells and progenitor cells (Figure 2). Thus, the mammary gland is a hierarchically structured organ (Stingl et al., 2005; Visvader and Lindeman, 2011). The presence of the undifferentiated cells within the adult gland enables mammary gland maturation and cyclic differentiation processes during the adult life (Stingl et al., 2006).

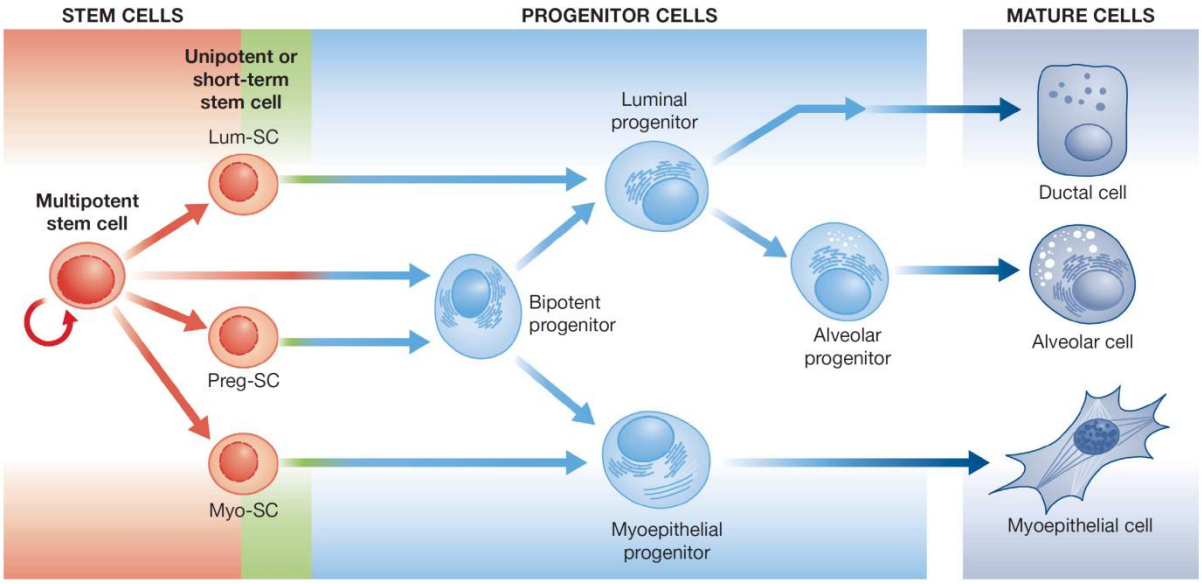

Figure 2. Hierarchical organization of the mammary gland. The adult mammary gland contains primitive adult stem cells which are able to reconstitute functional mammary gland. Figure is modified from the ref. (Visvader and Lindeman, 2011).

The adult mammary gland reaches functional maturity at pregnancy when branching TDLU are formed trough multi- step sequences of proliferation and differentiation processes (Sternlicht et al., 2006). Each pregnancy cycle ends with controlled reduction of the epithelial cell compartment by apoptosis (Radisky and Hartmann, 2009). These cyclical bursts of proliferation and subsequent apoptosis recur also during each menstrual cycle (Russo and Russo, 2004) and are enabled by the existence of the cells with differentiation and self-renewal ability, adult stem and progenitor cells (Dontu et al., 2003b).

The existence of a multipotent cellular type within the adult mammary gland able to reconstitute functional adult mammary gland has been shown by numerous independent experiments. The first mammary transplantation studies in the late 1950'ies by DeOme and colleagues suggested that the adult mammary gland contains a cell type able to reconstitute the mammary gland of the adult mice (Daniel et al., 1971; Deome et al., 1959). Furthermore, the engraftment of human tissue pieces into pre-cleared mammary fat-pads of immunodeficient mice suggested the existence of cells able to reconstitute the functional human mammary gland (Kuperwasser et al., 2004). The presence of the adult mammary stem cells was proven by Shakelton and colleagues who were able to reconstitute a functional mouse mammary gland form a single mammary cell (Shackleton et al., 2006). However, although today we have experimental evidences of adult mammary stem cells existence, the main problem for the study of mammary gland development and pathophysiology remained the isolation and molecular and functional characterization of the adult mammary stem and progenitor cells.

Although several subpopulations of mammary cells have been described, the existence and precise molecular profile of adult mammary stem cells is still intensively discussed (Keller et al., 2011; Stingl et al., 2005).

1.4. Isolation of the mammary stem and progenitor cells

Stem cells are defined as cells capable for multi-lineage differentiation and self-renewal (Luo et al., 2010; Smalley and Ashworth, 2003). It has been suggested that understanding mammary gland biology, development and pathophysiology mostly

depends on our ability to isolate, grow and manipulate undifferentiated cell types (Dontu et al., 2003a; Smalley and Ashworth, 2003). Therefore, the enormous efforts have been invested in the development of different strategies for the isolation and characterization of adult stem and progenitor cells.

1.4.1. Isolation of the mammary stem and progenitor cells based on marker expression

Scientists in mammary stem cell research were initially inspired by studies in the field of hematopoiesis and tried to develop various assays that help enrichment of the mammary stem and progenitor cells (Alvi et al., 2002; Eirew et al., 2008; Stingl et al., 2005).

One of the first methods for the isolation of stem and progenitor cells was based on the observation that due to over-expression of transmembrane transporter proteins stem cells are able to exclude vital marker dyes (Smalley and Ashworth, 2003). The so-called “side-population” remained unstained by DNA-binding dyes due to its ability to pump out the dye while more differentiated progenies were not able to exclude the DNA-binding dye (Charafe-Jauffret et al., 2009). Whereas the first reports convincingly demonstrated enrichment of stem cells and cancer stem cells (Alvi et al., 2002), later reports indicated many inconsistencies which hindered the experimental reproduction of the results and their validation (Montanaro et al., 2004).

On the other hand, empirical testing of surface marker combination enabled the definition of markers used for Fluorescence Activated Cell Sorting (FACS) methodology to identify and isolated adult stem and progenitor cells (Charafe-Jauffret et al., 2009; Ginestier et al., 2007a; Stingl et al., 2005). Thus, the cellular types defined by their functional characteristics, luminal and myoepithelial cells are described by the following cellular markers: 1) differentiated luminal cells are CK14-/CK18+/CK19+ and MUC1+ cells, while 2) myoepithelial cells are characterized as CK14+/SMA+ and CD10+ cells. The luminal progenitor cells are defined as as MUC1+/CD133+/EpCAM+/CD49f+/CD10-/THY-, while the myoepithelial progenitors express the marker following marker combination MUC1-/CD133-/EpCAM+/CD49f+/CD10+/THY+ (Bartek et al., 1990; Snedeker et al., 1991; Stingl et

al., 1998; Stingl et al., 2001; Stingl et al., 2005). It is important to say that the function of these markers is often unclear. Unfortunately, many attempts to define adult stem and progenitor cells based on marker expression led to inconsistent conclusions. Keller et al. used healthy mammary tissue specimens to define cellular populations within the adult mammary gland. They found that both, EpCAM+ and CD10+ population contain differentiation potential (Keller et al., 2011). On the other hand, the mentioned study (Keller et al., 2011) is opposed to the observation that mammary repopulating units were found to reside in EpCAM-/low phenotype (Eirew et al., 2008).

Taken together, our inability to isolate adult stem and progenitor cells by marker expression hampered the attempts for their perspective characterization and manipulation. Nevertheless, the alternative approaches demonstrated that the isolation and characterization of the adult mammary stem and progenitor cells is possible.

1.4.2. Mammospheres- enriched population of adult mammary stem and progenitor cells

Based on the neural stem cell research assays, Gabriela Dontu and colleagues applied a cell culture system for neural stem cells to propagate undifferentiated cells isolated from the adult mammary specimens (Dontu et al., 2003a). Basis of the mammosphere assay was the observation that rare undifferentiated cells survive anchorage independent conditions and proliferate to form multi-cellular spheroids while most of the cells isolated from mammoplasty tissue specimens underwent anoikis when grown under ultra-low attachment conditions. It was suggested that inability of differentiated cells surviving anchorage independent conditions underlies the selective propagation of adult stem and progenitor cells (Dontu and Wicha, 2005).

Mammospheres are highly enriched in undifferentiated cells, as demonstrated by the ability of single cells propagated as mammospheres to generate multi-lineage colonies, which is not the case in the presence of serum or when propagated on a collagen substratum (Dontu et al., 2003a; Liu et al., 2008). The primary mammospheres contain eight times more bi-lineage progenitor cells compared to the

tissue of origin. The secondary and later-passaged mammospheres consist of virtually 100% bi-potent progenitors (Dontu et al., 2003b; Dontu and Wicha, 2005). Moreover, mammospheres form complex structures in reconstituted 3-D culture systems in Matrigel©, resembling the observed morphology of the functional adult mammary gland (Dontu et al., 2003a).
In vivo experiments indicated that the secondary mammospheres are able to differentiate in complex ducto-acinar structures comparable to the TDLU when inoculated in NOD/scid mice, immunodeficient mice (Liu et al., 2006; Liu et al., 2008; Pece et al., 2010).

Growth and enrichment of the mammary stem and progenitor cells as spherical colonies was shown to be currently the most efficient way for the enrichment and propagation of the mammary stem and progenitor cells (Dontu et al., 2003a; Luo et al., 2010).

1.4.3. Isolation of the stem and progenitor cell fractions by functional properties

In 2010, Pece and colleagues developed another experimental strategy for stem cell enrichment of a pre-selected population of the mammary stem and progenitor cells. The mammary stem and progenitor cells were propagated under anchorage independent conditions. After the secondary mammospheres were formed stem and progenitor cells were selected on a basis on their functional characteristics (Pece et al., 2010).
The mammary stem cells are asymmetrically and slow dividing cells, which upon cell division give rise to two daughter cells; one is the self-renewed stem cell, while the other cell represents a progenitor cell (Harmes and DiRenzo, 2009; Smalley and Ashworth, 2003). The discrimination between two daughter cells is based on their cell division rates, stem cells are slower dividing cells compared to progenitor cells (Pece et al., 2010).

It was shown that single mammospheres can reconstitute the functional mammary gland *in vivo* and that mammospheres arise from single cells. Thus, the mammospheres are groups of cells, which arise from a single adult stem cell (Dontu

et al., 2003a; Shackleton et al., 2006). The isolation of the adult stem cells by Pece and colleagues relies on the following approach: If the cellular membrane of the cells propagated under anchorage independent conditions is labeled by a fluorescent marker, and the dye is equally distributed to the daughter cells upon each cellular division, then due to the slow cycling frequency of the stem cells, the label retaining cells represent the mammosphere stem cell, while the fast cycling cells within a mammosphere become quickly unlabeled and represent daughter cells (Lanzkron et al., 1999). Therefore, during the growth of a mammosphere, the rare quiescent/slowly dividing mammary stem cells retain dye, while the bulk of population derived from the proliferation of the progenitors progressively lose it by dilutions (Pece et al., 2010).

1.5. Differentiation ability of mammary stem and progenitor cells

Stem cells are characterized by the ability to self-renew and generate daughter cells that can form all the differentiated cell types found within the mature tissue (Smalley and Ashworth, 2003). Differentiation ability of the adult mammary stem and progenitor cells can be analyzed under *in vitro* and *in vivo* differentiation conditions (Eirew et al., 2008; Liu et al., 2008; Weaver and Bissell, 1999).

1.5.1. *In vitro* differentiation of mammary stem and progenitor cells

The human mammary gland develops and functions in a complex micro-environment composed of different cell types and an intricate network of extracellular molecules. It has been suggested that micro-environment influences epithelial cell homeostasis and differentiation (Nelson and Bissell, 2006) and therefore in the previous years different experimental strategies have been applied to unravel the micro-environmental influences on the cell fate of mammary cells (Campbell et al., 2011; Weaver and Bissell, 1999).

The most frequently applied matrix to study *in vitro* differentiation is Matrigel©, a reconstituted basement membrane of mice developing Engelbreth-Holm-Swarm sarcomas (Lee et al., 2007). The differentiation of adult human mammary stem and progenitor cells in such Matrigel© matrices results in a formation of (i) acinar structures resembling terminal end-buds of human mammary glands; (ii) TDLU-

complex terminal ductal-lobular structures and (iii) single cells which are not able to propagate (Dontu et al., 2003a). Therefore, the *in vitro* differentiation strategies in Matrigel© provide possibility to study development in a relevant micro-environment. Moreover, the Matrigel© is often used in cancer biology. One of the most important feature of malignancies is cellular invasion which enables tumor cell dissemination from the primary site and subsequent metastasis development (Hanahan and Weinberg, 2011). Cell propagation in Matrgel© can give information about the tumorigenic ability of the analyzed cells in a relevant milieu because it has been observed that the extracellular matrix can control the function of cells with aberrant genotype to some extent (Lee et al., 2007; Nelson and Bissell, 2006).

1.5.2. *In vivo* models for mammary stem and progenitor cell differentiation

Definitive evidence for the existence of adult stem cells within mammary gland is given by *in vivo* studies (Eirew et al., 2008).

The presence of stem cells within adult mouse mammary gland was demonstrated by reconstitution of normal mammary gland by a single cell (Shackleton et al., 2006), but the presence of adult stem cells within human mammary gland could not be shown due to the technical obstacles.
The first attempts to propagate normal human cells in mouse mammary fat-pad were not successful (Outzen and Custer, 1975) mainly because of the inability of normal human mammary cells to survive in recipient mice due to (i) the host immune system and (ii) micro-environmental differences between human and murine mammary gland (Howard and Gusterson, 2000; Proia and Kuperwasser, 2006). The problem of the immune rejection was circumvent by utilization and development of immune-deficient mice such as NOD.CB17-*Prkdc*^{scid}/J (Kuperwasser et al., 2004). The problem of the micro-environmental difference between human and murine mammary gland is in some reports overcame by engraftment of collagen plugs containing human mammary stem and progenitor cells subcutaneously or beneath the renal capsule (Eirew et al., 2008; Parmar et al., 2002), but such approaches do not consider the endocrine signaling of the adult mammary gland which is important for the gland development and regulation (Borellini and Oka, 1989; Kuperwasser et al., 2004).

Development of the orthotopic xenograft mouse models was enabled by "humanization" of the mouse mammary fat-pad by human immortalized fibroblasts (Kuperwasser et al., 2004; Proia and Kuperwasser, 2006). The recent progress made in isolation and propagation of human mammary stem and progenitor cells (i.e mammosphere culture) enabled study of normal and malignant mammary cells development and growth in immune-deficient mice (Liu et al., 2006; Liu et al., 2008; Pece et al., 2010). However, reconstitution of the human mammary gland in mice by "humanization" protocol (Liu et al., 2006; Proia and Kuperwasser, 2006) has shown many technical difficulties and risks for reproducibility due to sensitivity of the experimental approach what imposed the need for the development of more efficient orthotopic xenograft models.

1.6. Breast cancer

Breast cancer accounts as the most frequent cancer type among women. In 2008, breast cancer caused 458 503 deaths worldwide (WHO, 2008). The main culprit of the associated mortality is metastasis development at secondary, distant sites (Jemal et al., 2008).

Currently applied therapies against breast cancer depend on pathophysiological features determined by various methods (Downs-Holmes and Silverman, 2012). The frequently applied TNM classification subdivides breast cancer based on tumor size (T), number of lymph nodes containing infiltrated tumor cells (N) and presence of distant metastasis (M). The TNM classification is often supplemented by the morphological criteria, such as the differentiation grade of the observed tumor which indicates the probability of tumor recurrence (Bundred, 2001). The tumors may display characteristics of the differentiated mammary gland and therefore be subdivided into ductal carcinomas or lobular carcinomas. The grade is a summary score of values given to the mitotic index, percentage of tubular structures and nuclear pleomorphism (Elston and Ellis, 1991). Tumors with scores from 3 to 5 are well differentiated (grade 1), from 6 to 7 are moderately differentiated (grade 2), and 8 to 9 (grade 3) are poorly differentiated (Cianfrocca and Goldstein, 2004; Elston and Ellis, 1991). Grade 2 tumors make 50- 75% of all diagnosed breast tumors (Elston and Ellis, 1993; Parham et al., 1992) and show characteristics between differentiated

and poorly differentiated histological grades 1 or 3 status (with a low or high risk of recurrence, respectively) and therefore, to increase precision of cancer grades, further classification of the grade 2 tumors was preformed based on their gene expression. The applied re-classification divided the patients into two groups, groups with high versus low risk of recurrence (Sotiriou et al., 2006).

Poorly differentiated tumors exhibit the characteristics of the undifferentiated mammary cells. Hence, it has been suggested that poor differentiation of mammary cancers reflects the expression of stem-like traits (Ben-Porath et al., 2008). The reasoning raised the interest in studies of the mammary stem cell biology.

1.7. Cancer stem cell concept

Hyper-proliferation of cancer cells combined with genetic instability in the primary tumors results in their cellular heterogeneity (Hanahan and Weinberg, 2011). However, the cellular heterogeneity of the primary tumor is not only reflected in genetic differences among tumor clones, but also in functional hierarchy within the tumor cells (Ginestier et al., 2007a; Mani et al., 2008).

Cancer stem cells (CSC) are defined as tumor clones able to grow tumors in animal hosts and differentiate into non- CSC (Clarke et al., 2006). Rare but potent, CSC give rise to all other cancer cell types detected within the tumor and contribute to an invasive phenotype observed in metastatic breast tumors (Rudland, 1987; Sheridan et al., 2006). The current CSC concept indicates that disease relapses and later progression is largely due to the intrinsic therapy resistance of CSC (Gupta et al., 2009). The CSC concept does not suggest that the target cell of malignant transformation is a mammary stem cell, but the CSC possess characteristics of the normal counterparts (Bjerkvig et al., 2005).

The CSC concept further holds that successful eradication of a cancer is only possible if the applied therapies are able to target CSC. The analysis of CSC expression profiles showed that CSC utilize molecular pathways that are frequently a part of a stem cell program and moreover are correlated with the histopathological grading (Palmer et al., 2012). Therefore, it may be a plausible hypothesis that knowledge about the signaling networks governing the stem cell phenotype will also

improve our understanding of tumor biology and help to design novel targeted therapies.

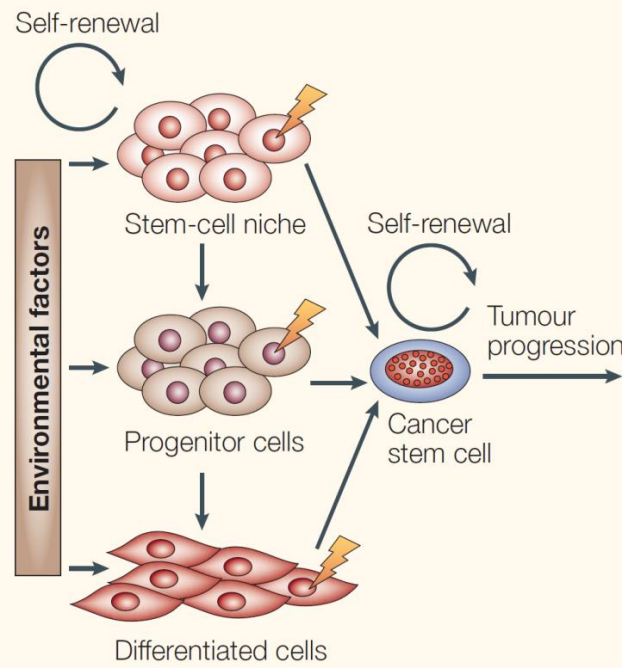

Figure 3. The adult mammary stem cells and breast cancer stem cells share certain characteristics. The cancer stem cells might arise either from specific adult stem or progenitor cells, but stem-like phenotype acquisition by the differentiated cells should be considered (Bjerkvig et al., 2005).

1.8. Interleukin 6 and breast cancer

Interleukin 6 (IL6), a multifunctional cytokine, plays a role in pro- and anti-inflammatory response and has a primary function in the pathophysiology of many diseases such as rheumatoid arthritis, Castleman's dieses and cancer (Grivennikov and Karin, 2008; Kishimoto, 2005).

IL6 signaling is mediated via IL-6 binding to IL6 receptor (IL6R) which induces homo-dimerization of the signal transducing receptor gp130 which leads to activation of multiple signaling networks (Keller et al., 2002). IL6 signaling is responsible for regulation of various biological processes as cell survival, apoptosis and proliferation in murine hematopoietic stem cells, hepatocytes and MCF7 breast cancer cell line (Gotze et al., 2001; Peters et al., 1998a; Sansone et al., 2007).

IL6 signals via a heterodimeric IL6/IL6R/gp130 complex, whose engagement triggers activation of Janus (JAK) kinases, and the downstream effectors STAT3, SHP-2/Ras,

NF-κB and PI3K/Akt (Kishimoto, 2005). The IL6/IL6R/gp130 complex can be build by either utilization of the membrane bound IL6R or the soluble form of IL6R (sIL6R) in the process known as IL6 trans-signaling (Peters et al., 1998b; Taga et al., 1989). The effect of the IL6 signaling on breast cancer was elaborated in various systems (Iliopoulos et al., 2011; Korkaya et al., 2012; Sansone et al., 2007), but in all of the mentioned reports it is not clear whether the IL6 signaling is maintained via membrane bound or soluble IL6R which is of high therapy design importance because high levels of sIL6R can be found in human sera.

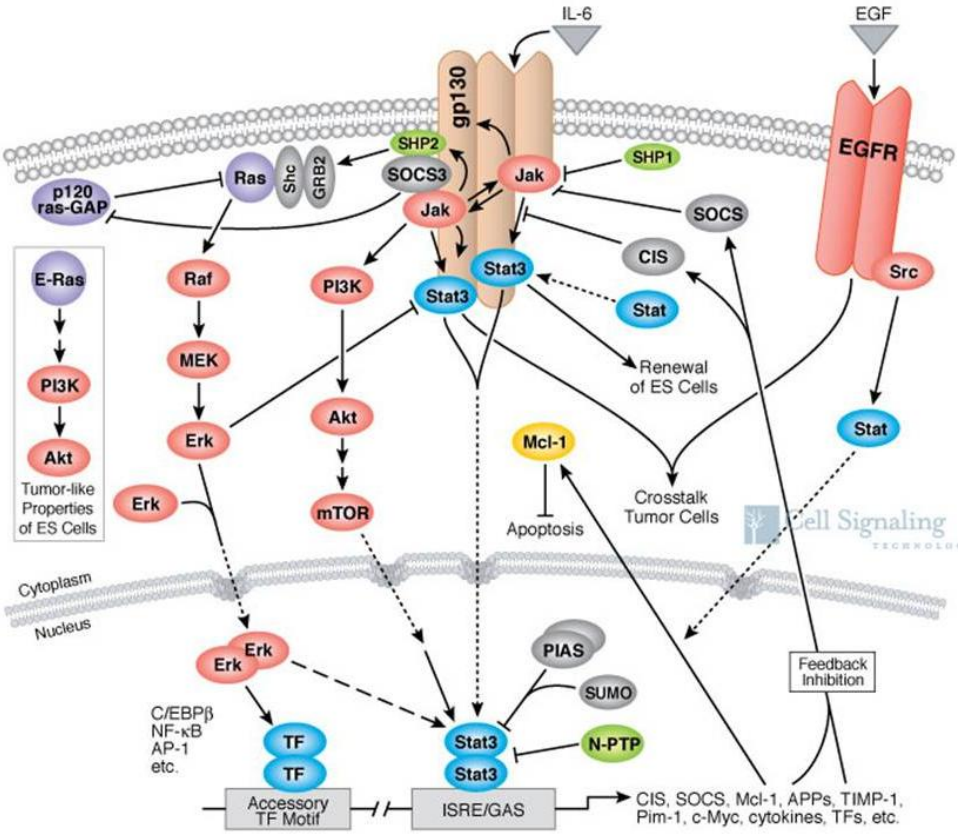

Figure 4. IL6 signaling pathway. IL6 signaling pathway is triggered by dimerization of the IL6 and IL6R. IL6-IL6R complex binds to gp130 and form a complex of 6 members complex (2 xIL6, 2xIL6R and 2x gp130). The complex triggers the signaling pathway via intracellular domain of gp130. IL6 signaling is madiated via complex signaling networks (i.e. JAK/STAT3, PI3K/Akt/mTOR, Raf/Mek/Erk). The figure is modified from the reference (CellsignalingTechnology, 2012).

Increased levels of IL6 in sera of breast cancer patients correlate with poor disease outcome and reduced prognosis (Bachelot et al., 2003). This might be a consequence of an overall IL6 influence on the growth rate of the primary tumor (Korkaya et al., 2012), but the exact mechanisms of these action is not yet

elucidated. Possible mechanism of action might be via CSC as deduced from the studies in the MCF7 cell line. Activation of the IL6 signaling induced self- renewal, hypoxia survival, and invasiveness of MCF7 cell line derived mammospheres (Sansone et al., 2007). Additionally, IL6 signaling has been proposed to regulate the conversion of the non- stem cancer cells into cancer stem cells (Iliopoulos et al., 2011) but this observation needs further clarification.

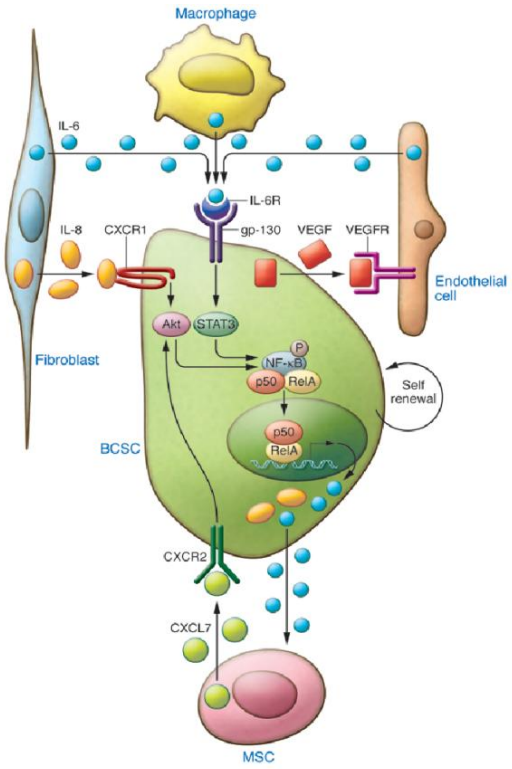

Figure 5. IL6 signaling in cancer cell. IL6 signaling in the cancer cells is maintained via IL6 secretion by various non-epithelial cells types. The IL6 signaling influences various biological processes enabling cancer cell survival, proliferation and self-renewal (Grivennikov and Karin, 2008; Korkaya et al., 2011).

Present knowledge suggests that IL6 signaling in cancer is maintained trough IL6 expression by cancer associated fibroblasts, macrophages and various different cell types (Bonafe et al., 2012) while it is not much known about the effect and sources of the sIL6R.

Having in mind the importance of the IL6 signaling the aim of this work was to further elaborate the effect of the IL6 trans-signaling in normal and malignant breast stem and progenitor cells.

1.9. The aim of the work

The mammary gland is hierarchically structured organ containing cellular types of various differentiation stages. The mammary gland development and extensive proliferation and differentiation during each pregnancy cycle are enabled by the presence of the adult mammary stem cells which phenotype is regulated by activation of stem signaling pathways. These signaling pathways are activated as a result of the dynamic interaction between mammary cells and micro-environment. Deregulation of stem cell signaling pathways has been suggested to drive breast cancer by maintaining cancer stem cells (CSC), cells which give rise to all other cancer cell types detected within the tumor and contribute to an invasive phenotype observed in metastatic breast tumors. As normal stem cells, CSC interact with micro-environment and these interactions involve inflammatory cytokines such as Interleukin 6 (IL6).

The aims of the proposed PhD thesis were:

1) To address how IL6 signals in normal mammary stem and progenitor cells,
2) To assess the effects of IL6 signaling in regulation of normal mammary stem and progenitor cell phenotype,
3) To assess the ability of cellular cooperation in triggering IL6 trans-signaling in mammary gland,
4) To evaluate the effects of the IL6 trans-signaling in CSC phenotype.

2. Materials and Methods

2.1. Materials

2.1.1. Reagents, solutions and cell culture media

Reagents, solution and cell culture media used in this work are listed in the following tables.

	Reagents	Company
1	**AB-Serum**	Bio-Rad, Dreieich
2	**Acetic acid**	Merck, Darmstadt
3	**Agarose**	Sigma-Aldrich, USA
4	**Ampicillin**	AppliChem GmbH, Darmstadt
5	**B27**	Invitrogen, USA
6	**BCIP/NBT (AP color reagent)**	BioRad, Munich
7	**Basic fibroblast growth factor (bFGF)**	Sigma-Aldrich, USA
8	**bio-dUTP, 1 mM**	Roche, Penzberg
9	**Bromphenol blue**	Sigma-Aldrich, USA
10	**Bovine serum albumin (BSA), 20 mg/ml**	Roche, Penzberg, Mannheim
11	**Bovine serum albumin (BSA), 30%**	Biotest, Dreieich
12	**Chloroform**	Sigma-Aldrich, USA
13	**Chloroquine**	Sigma-Aldrich, USA
14	**Cholera toxin**	Sigma-Aldrich, USA
15	**Collagenase**	Sigma-Aldrich, USA
16	**DAPI**	Roche, Penzberg
17	**dATP, 100 mM**	GE Healthcare, UK
18	**dCTP, 100 mM**	GE Healthcare, UK
19	**DEPC-H_2O**	Invitrogen, USA
20	**dGTP, 100 mM**	GE Healthcare, UK

21	**Dichlorodimethylsilane, 2% in 1,1,1-trichlorethane**	Merck, Darmstadt
22	**Diluent C**	Sigma-Aldrich, USA
23	**Disodium phosphate**	Sigma-Aldrich, USA
24	**Ditiotreitol (DTT), 0.1 M**	Invitrogen, USA
25	**DMEM**	Pan-Biotech, Aidenbach
26	**DMEM/F12**	Pan-Biotech, Aidenbach
27	**DNA ligase T4, 5 U/µl**	Roche, Penzberg
28	**DNA polymerase PanTaq, 5 U/µl**	Pan Biotech, Aidenbach
29	**DNA polymerase Taq, 5 U/µl**	Roche, Penzberg
30	**DNA polymerase Thermo Sequenase (TS), 32 U/µl**	GE Healthcare, UK
31	**DNA-Ladder 1kb**	Invitrogen, USA
32	**DNase I, 2000 U/mg**	Roche, Penzberg
33	**dNTPs, 100 mM**	GE Healthcare, UK
34	**DSL peptide**	Research Genetics, USA
35	**dTTP, 100 mM**	GE Healthcare, UK
36	**EB buffer – QIAquick PCR Purification Kit**	Qiagen, Hilden
37	**EDTA**	Sigma-Aldrich, USA
38	**Eosin**	Sigma-Aldrich, USA
39	**Epidermal growth factor (EGF)**	Sigma-Aldrich, USA
40	**Ethanol, absolute**	J.T.Baker, Griesheim
41	**Ethidium-bromide, 1%**	Fluka, Sigma-Aldrich, USA
42	**Eukitt**	O. Kindler GmbH, Freiburg
43	**Fetal bovine serum (FBS)**	Sigma-Aldrich, USA
44	**Fetal bovine serum (FBS)**	Pan Biotech, Aidenbach
45	**Formaldehyde**	Merck, Darmstadt
46	**Formamide**	Merck, Darmstadt
47	**Formamide, deionized**	Sigma-Aldrich, USA
48	**Gentamicin**	Sigma-Aldrich, USA

49	**H_2O, for HPLC**	Merck, Darmstadt
50	**Hank's salt solution**	Biochrom, Berlin
51	**Hematoxylin**	Ventana, USA
52	**Heparin**	Sigma-Aldrich, USA
53	**HEPES, 1M**	Sigma-Aldrich, USA
54	**Hyaluronidase**	Sigma-Aldrich, USA
55	**Hydrochloric acid, 37%**	J.T. Baker, Griesheim
56	**Hydrocortisone**	Sigma-Aldrich, USA
57	**Igepal CA-630**	Sigma-Aldrich, USA
58	**Insulin**	Sigma-Aldrich, USA
59	**Interleukin 6**	Sigma-Aldrich, USA
60	**Isopropanol**	Fluka, Sigma-Aldrich, USA
61	**L-Glutamine, 200 mM**	Pan-Biotech, Aidenbach
62	**Magnesium-chloride**	Sigma-Aldrich, USA
63	**Matrigel©**	BD Biosciences, Heidelberg
64	**MEBM**	Lonza, USA
65	**Methanol**	Merck, Darmstadt
66	**Mineral oil**	Sigma-Aldrich, USA
67	**Mouse serum**	DAKO, Hamburg
68	**mTRAP^{tm} kit**	Active Motif, Japan
69	**Sodium acetate, 2M pH 4**	Calbiochem, Hamburg
70	**Sodium citrate**	Applichem, Darmstadt
71	**NEB buffer 1**	New England Biolabs, USA
72	**NEB buffer 2**	New England Biolabs, USA
73	**NEB buffer 3**	New England Biolabs, USA
74	**NEB buffer 4**	New England Biolabs, USA
75	**N-Laurylsarcosin**	Sigma-Aldrich, USA
76	**Parablast embedding medium (Paraffin)**	Sigma-Aldrich, USA
77	**Penicillin/Streptomycin, 10 U/µl**	Pan-Biotech, Aidenbach
78	**Percoll**	GE Healthcare, UK
79	**Peroxidase Blocking Solution**	DAKO, USA

80	**Phytohemagglutinin, M form (PHA-M)**	Invitrogen, USA
81	**PolMix polymerase – Expand long template PCR system, 5 U/µl**	Roche, Penzberg
82	**Polybrene**	Sigma-Aldrich, USA
83	**Poly-HEMA**	Sigma-Aldrich, USA
84	**Potassium acetate, 5 M**	Sigma-Aldrich, USA
85	**Potassium chloride (KCl)**	Sigma-Aldrich, USA
86	**Potassium chloride (KCl), 1 M**	Fluka, Sigma-Aldrich, USA
87	**Potassium digydrogen phospate (KH_2PO_4)**	Merck, Darmstadt
88	**Propidiumiodid**	Sigma-Aldrich, USA
89	**Puromycin**	Sigma-Aldrich, USA
90	**Roti-Aqua-Phenol**	Carl Roth GmbH, Karlsruhe
91	**RPMI 1640**	Pan-Biotech, Aidenbach
92	**β-Mercaptoethanol**	Carl Roth GmbH, Karlsruhe
93	**Trisodium citrate dihydrate**	Merck, Darmstadt
94	**Trypan blue, 0.4%**	Sigma-Aldrich, USA
95	**Tris(hydroxymethyl)-aminomethan (TRIS)**	AppliChem, Darmstadt
96	**Tris-acetate**	Sigma-Aldrich, USA
97	**Tris-HCl (pH 8), 1M**	Sigma-Aldrich, USA
98	**tRNA, 100 mg**	Roche, Penzberg
99	**Trypsin neutralization solution**	Sigma-Aldrich, USA
100	**Trypsin/EDTA, 10x Trypsin, 0.5% + EDTA, 0.2% in 1x PBS**	PAA, Austria
101	**Tween 20**	Sigma-Aldrich, USA
102	**Ultra Pure^{tm} Herring sperm DNA solution**	Invitrogen, USA
103	**UltraPure^{TM} DEPC- Water**	Invitrogen, USA
104	**Xylol**	Roth, Karlsruhe
105	**Zeocin**	Invitrogen, USA

2.1.2. Antibodies

	Antibody	Company	Clone	Concentration
1	**Biotin anti-human CD126 (IL-6Rα)**	Biolegend, USA	UV4	0,5 mg/ml
2	**Mouse IgG_1, κ-Isotype control**	Biolegend, USA	MOPC-21	0,5 mg/ml
3	**Monoclonal anti-human IL6 blocking antibody**	Sigma-Aldrich, USA	6708.11	1,5 µg/ml
4	**Anti-human cytokeratin 18**	Chemicon	CK2	20 µg/ml
5	**Anti-IL6R (FITC)**	Abcam	B-R6	1 mg/ml

2.1.3. The composition of prepared buffers, media and solutions

	Solutions, Buffers and Media	Composition
1	**Carnoy Fixative**	7,5 ml methanol
		2,5 ml acetic acid
2	**Cell culture medium**	RPMI medium without L-glutamine
		10% FCS
		200 U/mL penicillin
		200 U/mL streptomycin
		2 mM L-glutamine
3	**DAPI solution**	10 µg/ml DAPI
		4x SSC / 0,2% Tween-20
4	**Hematoxylin solution**	2 g hematoxylin
		0,4 g sodium iodide
		100 g potassium aluminium

		sulfate
		100 g chloral hydrate
		2 g citric acid
5	**LB (liquid broth)**	1% NaCl
		1% tryptone
		5% yeast extract
		pH 7,0
6	**Mammosphere medium**	49 ml MEBM
		1x B27
		10 ng/ml EGF
		10 ng/ml bFGF
		4 µg/ml heparin
7	**Medium for the HME cell lines**	DMEM/F12
		10% FCS
		200 U/ml penicillin
		200 U/ml streptomycin
		10 ng/ml EGF
		0,5 µg/mL hydrocortisone
		10 µg/mL insulin
8	**Medium for the MCF7 and MDA-MB-231 cell lines**	DMEM/F12
		10% FCS
		200 U/ml penicillin
		200 U/ml streptomycin
		2 mM L- glutamine
9	**Mammary tissue digestion medium**	DMEM/F12
		1% HEPES
		200 U/ml penicillin
		200 U/ml streptomycin

		2 mM L- glutamine
		2% BSA
		10 mg/ml hyaluronidase (100 U/ml)
		33 µg/ml collagenase (300 U/ml)
		10 µg/mL insulin
		0,5 µg/mL hydrocortisone
		100 ng/ml cholera toxin
10	**PBS (Phosphate Buffer Saline)**	8,5 mM Na_2HPO_4
		2 mM KH_2PO_4 NaCl
		150 mM NaCl
		pH 7,4
11	**PCR-Buffer + dNTPs**	100 mM Tris-HCl
		500 mM KCl
		10 mM $MgCl_2$
		1mM nucleotids
12	**TE-Puffer**	10 mM TRIS-HCl
		1 mM EDTA
		pH 7,4

2.1.4. Cell lines

Identity of used cell lines was regularly controlled by the ATCC recommended DNA fingerprinting.

	Cell line	Description
1	**C3H10T 1/2**	Mouse embryonic fibroblasts
2	**hTERT-HME1**	Non-tumorigenic breast epithelial cell line
3	**hTERT-HME1 BRAF**	hTERT-HME1 cell line carrying mutation in BRAF gene
4	**hTERT-HME1 EFGR**	hTERT-HME1 cell line over-expressing EGFR receptor

5	**hTERT-HME1 PI3KCA ex. 20**	hTERT-HME1 cell line carrying mutation in exon 20 of PI3KCA gene
6	**hTERT-HME1 shPTEN**	hTERT-HME1 cell line expressing reduced levels of PTEN
7	**hTERT fibroblasts**	Immortalized human fibroblasts
8	**MCF10A**	Non-tumorigenic breast epithelial cell line
9	**MCF7**	Breast cancer cell line- metastatic pleural effusion cells
10	**MDA-MB-231**	Breast cancer cell line- metastatic pleural effusion cells
11	**MDA-MB-231 1833**	Breast cancer cell line- metastatic pleural effusion cells
12	**SK-BR-3**	Luminal breast cancer cell line
13	**HEK-293T**	Human embryonic kidney cell line

2.1.5. Devices

	Device	Company
1	**Axio Imager Z1 Fluorescence microscope**	Zeiss, Göttingen
2	**Balance**	Kern, Balingen
3	**BenchMark Ultra**	Ventana, USA
4	**Capillary holder for micromanipulation**	Eppendorf, Hamburg
5	**Cell culture incubator**	Heraeus, Hanau
6	**Cell culture incubator**	Heraeus, Hanau
7	**Cell culture laminar flow**	Heraeus, Hanau
8	**Centrifuge**	Heraeus, Hanau
9	**Centrifuge**	Eppendorf, Hamburg
10	**Centrifuge, tabletop**	Grant Bio, USA
11	**Centrifuge, tabletop**	Eppendorf, Hamburg
12	**Cytospine Centrifuge**	Hettich, USA

13	**DM RXA Fluorescence microscope**	Leica, USA
14	**Cauterizer**	Fine Science Tools, Hedelberg
15	**FACS Canto II**	BD Biosciences, USA
16	**Electrophoresis gel chamber**	Biostep, Jahnsdorf
17	**Photometer, GeneQuant II**	Pharmacia Biotech, USA
18	**Laser micro-dissection microscope**	P.A.L.M, Bernried
19	**LSR II flow cytometer**	BD Bioscience, USA
20	**Magnetic stirrer**	VELP Scientifica
20	**MJ Research Peltier Thermal Cycler PTC-200**	Bio-Rad, USA
21	**MJ Research Peltier Thermal Cycler Tetrad**	Bio-Rad, USA
22	**Multipipette Stream**	Eppendorf, Hamburg
23	**Neubauer- Cell counter**	Schubert und Weiß, Munich
24	**Optical microscope**	Optech, Canada
25	**Pipette controller**	Brand, Wertheim
26	**pH-meter**	Eutech Instruments, The Netherlands
27	**Pipettes (2 µL, 20 µL, 200 µL, 1000 µL)**	Eppendorf, Hamburg
28	**Power Supply for gel chamber electrophoresis**	MRC, Israel
29	**Pump**	KNF, Freiburg
30	**Stuart™ Scientific roller mixer**	Stuart Scientific, UK
31	**Thermo mixer**	Eppendorf, Hamburg
32	**UV illuminator**	Intas, Göttingen
33	**Vortex mixers**	VELP Scientifica, Italy
34	**Water bath**	Memmert, Schwabach

2.1.6. Software

Software	Company
AxioVision 4.5	Zeiss, Göttingen
FACS Diva 6.1.1	BD Biosciences, USA
FlowJo 8.8.6	TreeStar, Inc.USA
NEBcutter V2.0	New England Biolabs, USA
Vector NTI	Invitrogen, USA
GraphPad Prism	Graph Pad software, USA
http://faculty.vassar.edu/lowry/VassarStats.html	Website for statistical computation

2.1.7. Primers used for the PCR amplification

Gene of interest		Oligonucleotide sequence
β-Actin	Forward	5'-GTG ACA GCA TTG CTT CTG TG-3'
	Reverse	5'-TCT CAA GTC AGT GTA CAG GC-3'
EF1-α	Forward	5'-CCA GTT ATG TGG CAA GAC GTT-3'
`	Reverse	5'-TCT GGG GAG AAT GGG TAG C-3'
GAPDH	Forward	5'- AAT CCC ATC ACC ATC TTC CAG-3'
	Reverse	5' GCC ATC ACG CCA CAG TTT CC -3'
IL6	Forward	5'- GAG AAG GCT GAG ATA AAA GGA GA -3'
	Reverse	5'- CAT GAT ATA GAC GTT GTG GCT G -3'
IL6R	Forward	5'- GCG ACA AGC CTC CCA GGT TC -3'
	Reverse	5'-GTG CCA CCC AGC CAG CTA TC -3'

m-dio	Forward	5'-GCT CCT TAC AGT GAC TGC AG-3'
	Reverse	5'-TCA ATG GTC ATA TTG CAG CC-3'
m-IVL	Forward	5'-GAA GCA GGT AGG TGT GCA G-3'
	Reverse	5'-GCC CTA CTC AAC CTG AGA G-3'
P53 exon 2/3	Forward	5'-AGG ACC TGA TTT CCT TAC TGC-3'
	Reverse	5'-GAG GTC CCA AGA CTT AGT AC-3'
Pseudo CK 19	Forward	5'-GAA GAT CCG CGA CTG GTA C-3'
	Reverse	5'-TTC ATG CTC AGC TGT GAC TG-3'
CFL15CT24		5'-CCCCCCCCCCCCCCCGTCTAGATTTTTTTTTTTTTTTTTTTTTTVN-3'
CFL15CN8		5'-CCCCCCCCCCCCCCCGTCTAGANNNNNNNN-3'
CP2		5'-TCAGAATTCATGCCCCCCCCCCCCCC-3'
CP2-BGL		5'-TCAGAATTCATGCCGCCCCCCCGGCCC-3'
Lib1		5'-AGTGGGATTCCTGCTGTCAGT-3'
ddMse11		5'-TAACTGACAGddC-3'

2.2. Methods

2.2.1. Methods for *in vitro* cell propagation and characterization

The list of used cell lines is shown in the chapter 2.1.4. The identity of the used cell lines was controlled on a regularly basis by ATCC recommended DNA fingerprinting.

2.2.1.1. *In vitro* cell line propagation under conventional 2D conditions

Cell lines were preserved in liquid nitrogen in appropriate medium containing 5% DMSO. Cell lines were propagated until 70% confluence apart from the cases when the experimental strategy did not imply differently. Cell lines were de-attached using Trypsin/EDTA and re-plated in an appropriate cell density. The medium was changed following the recommendation of the ATCC.

2.2.1.2. *In vitro* cell line propagation under anchorage independent (3D) condition

The aim of 3D cell propagation system is to enrich mammary stem and progenitor cell populations.
Mammary cell lines were propagated in 2D condition until the cells reached the 70% confluence. Propagated cells were de-attached and washed in PBS at least two times. The washing steps were introduced to remove traces of serum used in the 2D cell line propagation culture strategy. Cell lines were propagated in ultra-low attachment plates in cell culture incubator at 37 °C, 5% CO2. The cell lines were propagated at a seeding density of 10 000 cells/ml.

Mammosphere forming ability was assessed 7 days post-plating. During this period, medium was not changed. All cell lines were propagated in the same mammosphere medium, as listed in the chapter 2.1.2.

2.2.1.2.1. Preparation of poly-HEMA plates

The mammary stem and progenitor cells are able to survive anchorage independent conditions while more differentiated progenies are undergoing anoikis. Cells are not able to anchorage to the dish bottom if the dishes are covered by poly-HEMA, an organic substance soluble in ethanol. Poly-HEMA ethanol suspension was applied to the culture dishes 24 h before the cells are plated. On the next day, a fine layer of poly-HEMA covers the culture dish and prevents the cells to adhere. Poly-HEMA (2,4 g) was dissolved in 95% ethanol (20 ml) at 65 ^{0}C. Eight hours later ethanol dissolved poly-HEMA was diluted 10x in 95% ethanol and added to the cell culture dishes at the final concentration of 12 mg/ml. Poly-HEMA coated plates were sterilized by the UV light in prior to cell seeding. The ethanol traces were removed by washing with PBS.

2.2.1.3. *In vitro* differentiation of mammary cells

Cell lines propagated in 3D conditions or the secondary mammospheres obtained from the donor's tissue specimens were used for the *in vitro* differentiation in Matrigel©. Matrigel© is a gelatinous protein mixture secreted by Engelbreth-Holm-Swarm mouse sarcoma cells. This mixture resembles the complex extracellular environment found in many tissues. Different differentiation strategies were tested and as a results Matrigel© "sandwich" strategy was adopted as the most efficient. Cells were propagated in Ham's F-12 medium supplemented with 5% FBS, 5 µg/ml insulin, 1µg/ml hydrocortisone, 10 µg/ml cholera toxin, 10 ng/ml EGF, and 1× Pen/Strep Mix.
Briefly, Matrigel© was diluted 1:1 with differentiation media and placed in a differentiation dish for 15 minutes at 37 ^{0}C. On the top of the stiff gel, the mammary stem and progenitor cells were placed in an incubator at 37 ^{0}C for 30 minutes. The cells were covered with an additional Matrigel© layer and left for additional 15 minutes at 37 ^{0}C. Differentiation medium was added at the end of the embedding procedure. Differentiation medium was changed regularly each fourth day.

Cells propagated in Matrigel© were examined 3-4 weeks post embedding for the development of the complex duct and acinar structures.

2.2.2. *In vitro* cell propagation of the donor's tissue specimens

2.2.2.1. Tissue collective

Mammary tissues were obtained from women undergoing mammary reduction surgeries at Caritas-Krankenhaus St. Josef, Regensburg in collaboration with Dr. Claus Lattrich and Dr. Norbert Heine. Mammary tissues were examined by pathologists at Institut für Pathologie, Universitätsklinikum Regensburg, Regensburg. The tissues showing the signs of breast cancer were excluded from the study and not used for this work (Figure 1).

Eighty seven healthy mammary tissues were received in the period 2007-2012. The median age of the cohort was 27. Due to hormone changes during menopause and proposed hormonal influence in mammary stem and progenitor cells, tissue were selected based on an arbitrary age limit (45 years). However, the samples received from the donors older than 45 were used for the modifications of the mammosphere protocol presented in result section.

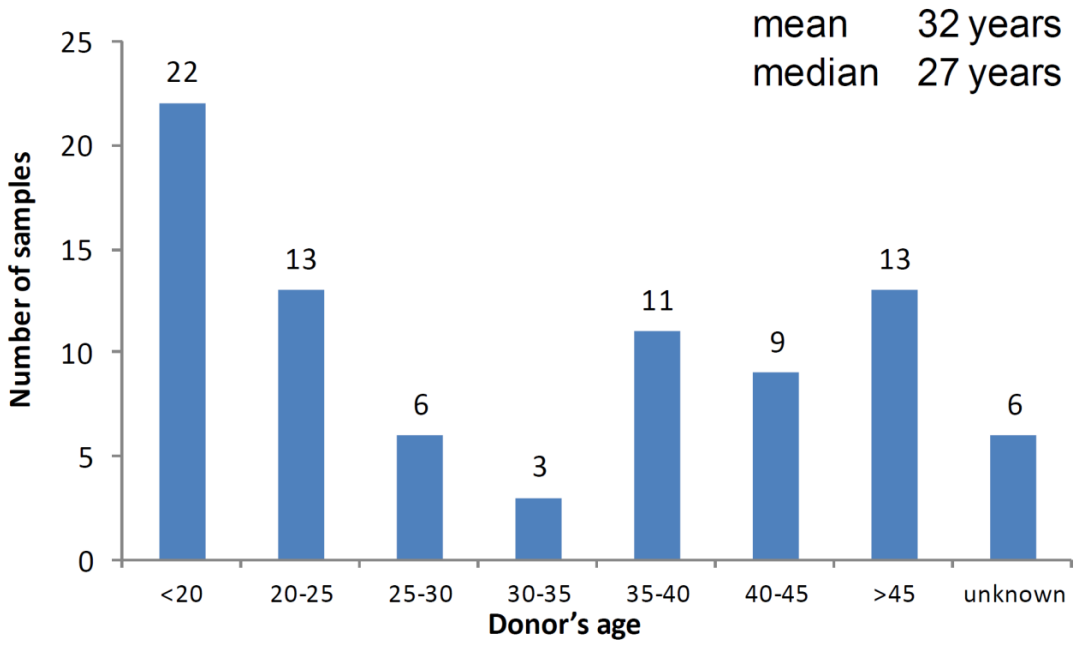

Figure 1. The overview of the mammary tissues received in the period 2007-2012.

2.2.2.2. Mammary tissue digestion and cell isolation

Mammary tissue was minced and dissociated in Ham's F12/Dulbecco's modified Eagle's medium [F12:DMEM; 1:1 (v:v)] supplemented with 10 mM HEPES, 2% bovine serum albumin (BSA; Fraction V), 5 µg/ml insulin, 0.5 µg/ml hydrocortisone, 10 ng/ml cholera toxin, 300 U/ml collagenase and 100 U/ml hyaluronidase at 37°C for 18 h (Figure 2).

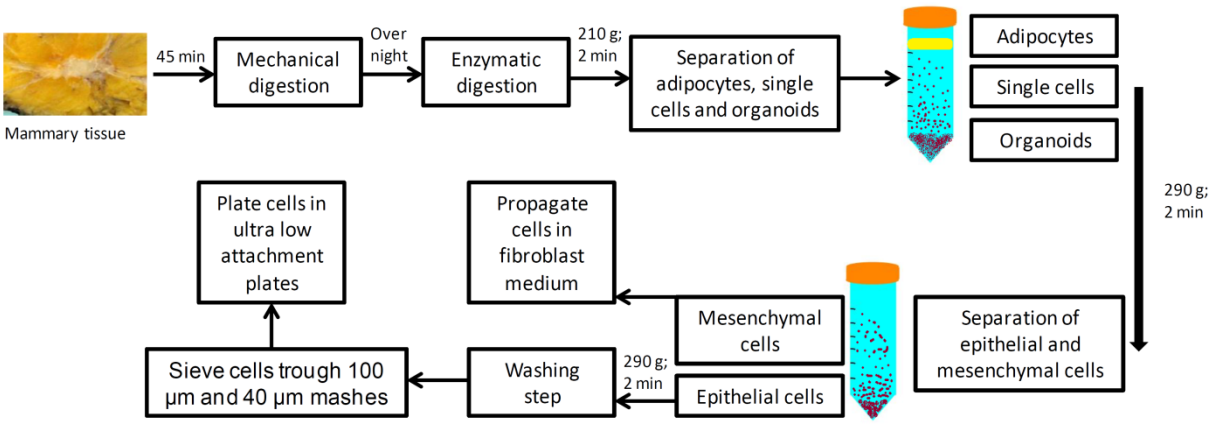

Figure 2. Digestion of the tissue specimen and cell isolation.

At the next day, the digested cell suspension was centrifuged at 210 g for 2 minutes at room temperature. Supernatant from the first centrifugation step contained single mammary epithelial and stromal cells (fibroblasts), while in the pellet were undigested tissue pieces, known as organoids. Single epithelial cells were subjected to an additional centrifugation step (290 g; 2 minutes; room temperature) and the epithelial cells found in pellet were re-suspended in the basal medium, washed and propagated in mammosphere medium in ultra low attachment plates. Mammary gland fibroblasts were obtained by centrifugation of the supernatant (500 g; 5 minutes; room temperature). Fibroblasts were propagated in standard tissue culture flasks in DMEM medium supplemented by 10% fetal bovine serum (FBS).

The organoids obtained in the first centrifugation step were either processed immediately for single cell isolation or preserved by freezing (-80 ºC) in organoid freezing medium (DMEM supplemented with 10% DMSO and 20% FCS).
If obtained number of epithelial cells was not sufficient, organoids would be processed immediately by further digestion steps in DMEM/F12 supplemented with 5 U/ml dispase and 0,25% trypsin. Trypsin was inactivated by trypsin inactivation

solution (TNS) or medium supplemented with serum. Digested organoids were centrifuged (300 g; 3 min at RT) and the epithelial cells found in the pellet were re-suspended in mammosphere medium.

2.2.2.3. Mammosphere protocol

Single cells obtained from digested tissues were plated in ultra-low attachment plates at a density of 20,000 cells/ml. The number of plated cells was later modified according to the results shown in the chapter 3.2.3.
Cells were grown in a serum-free mammary epithelial growth medium (MEBM) supplemented with B27, 20 ng/ml EGF and 20 ng/ml bFGF and 4 µg/ml heparin. Mammospheres were collected by gentle centrifugation (100 g) after 7 days and dissociated enzymatically (10 min in 0.05% trypsin, 0.53 mM EDTA-4Na).
The obtained secondary mammosphere were used for the most of the downstream assays elaborated in this work (Figure 2).

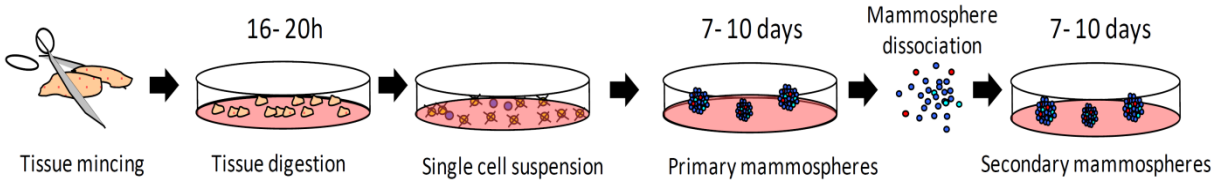

Figure 3. Mammosphere propagation.

2.2.3. *In vivo* human mammary stem and progenitor cells differentiation

In vivo experiments were undertaken in the animal facility of the University Hospital Regensburg. All the experiments considering NOD.Cg-*Prkdc*^{scid} *Il2rg*^{tm1Wjl}/SzJ (NSG) mice were done in accordance with animal application 54-2532.1-15/09 Government of Oberpfalz (54-2532.1-15/09; Antrag auf Genehmigung eines Versuchsvorhabens mit Wirbeltieren; Riegirung der Oberpfalz).

2.2.3.1. *In vivo* human mammary stem and progenitor cells differentiation

In vivo differentiation of the human mammary stem and progenitor cells was based on published protocols (Liu et al., 2006; Proia and Kuperwasser, 2006). Briefly, the experimental strategy consists of the two surgical steps undertaken at week 3 and week 5 of the mouse post-natal (Figure 3). During the first surgical step the 4th mammary glands of 3-4 weeks old NSG mice were pre-cleared of endogenous mammary epithelial tissue and humanized. Mouse mammary gland humanization was undertaken by injecting human immortalized fibroblasts in mammary fat-pad. Two weeks after the first surgical step the mixture of human secondary mammospheres and fibroblasts of the matched tissue specimen were inoculated into humanized fat-pad. Mice were analyzed 8 weeks post cell inoculation.

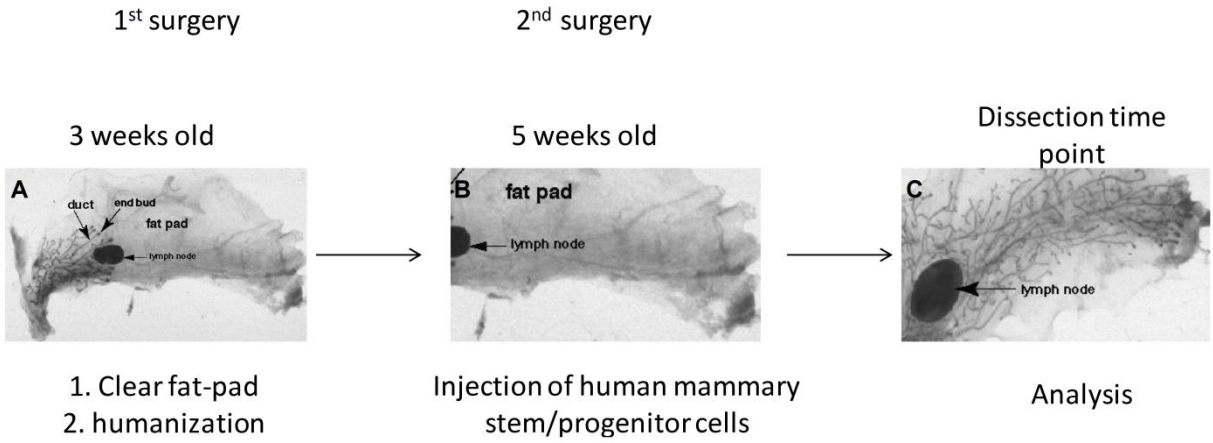

Figure 4. *In vivo* differentiation of the human mammary stem and progenitor cells in NSG mice. (A) The mammary fat-pad of the 3 weeks old females were cleared of endogenous mouse epithelia and humanized by the injection of the human immortalized fibroblasts; (B) Two weeks later, human mammary stem and progenitor cells co-mixed with the fibroblasts of the matched tissue sample were injected into humanized fat-pad; (C) Dissection and analysis of the engraftment and differentiation of the human mammary stem and progenitor cells in NSG mice.

2.2.3.1.1. Preparation of human immortalized fibroblasts used for xenotransplantation procedure and injection of human mammary stem and progenitor cells

Human, h-TERT immortalized, fibroblasts were a kind gift of Professor Dr. Robert A. Weinberg (MIT Ludwig Center for Molecular Oncology, USA). Fibroblasts were propagated in DMEM media supplemented with 10% FCS and L-glutamine. The cells were passaged 3 times per week taking into account that cell growth confluence of 100% should not be reached.

Before the injection of h-TERT immortalized fibroblasts was undertaken, fibroblasts were de-attached and counted. Humanization of the mouse mammary fat-pad was performed by inoculation of a half of million cells in a pre-cleared mammary fat pad. Of these, 250 000 cells were washed, irradiated (4 Gy) and subsequently mixed with 250 000 non-irradiated cell. Fibroblasts were injected into a pre-cleared 4th mouse mammary fat-pad ensuring the point of injection is not too deep and thus does not pressure any leakage. Formation of a bubble in the mammary fat pad was taken as a proof of a suitable inoculation.

Two weeks after humanization, 200 000 cells obtained from the propagation of the secondary mammospheres and 500 000 fibroblasts of the same tissue specimens were co-mixed 1:1 (v/v) with Matrigel© and injected into the humanized fat-pad of NSG mouse. Eight weeks post inoculation mouse mammary fat-pad was analyzed.

2.2.3.1.2. Preparation of C3H10T1/2 fibroblasts for orthotopic xenotransplantation

C3H10T1/2 mouse immortalized fibroblasts are derived from mouse embryonic fibroblasts obtained from C3H mouse strain. Fibroblasts were kind gift of Dr. John Stingl (Cancer Research UK, Cambridge Research Institute, Li Ka Shing Centre, Cambridge, UK). Fibroblasts were propagated in DMEM media supplemented with 5% FCS and L-glutamine as previously described (Eirew et al., 2008). On the surgery day, 225 000 fibroblasts were detached, washed and irradiated by 15 Gy. Irradiated

fibroblasts and 200 000 mammosphere cells were commixed, centrifuged at 500 g for 5 min and re-suspended in 40 µl of 1:1 mixture of differentiation medium and Matrigel©. Cells were kept on ice until the surgery.

2.2.3.2. Orthotopic xenotransplantation

Three to four weeks old NSG female mice were used as recipient animals for the *in vivo* differentiation experiments. The limiting factors for the recipient selection were the weight (8 - 12 g) and age (3 - 4 weeks old). Despite the challenges working with pre-pubertal mice due to their size, the utilization of older mice was omitted due to the risk of incomplete clearance of the endogenous mammary epithelia. On the other hand, the radical surgical steps were lethal for the mice younger than 3 weeks or lighter than 8 g.

Two different types of anesthetic solutions were compared.

The composition of the first anesthetic solution:

Volume	Drug (concentration)	Active substance	Dose
0.5 ml	Ketavet (100 mg/ml)	Phecyclidine/ketamine	200 mg/kg
0.25 ml	Rompun (20 mg/ml)	Xylazine	10 mg/kg
5 ml	PBS		
13 ml			

The amount of the injected anesthetic solution depended on the mouse weight. In general, the recommended dosage of the prepared solution is 10 µl/g. However, the administration of the described anesthetic solution caused the death of 20% of used mice. Because of this drawback alternative anesthetic solution was tested and later on used in experimental procedure.

The composition of the second anesthetic solution:

Volume	Drug (concentration)	Active substance	Dose
10 ml	Dormicum (1mg/ml)	Midazolam	**5 mg/kg**
2 ml	Fentanyl (0,05mg/ml)		**0,05 mg/kg**
1 ml	Domitor (1mg/ml)	Medetomidin	**0,5 mg/kg**
13 ml			

The amount of the injected anesthetic depended on the mouse weight. In general, 100 µl of the solution was administrated intra-peritoneally to mice weighting 8-12 g. The anesthetized animals were awakened by the administration of the 50 µl of the antagonist solution:

Volume	Drug (concentration)	Active substance	Doses
5 ml	Anexate (0,1mg/ml)	Flumazenil	0,5 mg/kg
0,5 ml	Antisedan (5 mg/ml)	Atipamezol	2,5 mg/kg
3 ml	Narcanti (0,4 mg/ml)	Naloxon	1,2 mg/kg
8,5 ml			

Mice were anesthetized by intra-peritoneal injection of described solutions and closely monitored during the sleep due to the possible complications. Once the mouse was anesthetized, the fur around the incision area was shaved and sterilized in order to prevent the recipient mouse of any post surgical infection. The body temperature was adjusted to prevent possible hypothermia. The skin of anesthetized mouse was then cut in a half "Y" intersection. With gentle moves the fourth mammary gland was released of peritoneum. Large vessels in the area of surgery were destroyed with an electric cauterizer to prevent accidental injury of the blood vessels. The cell mixture was injected into clean adipose tissue of the recipient mouse in a volume not higher than 40 µl. Finally, the wound was sued and mice were awakened by intra- peritoneal administration of “antagonist” solution.

2.2.3.3. *In vivo* breast cancer mouse model

MDA-MB-231-GFP (231-GFP cells line) and MDA-MB-231 1833-GFP (1833-GFP) cell lines were used either to (i) address the role of the IL6 signaling in the breast cancer and (ii) establish the *in vivo* mammary stem and progenitor cell differentiation protocol. The cell lines were propagated by already described strategies in chapter 2.2.2.1 and 2.2.2.2. The cell lines were injected into a pre-cleared mammary fat-pad of NSG mice. The first palpable tumors in either cancer cell lines, 231-GFP and 1833-GFP, formed 20 days post inoculation. Mice were analyzed and dissected when the size of the primary tumor reached 10 mm in the diameter.

2.2.3.4. Mice dissection

Mice were sacrificed by cervical dislocation. The organs of interest were either embedded in paraffin or snap frozen (-80 ºC). The following organs were preserved for the later immunohistochemical analysis: 1) mammary glands, 2) tumors, 3) lungs, 4) liver and 5) spleen. The bone marrow was prepared by the protocol described in the chapter 2.2.3.4.2

2.2.3.4.1. Paraffin embedding of mice tissue samples

The dissected tissue samples were fixed in a 4% paraformaldehyde (PFA) solution for 12 h. Following fixation, the samples were washed 3 times in PBS. The major obstacle during the tissue sectioning represents residual water in the embedded tissue. Therefore, dehydration of the paraffin embedded samples was achieved by series of washing steps in alcohol (70%, 85% and 100% ethanol, each step 1 hour). Then the fixed and dehydrated tissue was washed twice for 30 min in 100% xylene. This step serves not only the removal of alcohol from the tissue, but also facilitates the penetration of the paraffin during the subsequent embedding. After three incubation steps with paraffin (parablast embedding media), tissues were embedded. Paraffin embedded tissue is stored at room temperature.

2.2.3.4.2. Preparation of the bone marrow

Tibiae and femora of experimental mice were unconstrained of skin and muscles. The distal parts of the bones were cut in order to make space for 26G canula to enter and flush the bone marrow. The bone marrow was flushed by PBS and washed with up to 10 ml Hank's salt solution. Next, bone marrow was centrifuged at 170 g for 10 min to remove impurities such as fat, muscles cells and platelets. Supernatants were removed and the cells were re-suspended in 7 ml of PBS. Re-suspended cells were subjected to the gradient centrifugation (65% percoll solution). The aim of the gradient centrifugation was to enrich bone marrow cell suspension for the mononuclear cells.

Cell suspension was carefully layered on top of the 7 ml 65% percoll solution and centrifuged (10 min, 1000 g). Mononuclear cells in the density gradient remain in the inter-phase. Inter-phase was cleaned of percoll by PBS and then subjected to centrifugation at 500 g for 10 min. Precipitated cells were re- suspended in 2 ml of PBS. Cells were counted and placed on adhesion slides (250 000 cells per field). Adhesion slides were dried overnight and then stored at -20 °C.

2.2.3.4.3. Paraffin tissue sectioning, H&E staining and micro-dissection

Hematoxylin and eosin (H&E) staining was performed in paraffin embedded samples Paraffin blocks containing embedded tissue were sectioned in a 5 µm thick slices using a microtome. Slides used for laser micro-dissection contained polyethylene membrane (1, 35 µm) while slides used for immunohistochemical staining were conventional glass slides. After sectioning slides were dried in the oven for 45 min at 65 ºC. Paraffin sections were then de-paraffinized twice for 10 min in 100% xylene and subsequent series of ethanol steps were applied (2 min 100%, 90%, 70% ethanol), samples were then rehydrated with bi-distilled water and ready for staining. Hematoxylin staining was performed by applying Mayer's hematoxylin (0.1%) for 2-3 min while the staining of the cytoplasm was carried out with acidified eosin (0.1%) for 2 min. The slides were washed in ethanol (1 min in 70%, 90% and 100% ethanol) and later in xylene (10 min, 100% xylene). At the end of the procedure, slides were

mounted with Eukitt and preserved at room temperature. Slides used for the laser micro-dissection were not stained with eosin because the samples were later used for the primary PCR strategy. Eosin shows inhibitory effect on the primary PCR.

Examination of stained material was carried out by Dr. med. Fabian Eder from Institute for Pathology, University Hospital Regensburg, Regensburg.

2.2.4. Generation of GFP labeled cells lines by lentiviral vector-mediated gene transfer

Cancer cells lines expressing green fluorescent protein (GFP) were established for the purpose of the easier detection of the disseminated cancer cells in distant organs.

Lentiviral gene transfer is an efficient methodology for the establishment of the genetically modified organisms. Lentivirus containing GFP were constructed and later target cell lines over-expressing GFP were established.

2.2.4.1. Construction of the lentiviral particles- Transfection of the HEK-293T cells

HEK-293T cells (293T cells) are derived from the human embryonic kidney. The 293T cells are frequently used as lentiviral producer cells due to their high transfection ability.

The 293T cells were propagated in DMEM media supplemented with 10% FCS and l-glutamine. The transfection ability of the 293T cells depends on the culture conditions. Therefore, cells were never allowed to reach 100% confluence before the transfection. Ten million cells were seeded in a 10 cm cell culture dishes 15h before the transfection. Transfection was performed once the cells reached 70% confluence. Transfection medium (DMEM; 10% FCS) containing 25 µM chloroquine was added 45 min before the start of transfection. Chloroquine's function is to block plasmids degradation in the endosome/lysosome system which increases transfection rate (Ciftci and Levy, 2001; Erbacher et al., 1996). Half an hour to two hours after chloroquine addition the medium was replaced by transfection mixture.

The composition of the transfection mixture was:

5 µg pMD2G (envelope plasmid),
20 µg psPAX2 (packaging plasmid),
20 µg lentiviral plasmid (containing the target genes),
add water up to 250 µl,
add 250 µl of 0.25 M CaCl2 solution.

This mixture was diluted into 2x HEBS buffer. The transfection mixture was added drop wise to HEK-293T cells. The medium was replaced 6h after the transfection mixture was added. The addition of the transfection mixture is taken as the start point of the S2 work. Therefore, all work was performed according to the safety recommendation prescribed for the S2 work. The lentiviral particles containing GFP were collected 48h and 72h post transfection. Lentiviral particles were stored at -80ºC.

2.2.4.2. Determination of virus titer

Virus titer represents the number of the virus particles in 1 ml. Determination of the virus titer was performed using 231-GFP or 1833-GFP cell lines. Cells were propagated in a 12-well plate. The cells (4×10^4 cells/well) were plated and propagated overnight at 37 °C. On the next day, medium was removed, cells were washed and virus diluted in 1:10, 1:100, 1:1000, 1:10000 as well as undiluted virus were added to the cells. GFP fluorescent cells were noticeable 24h post infection.

Titer of the produced virus was determined by measuring the number of the GFP positive cells in a given population by the following equation:

Titer = percent of GFP-positive cells * number of seeded cells / infection volume

2.2.4.3. The selective propagation of the transduced cells

Lentiviral vector used for the stabile integration and expression of the GFP contain a gene for the puromycin resistance. Therefore, transduced cell have stabile integrated and expressed gene for puromycin resistance. Treatment of transduced cell with puromycin depletes uninfected cells. To determine puromycin concentration, 50 000

non-transduced target cells were seeded in a 24-well plate. Day after seeding the growth media was supplemented with in grading puromycin concentration ranging from 0-20 µg/ml. The cells were propagated 4 days and the optimal concentration required for the selection of transduced cell population was determined as a minimal concentration in which 100% of un-transduced cells are dead after 4 days.

2.2.5. Gene specific PCR

The assessment of the transcription of gene of interest, verification of the epithelial origin of the *in vivo* engrafted epithelial structures and assessment of the cDNA libraries was performed by PCR.

PCR reaction was prepared following Table 8.

Volume	Reagent
7,15 µl	Ultra pure DEPC- water
1 µl	PCR buffer + dNTP
0,5 µl	Forward oligonucleotide (8 µM concentration)
0,5 µl	Reverse oligonucleotide (8 µM concentration)
0,25 µl	BSA
0,1 µl	Taq DNA-polymerase
0,5 µl	DNA

Table 8. PCR reaction mixture.

The standard program for gene specific PCR is listed in Table 9.

	Temperature	Time
1.	94 ºC	2:00 min
2.	58 ºC	0:30 min
3.	72 ºC	2:00 min
4.	94 ºC	0:15 min
5.	58 ºC	0:30 min
6.	72 ºC	0:20 min
7.	Repeat steps from step 4 to 6 (14 times)	
8.	94 ºC	0:15 min
9.	58 ºC	0:30 min
10.	72 ºC	0:20 min
11.	Repeat steps from step 8 to 10 (24 times)	
12.	72 ºC	2:00 min
13.	4 ºC	∞

Table 9. Program used for the PCR reaction.

Result of PCR was visualized with agarose gel electrophoresis using ethidium-bromide.

2.2.5.1. Agarose gel electrophoresis

Amplified products of the specific PCR were separated with gel electrophoresis,1.5% agarose concentration in TBE buffer with addition of ethidium-bromide (0,5 µg/ml). Samples were mixed with a loading dye and loaded in the gel. PCR amplicons were separated at 160 V for 45 min.

2.2.5.2. Total mRNA reverse transcription and cDNA amplification from single or few cells

Total mRNA reverse transcription and cDNA amplification from single or few cells was performed as described elsewhere (Hartmann and Klein, 2006).

2.2.6. Unspecific labeling of cell membrane- PKH26 staining

The unspecific labeling of the cellular membrane by PKH26 dye was used for the detection and isolation of the single mammary stem and progenitor cells.

PKH26 dye labels phospholipids in the cell membrane. During each cell division membrane is divided between daughter cells. Therefore, fluorescent dye is diluted by half after each cell division. Optimal dye concentration depends on proliferative rate of cell type; if a cell is over-saturated by PKH26 daughter cells despite the cell divisions would be fluorescent. Therefore, determination of the optimal concentration is a crucial step in the protocol. Staining of the 107 cells at final concentrations of 2 X 10^{-6} M PKH26 dye was performed by the following protocol:
Cells were washed using medium without serum and then centrifuged at 400 g for 5 min. Pellet was re-suspend in 1 ml of diluent C by pipetting to ensure complete dispersion. Prior to staining, 4 X 10^{-7} M PKH26 dye was prepared using diluent C. Cells were added rapidly to 1 ml of dye and mixed. Rapid and homogeneous mixing is a critical point for the uniform labeling. Cells were incubated at 25 °C for 5 min. Staining reaction was stopped by adding an equal volume of serum or compatible protein solution (i.e., 1% BSA). Cells were washed with an equal volume of serum-free medium or PBS and centrifuged at 400 g for 10 min at 25 °C to remove cells from staining solution. Centrifugation step was repeated at least 3 times in order to clean cells of ethanol traces and diluent C. Cells were examined using fluorescence microscopy. Staining should be uniform and is typically 100 - 1 000 times brighter than background auto-fluorescence.

2.2.7. Quantification of Interleukin 6 and soluble Interleukin 6 receptor

Interleukin 6 (IL6) and soluble Interleukin 6 receptor (sIL6R) expression were quantified in growth media of used cell lines or media of patient tissue culture.

Measurements of human IL6 production was performed by "Human IL-6 DuoSet" elisa kit following manufactures protocol (R&D Systems).
Human sIL6R production was measured by "Human sIL-6R alpha DuoSet" elisa kit following manufactures protocol (R&D Systems).

Briefly, after cells were propagated under experimentally required conditions growth media was collected and 100 µl of supernatant were applied on 96-well plates prepare by provided manufacturer protocols. Final results were obtained by using micro-plate reader set at 450 nm. Positive and negative controls were used. Moreover, for both proteins 7 points standard curves were used for obtaining the final results.

2.2.8. Flow cytometry

The analysis of membrane-bound IL6R was performed in collaboration with Dr. Melanie Werner-Klein. The expression of membrane bound IL6R was assessed by flow cytometry by using LSR II flow cytometer (BD Biosciences). Briefly, cells propagated under anchorage independent conditions or under standard conditions were blocked with 10% AB-serum and incubated with anti-IL6R antibodies. Obtained results were analyzed with FACS Diva 6.1.1 and FlowJo 8.6.6 software.

3. Results

3.1. Overview of the research rationale

To study the effect of IL6 signaling in mammary gland several aspects had to be addressed. First, novel approaches and methodological strategies had to be developed, while some of the published methods had to be adapted. These issues are elaborated in the chapter 2 of the Result Section.
Once the modified approaches and novel methods were developed, the mechanism and phenotypic consequences of the IL6 signaling in mammary cells had to be identified. The obtained results indicated a role of IL6 signaling in normal mammary stem and progenitor what enabled me to address the impact of IL6 signaling in cancer stem cells (Figure 1).

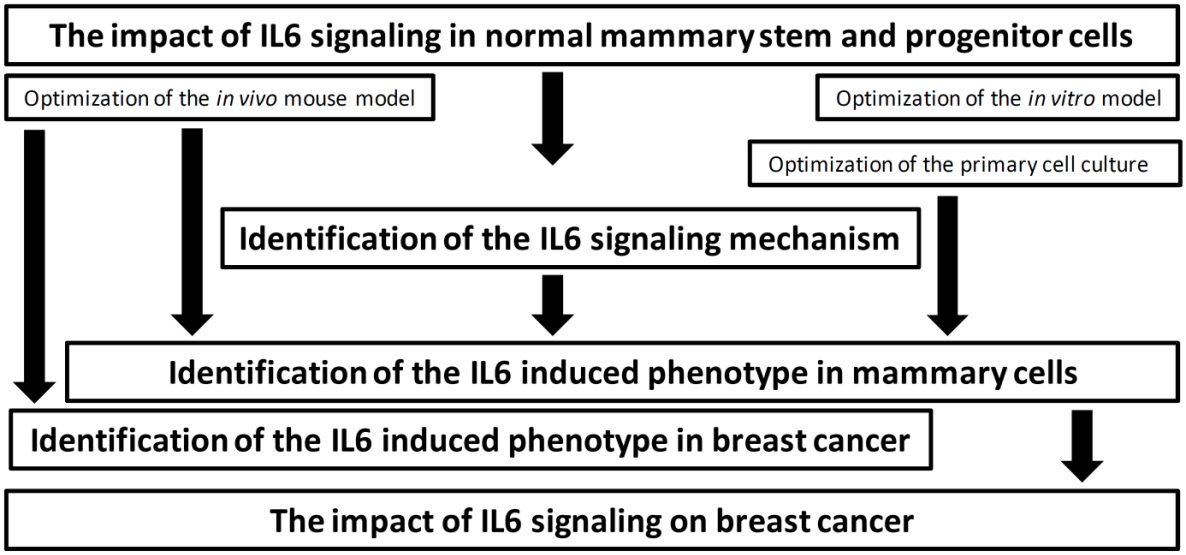

Figure 1. The rationale of the PhD work.

3.2. Development and modification of the protocols used for the study of IL6 signaling influence in the mammary gland

The work on normal adult mammary stem and progenitor cells is challenging due to: 1) the low absolute and relative number of adult mammary stem cells; 2) difficulties in maintaining and propagating adult stem and progenitor cells for longer time period *in vitro* and 3) technical obstacles, such as low efficiency of protocols used for isolation

and propagation of adult mammary stem and progenitor cells *in vitro* and low efficiency of protocol used for *in vivo* mammosphere differentiation in immunodeficient mice.

Isolation of mammary stem and progenitor cells is highly relevant because it determines the number of cells which can be used for the downstream assays. Therefore, the first aim was to increase the efficiency of the mammary stem and progenitor cell isolation and propagation.

3.2.1. Improvement of the cell isolation protocol

The aim of the mammosphere assay is propagation of normal human mammary stem and progenitor cells. Isolation of the single mammary epithelial cells was achieved by digestion of donor's tissue specimens. The mammary tissues of patients undergoing mammary reduction-plasty were first examined by a pathologist. Samples containing potential cancerous lesions were excluded from downstream approaches. Tissue examination was performed in semi-sterile conditions resulting in contamination of 3 out of 87 samples. Isolation of single cells from the mammary specimens was achieved by mechanic and enzymatic digestion, while subsequent isolation of epithelial cells was accomplished by differential centrifugation steps.

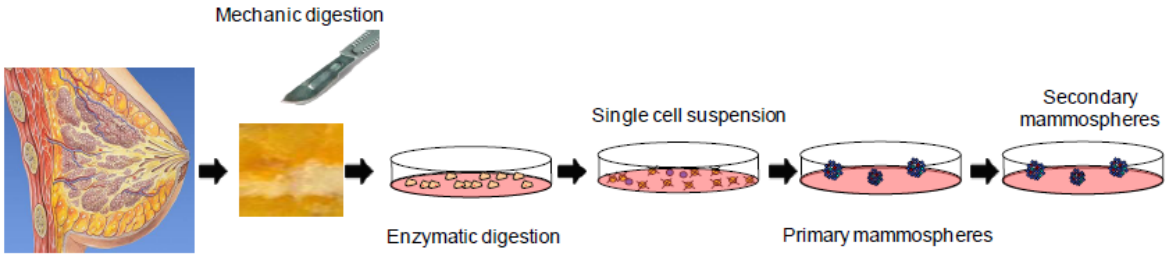

Figure 2. Isolation and growth culture of the normal mammary stem and progenitor cells. Mammosphere protocol. Growth of enriched stem and progenitor cell population is enabled by propagation of cells under anchorage independent conditions. While differentiated cells are not able to survive anoikis, mammary stem and progenitor cells form spherical colonies, named as mammospheres.

The centrifugation steps of the cell isolation protocol were identified as import determinants of overall efficiency of the method. Application of lower centrifugation speeds in shorter time can reduce the number of obtained cells. Therefore, the

influence of the centrifugation time and speed during cell isolation on the overall number of obtained secondary mammospheres was tested. Separation of epithelial and mesenchymal cells was achieved by 290 g centrifugation for 2 minutes at room temperature. To test whether higher g- forces increase epithelial cells recovery, centrifugation conditions were modified to 350 g for 4 minutes (Figure 3).

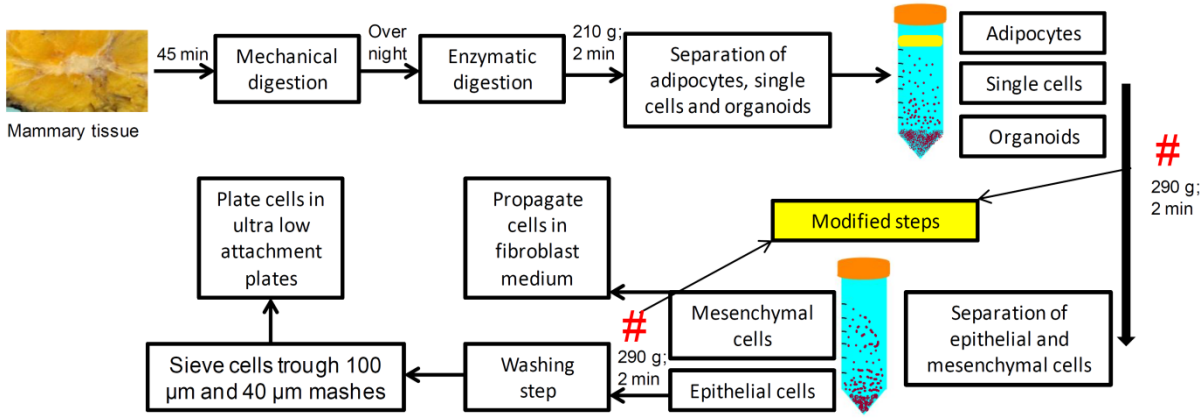

Figure 3. Isolation of single cells from mammary tissue. Mammary tissue was mechanically and enzymatically digested. Epithelial and mesenchymal cells were isolated by application of multiple centrifugation steps. Modified steps are indicated by #.

The second centrifugation step during cell isolation has the aim to separate epithelial and mesenchymal cells (Figure 3). The increased centrifugation speed and time resulted in an increase of number of pelleted cells (Figure 4 a). These cells were tested for their ability to form secondary mammospheres. It was found that increased centrifugation parameters resulted in increased numbers of isolated cells with the mammosphere forming ability (Figure 4 c).

On the other hand, increased centrifugation parameters resulted in considerably less cells isolated from the supernatant (Figure 4 b). Cells found in supernatant were later used for *in vivo* mammosphere differentiation and thus the number of obtained cells is a relevant parameter. However, propagation of supernatant-derived cells resulted in slightly reduced numbers of cells after 7 days of propagation under anchorage dependant conditions when centrifuged at 350 g for 4 min as compared to 290 g for 2 minutes. *In vitro* propagated cells obtained from both centrifugation conditions were reaching confluence in a short time. Therefore, decreased number of

isolated mesenchymal cells due to increased centrifugation conditions had no consequences for later experiments (Figure 4.d). Subsequently, the following step, the washing centrifugation step, was adjusted to the modified parameters (350 g; 4 minutes; RT instead of 290 g; 2 minutes; RT).

Optimization of the cell isolation protocol from mammary gland specimens resulted in a 2 fold increase of cultivated secondary mammospheres (Figure 4 c).

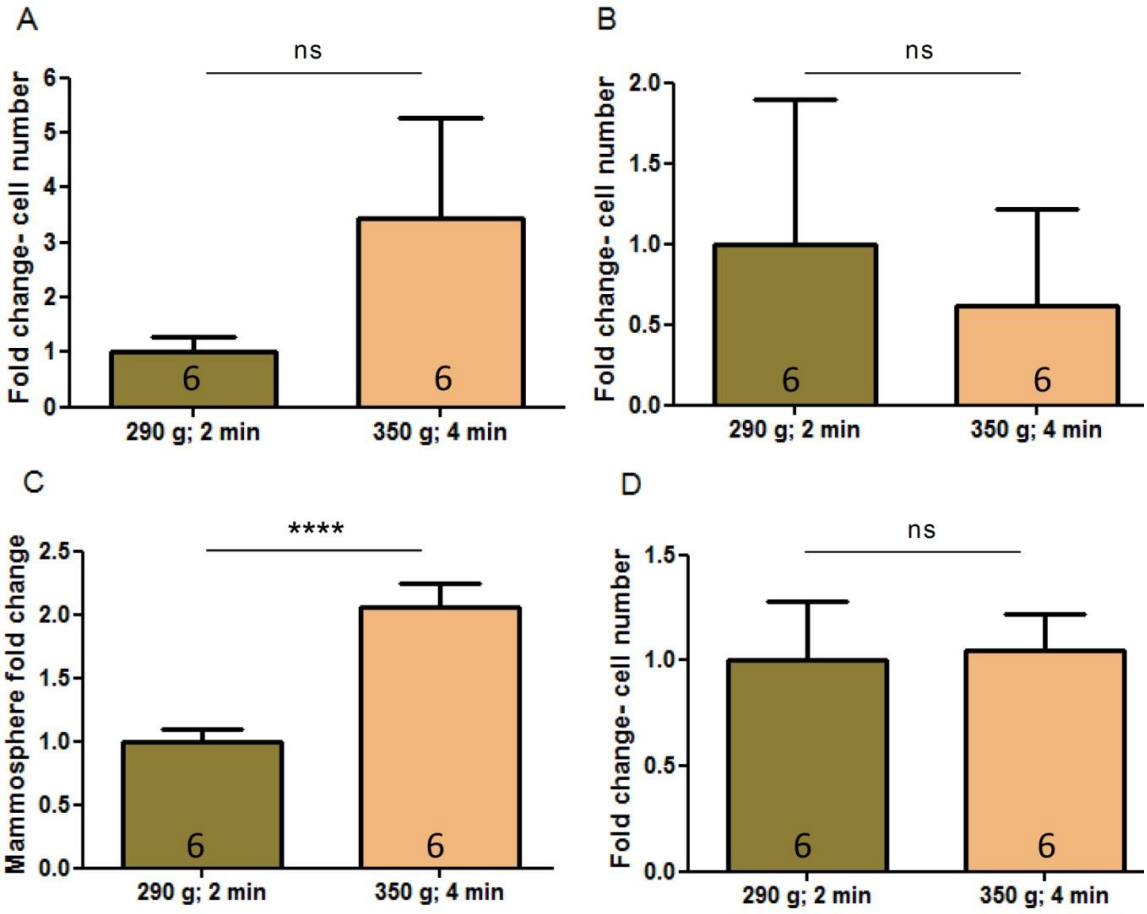

Figure 4. Modification of the cell isolation protocol. Increased numbers of mammosphere forming cells were achieved by modification of the centrifugation parameters. (A) Increased centrifugation speed and time resulted in the sedimentation of higher cell numbers ($p = 0.08$, two- tailed unpaired t-test); (B) Due to the higher centrifugation speed for prolonged time, the number of the cells isolated from the supernatant was reduced ($p = 0.57$, two- tailed unpaired t-test); (C) The increased number of the pelleted cells resulted in overall higher number of the propagated secondary mammospheres ($p < 0.0001$, two- tailed unpaired t-test); (D) Reduced number of plated cells from supernatant did not influence fibroblast propagation ($p = 0.82$, two- tailed unpaired t-test). After 7 days equal numbers of fibroblast were counted in both conditions. Results were obtained using 3 different donor's tissue specimens (n=3). Experiments were performed in technical duplicates.

The higher number of isolated and plated cells might cause the problem during the mammosphere outgrowth due to higher cells densities. Increased number of isolated epithelial cells raised the question about the most effective cell density for the mammosphere propagation. Therefore, the optimization of the mammosphere protocol was performed.

3.2.2. Improvement of the mammosphere culture protocol

The numbers of plated epithelial cells isolated from mammary tissue range from 10 000 cells/ml to 100 000 cells/ml in various published protocols.

The aim of this experiment was therefore to define the optimal number of seeded cells for obtaining maximal mammosphere counts in the second and higher passages. Two limiting factors were considered to determine the range of cell density values: (1) Higher cell density may induce mammosphere fusion while (2) lower density can reduce paracrine cell stimulation. Therefore, 3 different cell densities were tested: 10 000 cells/ml, 50 000 cells/ml and 200 000 cells/ml. Mammospheres obtained after propagation of the cells isolated from the tissue specimen were counted, dissociated and further propagated in ultra-low attachment plates. Seven days after the first passage, mammospheres were again counted, dissociated and re-plated. This cycling procedure was repeated up to 6 times in case of the highest density; while in the case of 10 000 seeded cells per ml mammospheres were maintained up to 4 passages (Figure 5).
Mammospheres grown in different cell densities showed differences in the size and number. Mammospheres grown in 200 000 cells/ml condition were the largest in size and showed increased fusion level (Figure 5). As a result, the final number of mammosphere forming cells in this condition might be under-estimated. Mammospheres were found for up to 6 passages upon tissue dissociation in the condition 200 000 cells/ml. However, in the condition 10 000 cells/ml mammospheres were detected for up to 4 passages (Figure 5 a).

In the first week, percentages of mammosphere forming cells (MFC) were similar for different conditions while in the second week overall percentages of MFC were significantly increased compared to the first week (Figure 5 b). Such an effect is

mainly because cells plated in the second week had been already selected for the anoikis survival. In later passages the percentage of MFC was rapidly decreased. The strongest reduction was observed in case of 10000 cells/ml propagated cells.

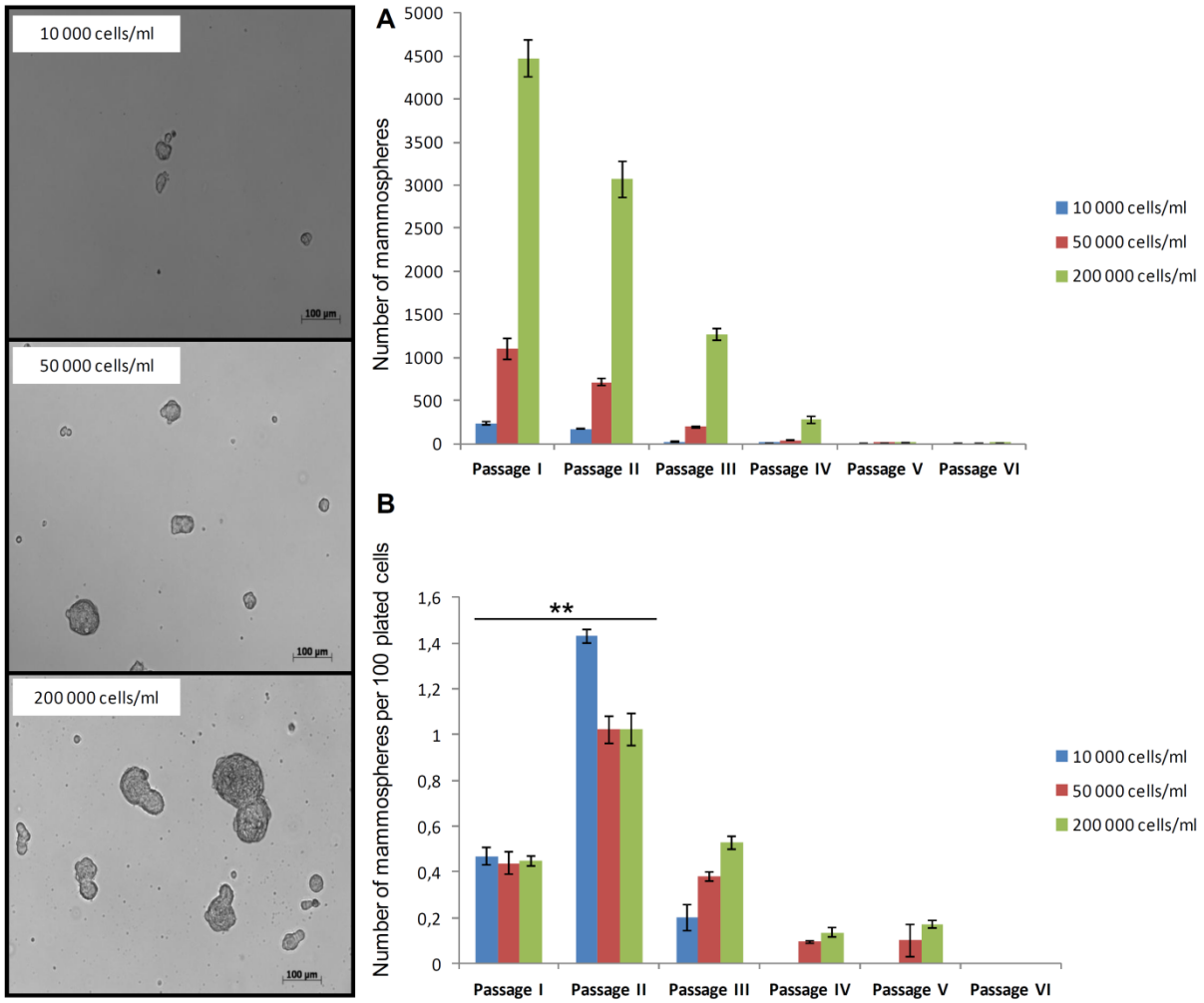

Figure 5. Influence of the cell density on mammosphere outgrowth and propagation. (A) Cell density had no influence on mammosphere outgrowth. Ratios between differential seeded cell numbers were retained for secondary mammospheres. The highest seeding density gave possibility to maintain mammospheres for longer period (up to 6 passages); (B) Frequency of the mammosphere forming cells in population of seeded cells. The cells obtained from the secondary mammospheres showed the highest relative number of mammosphere forming cells ($p<0.01$, two- tailed unpaired t-test). Results were confirmed using 2 additional donor's tissue specimens (n=3). Representative results are shown. Experiments were performed in technical duplicates.

If the seeding density does not influence mammosphere propagation then the numbers of obtained mammospheres in higher densities (50000 cells/ml and 200000 cells/ml) would be in accordance to the number of mammospheres obtained under

10000 cells/ml condition multiplied by seeding factor.
Influence of the seeding density on mammosphere propagation was measured by setting the numbers of mammospheres counted in the 10000 cells/ml conditions as a reference for mathematical prediction. The number of counted mammospheres in 10000 cells/ml conditions was amplified 5 or 20 times to get the predicted numbers of secondary mammospheres in 50000 cells/ml or 200000 cells/ml conditions, respectively (Figure 6). Experimental and predicted data were comparable during the first 3 passages.

Mathematical prediction	10 000 cells/ml	50 000 cells/ml	200 000 cells/ml
Passage I	234,5	1172,5	4690
Passage II	171,5	857,5	3430
Passage III	20	100	400
Passage IV	1	5	20
Passage V	0	0	0
Passage VI	0	0	0

Experimental data	10 000 cells/ml	50 000 cells/ml	200 000 cells/ml
Passage I	234,5	1098,5	4473,5
Passage II	171,5	714,5	3066,5
Passage III	20	190	1266
Passage IV	1	37,5	273
Passage V	0	2	51,5
Passage VI	0	0	0,5

Figure 6. Experimentally observed mammosphere numbers and mathematical prediction of the mammosphere numbers. Mathematical prediction was done by amplifying the numbers of mammospheres obtained at 10 000 cells/ml 5 or 20 times for seeding densities 50 000 cell/ml or 200 000 cells/ml, respectively. Comparison showed no influence of a seeding number on mammosphere outgrowth and propagation. Experiment was performed with 3 different tissue specimens confirming presented results (n=3). Each experiment was performed in technical duplicates.

Altogether, outgrowth and propagation of epithelial cells isolated from mammary tissue in the density of 200000 cells/ml gives the optimal conditions for outgrowth of sufficient number of the secondary mammospheres.

3.2.3. Establishment of *in vitro* differentiation on a panel of HME cell lines- *In vitro* differentiation of the selected mammary cell lines

Characteristic of stem and progenitor cells is the ability to differentiate down in several lineages to form all of the cell types that are found in the mature tissue. Thereby, *in vitro* differentiation is frequently used to assess differentiation ability of tested cells.

The adult human mammary gland is organized in a complex network of 3D duct and alveolar structures. The mammosphere propagation in the 3D matrices (i.e. collagen,

Matrigel©) promotes development of structures similar to those of the adult human mammary gland. The aim of the following experiment was to compare different Matrigel© differentiation strategies for reaching the best conditions for differentiation of the secondary mammospheres. Comparison of different strategies was performed by testing differentiation ability of different HME cell lines (Figure 7).
The panel of HME isogenic cell lines showed differential morphological structures upon differentiation in Matrigel© by using two different embedding approaches: "3D on top" assay and "sandwich" model. The differentiation ability was analyzed by the ability of cells to form branching and acinar structures when embedded in Matrigel©. Differentiation ability of cells embedded following the recommendations of "3D on top" assay could not be analyzed due to the cell death shortly after cells embedding. However, the HME cell lines showed high proliferative and differentiation abilities upon embedding following recommendation given for the "Sandwich" model.
HME cell line containing BRAF mutation failed to survive in extracellular matrix. HME EGFR and HME wt cell lines differentiated in mass-like structures after 3-4 weeks in Matrigel©. Observed mass-like structures resulted from proliferation of single cells indicating high proliferative ability of HME EGFR cell line. HME PIK3CA cell line had a grape-like morphology, while HME cell line down-regulated for PTEN grown in branching structures similar to duct morphology of functional breast tissue (Figure 7). Duct morphology of HME PIK3CA cell line is similar to the ducts observed in adult mammary gland.

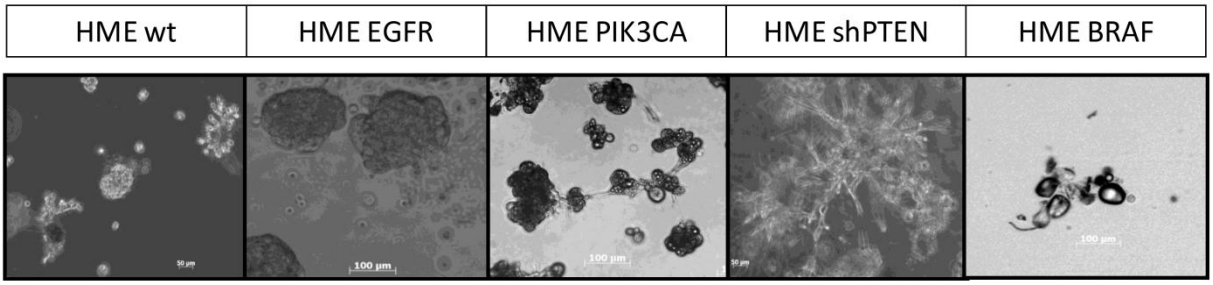

Figure 7. Differentiation of HME cell lines in 3D reconstituted extracellular matrix. HME cell lines, containing oncogene mutation, showed different morphologies. HME wt and HME EGFR cell lines have mass like wile HME PIK3CA cell line have grape-like morphological differentiation pattern. HME shPTEN showed stellate type of differentiation. HME BRAF failed to survive in Matrigel©. "Sandwich" Matrigel© embedding was applied for the *in vitro* differentiation.
Experiments were repeated 3 times with cells of 3 different passages (n=3). Each experiment was performed in technical duplicates.

Altogether, modified "sandwich" embedding Matrigel© differentiation approach was applied for the purpose of this work. The modification of the "sandwich" model concerned the dilution of Matrigel©. Matrigel© was diluted in prior to use 1:1 in differentiation medium and in this way the overall cost of the experiment was reduced while the high differentiation ability of the analyzed cells was achieved.

3.2.4. *In vivo* engraftment and propagation of the human mammary cells

The *in vivo* differentiation ability of human adult stem and progenitor cells is usually analyzed by xenograft models which utilize immune-deficient mice, such as NOD.Cg-Prkdc^{scid} Il2rg^{tm1Wjl}/SzJ (NSG) mice.

3.2.4.1. *In vivo* engraftment and growth of human mammospheres in NSG mice

The most frequently used published protocol describes important steps for the successful engraftment and differentiation of the adult stem cells (Liu et al., 2006; Proia and Kuperwasser, 2006). Following this protocol I tried to transplant and differentiate HME wt cells in the mammary fat-pad of NSG mice. The procedure was performed in two surgical steps. During the first surgical step, the mouse mammary fat-pad of 3-4 week old NSG mice was cleaned of endogenous mammary cells and "humanized" with human immortalized fibroblasts (HIF). Two weeks post HIF injection, human mammospheres were injected into the "humanized" area. Eight to twenty weeks after mammospheres had been injected mice fat-pads were examined for the presence of human mammary cells (Figure 8).
For the establishment of the protocol, 114 mice were used. Mammospheres of the HME cell line were inoculated in 80 mice while 34 mice were inoculated with human secondary mammospheres derived from the donor's tissue specimens. None of the isolated mouse mammary fat-pads contained human cells indicating problem of engraftment or survival of human cells into the mammary fat-pad of NSG mice.

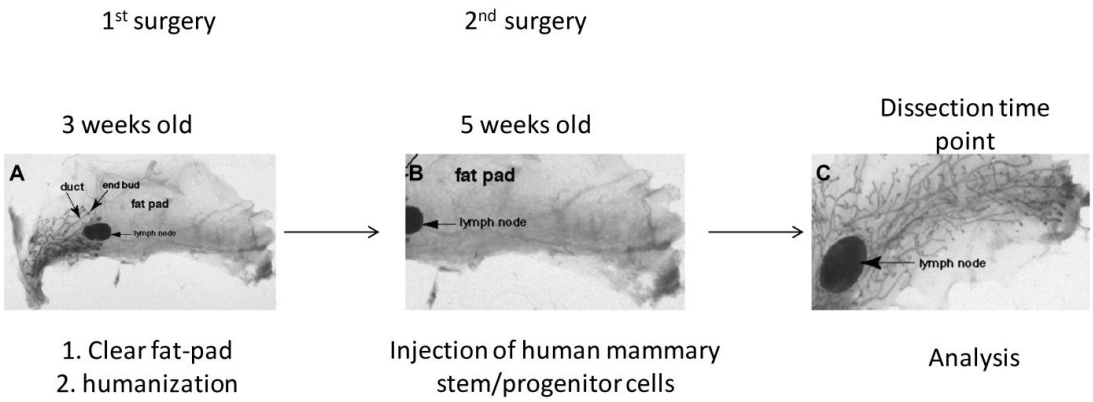

Figure 8. *In vivo* differentiation of the human mammospheres in NSG mice.
(A) Three weeks old female mice were subjected to resection of endogenous mammary epithelial compartment. In the cleared fat cell compartment irradiated human fibroblasts were inoculated. (B) Humanized mammary fat-pad serves as matrix for engraftment and propagation of mammospheres. (C) Mouse mammary fat-pad was analyzed eight to twenty weeks post inoculation. Detailed protocol is in (Liu et al., 2006; Proia and Kuperwasser, 2006).

MDA-MB-231 1833 GFP (1833 GFP) cell line was used as a positive control for the engraftment and propagation of human cells in immune-deficient mice. The expression of green fluorescent protein in (1833 GFP) was achieved by stable integration of *GFP* by using lentiviral gene transfer. In a group of 6 mice 1833-GFP cell line was inoculated by the already described protocol. Two weeks post inoculation the first signs of primary tumor formation were observed. All of 6 mice developed primary tumors. Due to the size of the primary tumor, mice had to be sacrificed 10 weeks post inoculation (Figure 9).

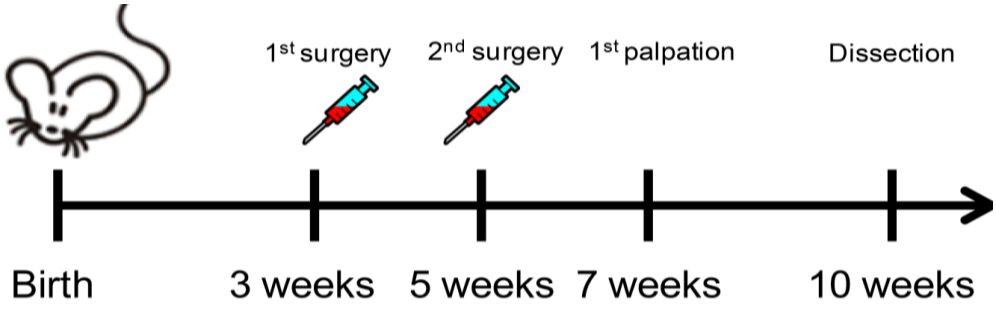

Figure 9. The MDA-MB-231 1833 cell line forms mammary tumors in NSG mice. 1833-GFP cell line was inoculated in the pre-cleared mouse mammary fat pad. The fourth mouse mammary fat-pad was pre-cleared and endogenous mouse epithelia was removed. In the remnant fat-pad human immortalized fibroblasts were injected. Two weeks after first surgical step 200 000 cancer cells were injected. Tumors were palpable 2 weeks after injection, 3 weeks later mice were dissected. Results were obtained from group of 6 mice (n=6).

Postmortem examination revealed the presence of macroscopic mammary tumors (~1 cm in diameter) and the presence of macroscopic lung and liver metastasis (Figure 10 a-f). Histo-pathological examination confirmed the mammary origin of the primary tumor. Macro-metastases were present in distant organs (lungs and liver) of all mice. Focal liver macro-metastasis were found in one of six mice (1/6; 16%) while lung metastasis were found in all of the experimental mice (6/6). Brain metastases were not detectable. Bone marrow was isolated from the tibiae and femura of the experimental mice. Examination of bone marrow by fluorescent microscopy showed up to 1,8% of GFP positive cells (Figure 10 g-i).

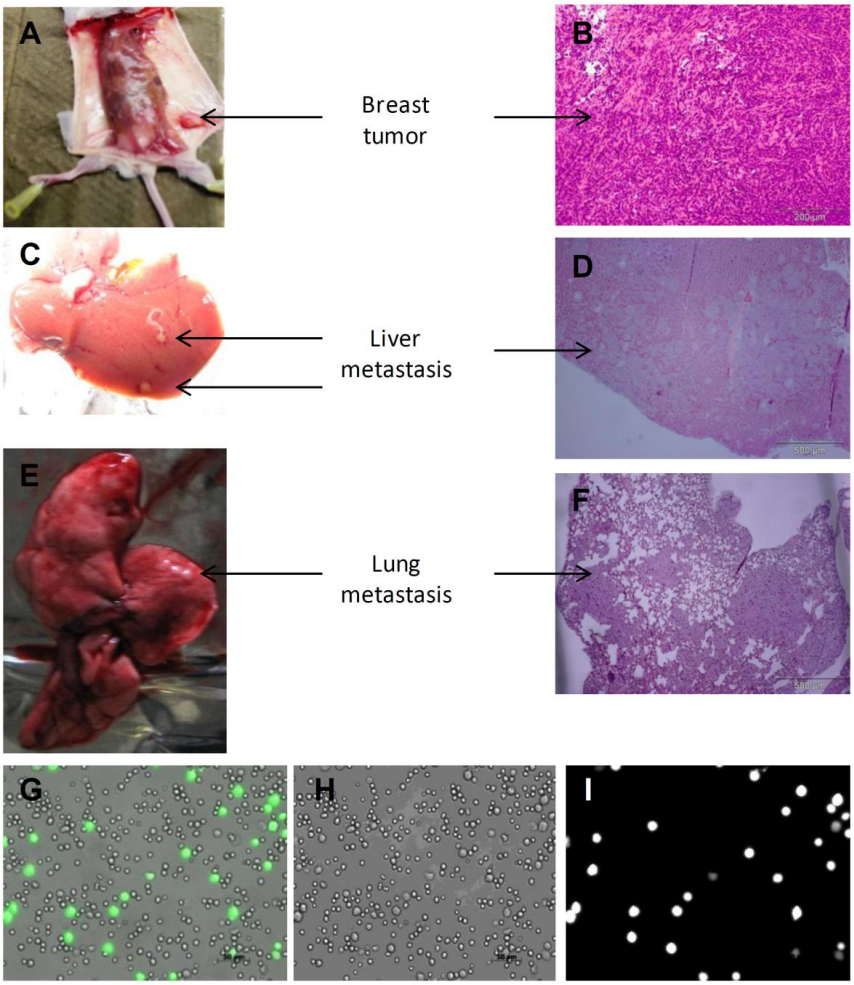

Figure 10. The MDA-MB-231 1833-GFP cells form mammary metastatic tumors and metastasize in NSG mice. (A-B) MDA-MB-2311833-GFP cell line developed mammary tumors. Mice were killed 7 weeks post cell inoculation. (C-D) Focal liver macro-metastases were confirmed by H&E staining. (E-F) Lung metastasis and big deposits in pleural effusion were observed. (G-I) Bone marrow was isolated and examined for the presence of GFP positive cells. Six mice were used for this experiment (n=6).

Engraftment and growth of robust human cancer cell line in NSG mice but the lack of HME wt cell line engraftment and propagation indicates necessity for protocol improvement. The MDA-MB-2311833-GFP cell line experiment suggested that engraftment and survival of human cells in NSG mice might depend on the environmental signals provided mainly by fibroblasts used for mammary fat-pad humanization. Therefore, the next step was to check whether the human immortalized fibroblasts engraft into mammary fat-pad and do they support the growth and differentiation of adult mammary stem and progenitor cells.

3.2.4.2. *In vivo* engraftment and growth of human mammospheres in NSG mice- protocol modification

Human mammary glands contain as larger fibrotic compartment compared to murine glands and moreover, fibroblasts play an important role in the development of human mammary stem cells. For these differences, engraftment of human immortalized fibroblasts (HIF) into pre-cleared mouse mammary fat-pad is tought to be necessary for the subsequent engraftment and differentiation of adult human mammary stem and progenitor cells.
Described failure of normal human mammary epithelia to engraft, but ability of human cancer cell line to engraft and propagate in NSG mice suggested that “humanization” of the recipients’ fat-pad failed. The failure of mammary fat-pad “humanization” may be due to the lack of HIF engraftment into pre-cleared mouse mammary fat-pads. Therefore, the fat-pads of animals where no engraftment of human epithelial cells could be detected were examined for the presence of HIF.

HIF were not detectable by histological and immunohistochemical examination, while humanized mammary fat-pads showed similar morphology to pre-cleared but not humanized fat-pads (Figure 11 a-b).
This finding suggested that the used HIF were not able to engraft and subsequently support development of human mammospheres in mouse mammary fat-pad.

Therefore, mouse mammary C3H10T1/2 fibroblasts were checked for the ability to form a fibroblast-containing stroma in mouse mammary fat-pad.
Interestingly, murine fibroblasts rapidly engrafted in the fat-pad and formed large fibroblast-containing regions (Figure 11 c).

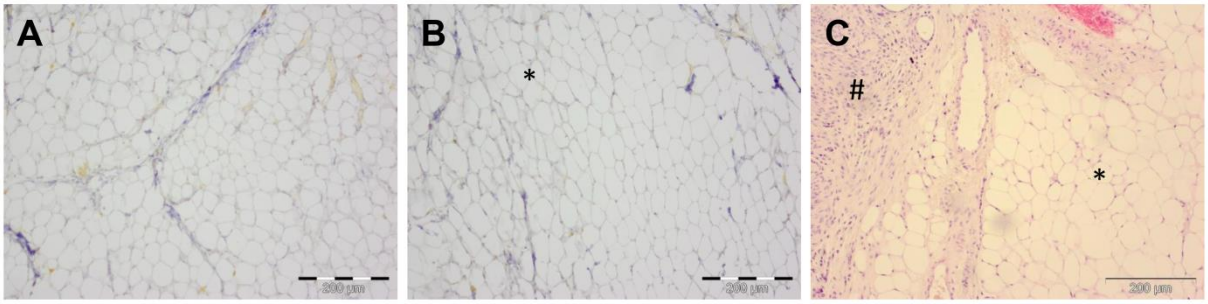

Figure 11. Inoculation and propagation of fibroblasts in the mouse mammary fat-pad. (A) Mammary fat-pads were cleared of endogenous mouse epithelial cells; (B) Engraftment of human immortalized fibroblasts in cleared mouse fat-pad was not detected as indicated by *; (C) Engraftment of C3H10T1/2 murine fibroblasts (engraftment of C3H10T1/2 fibroblasts is indicated by #, while mouse endogenous mammary fat-pad stroma is tagged by *).

Engraftment of C3H10T1/2 fibroblast into mouse mammary fat pad suggested that inoculation of human epithelial cells co-mixed with C3H10T1/2 fibroblasts may result into successful engraftment of human cells.

Human mammary HME wt cells and HME EGFR cells were co-mixed with C3H10T1/2 fibroblasts and injected into pre-cleared fat-pad of NSG mice. Five to eight weeks post inoculation mice were examined for the outgrowth of human cells. HME wt and HME EGFR cells were found to have successfully engrafted in mouse mammary fat-pads. Their human origin was confirmed by immune-staining using an antibody which specifically binds to human cytokeratin 18 (Figure 12 a).

Moreover, the analysis of mouse mammary fat-pads inoculated with HME cells confirmed presence of cytokeratin 5/14 expressing cells (Figure 12 c). Estrogen receptor expression of observed human epithelial cells could not be observed (Figure 12 d).

To exclude the possibility that C3H10T1/2 fibroblasts form tumors over time, a control group of mice (n=4) was observed after inoculation. During 60 weeks, none of the mice showed any sign of illness, tumor formation or other side effects promoted by immortalized fibroblasts. Dissection and analysis of control mice confirmed absence of tumor formation by C3H10T1/2 fibroblasts.

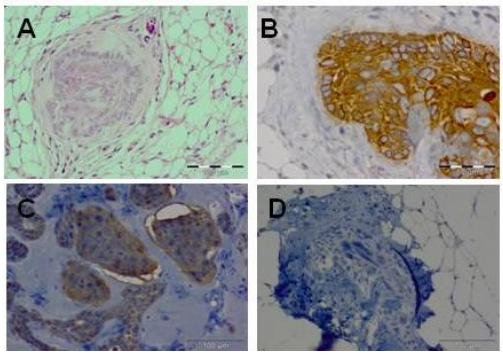

Figure 12. Engraftment of HME EGFR cell line in mammary fat-pad. (A) HME EGFR cell line successfully engrafted and propagated in mouse mammary fat-pad; (B) Engrafted cells expressed human cytokeratin 18; (C) Developed structures express cytokeratin 5 and 14; (D) Expression of estrogen receptor could not be detected. Twenty mice were used for the purpose of the protocol improvement (n=20).

After, HME cells had successfully engrafted, human mammospheres obtained from the reduction mammoplasty were tested. The secondary mammospheres were co-mixed with C3H10T1/2 fibroblasts and transplanted into pre-cleared mammary fat-pad of NSG mice and supplemented with estrogen pellets. Analysis of the mammary fat-pads 8 weeks post-inoculation showed that in case of 4 animals (67%) engraftment of mammospheres was successful what confirmed that utilization of C3H10T1/2 fibroblasts for the engraftment of human cells into mammary fat-pad of NSG mice results in an improved *in vivo* differentiation protocol (Figure 13 b and c).

Development of a novel strategy for the *in vivo* differentiation of human mammary stem and progenitor cells by utilization of C3H10T1/2 murine fibroblasts enabled the start of study of IL6 trans-signaling influence in normal and malignant stem and progenitor cells.

A

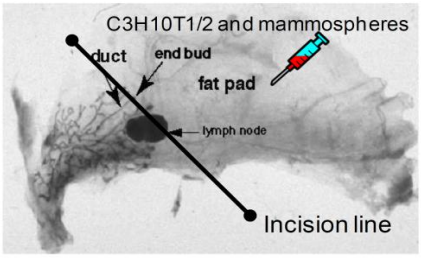

B

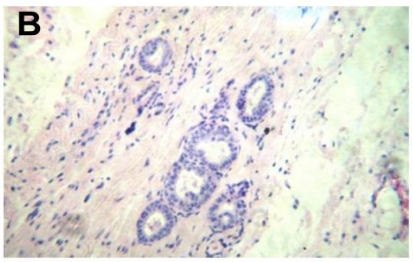

C

	Injection		Engraftment		p-value (χ^2 test)
	HME cells	NM	HME cells	NM	
HIF	80	34	0	0	p< 0.001
C3H10T 1/2	20	6	20	4	

Figure 13. Engraftment of human mammospheres in mouse mammary fat-pad of NSG mice and protocol modification. (A) Mammary fat-pads of 3 weeks old NSG mice were pre-cleared and inoculated with co-mixed murine C3H10T1/2 fibroblasts and mammospheres; (B) Eight weeks post-inoculation human engrafted cells were detected. (C) Comparison of engraftment efficiency by using two different fibroblasts types (HIF vs. C3H10T1/2). Utilization of C3H10T1/2 fibroblasts instead of HIF resulted in improvement of *in vivo* differentiation protocol (NM = mammospheres obtained from propagation of normal mammary gland; normal mammospheres).

3.3. IL6 signaling in normal mammary cells

Activation of the IL6 signaling has been implicated in regulation of important cell signaling pathways, such as Notch and Wnt (Ben-Porath et al., 2008; Sansone et al., 2007). Therefore, I tried to assess the impact of IL6 signaling and how IL6 signals in normal mammary stem and progenitor cells.

3.3.1. The activation of the IL6 signaling promotes survival and proliferation of the mammary cells under anchorage independent conditions

Stem and progenitor cell proliferation can be assessed by cell propagation under anchorage independent conditions. Thus, the sphere forming ability of MCF10A and HME wt was analyzed upon activation or blockage of IL6 signaling. The cell lines were propagated under sphere conditions for 7 days in medium supplemented either with IL6, anti-IL6 blocking antibody or PBS. Activation of IL6 signaling promoted survival and propagation of HME wt and MCF10A cells under anchorage

independent environment. On the other hand, the number of spherical colonies was slightly reduced upon application of IL6 blocking antibody (Figure 14).

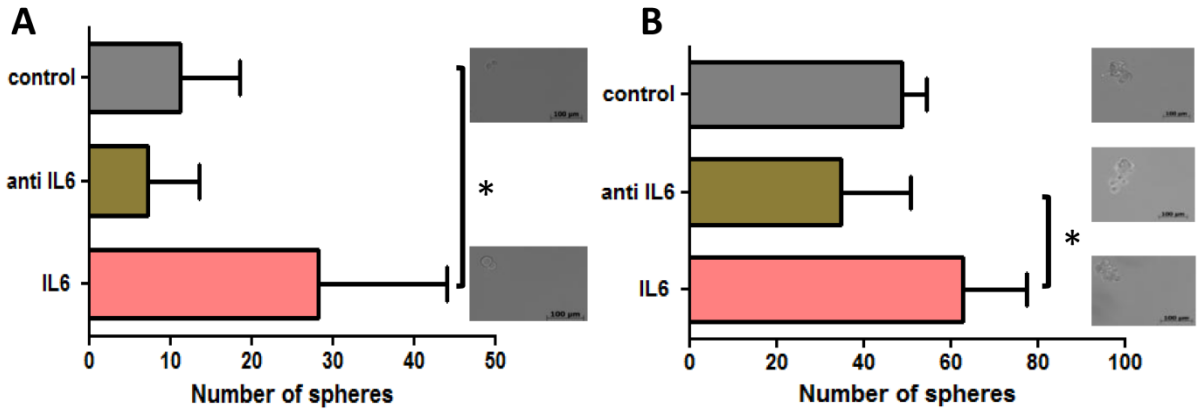

Figure 14. IL6 increases cell survival and sphere numbers of human mammary cell lines under anchorage independent environment. (A) Sphere forming ability of MCF10A cell line in presence of IL6 or anti-IL6 (One way ANOVA p=0.009; control vs. IL6, p=0.03, two- tailed unpaired t-test); (B) Sphere forming ability of HME wt cells in presence of IL6 or anti-IL6 (One way ANOVA p=0.008; anti IL6 vs. IL6, p=0.01, two- tailed unpaired t-test). Results represent a mean of 3 experiments performed with cells of different passages (n=3). Each of 3 experiments was performed in technical duplicates.

Taken together, these results suggest that IL6 signaling impacts on survival and propagation of mammary cell lines when propagated under anchorage independent condition.

3.3.2. IL6 signals in mammary cells via trans-signaling

The increase of sphere forming ability by addition of IL6 signaling poses the question for the mode of IL6 signaling. To test whether the signal can be transmitted through membrane-bound IL6 receptor (IL6R), mammary cell lines were propagated under conventional (2D) conditions and under anchorage independent (3D) conditions, isolated and stained with antibodies directed against the IL6R (anti-IL6R). IL6R surface expression was quantified by FACS.

FACS analysis suggested the absence of mammary cells expressing membrane-bound IL6R in MCF10A and HME wt cells. Moreover, cell propagation under 3D conditions did not result in detectable expression of membrane-bound IL6R. Of note,

fibroblasts isolated from the normal mammary gland and propagated for two weeks did not show any detectable membrane-bound IL6R expression.

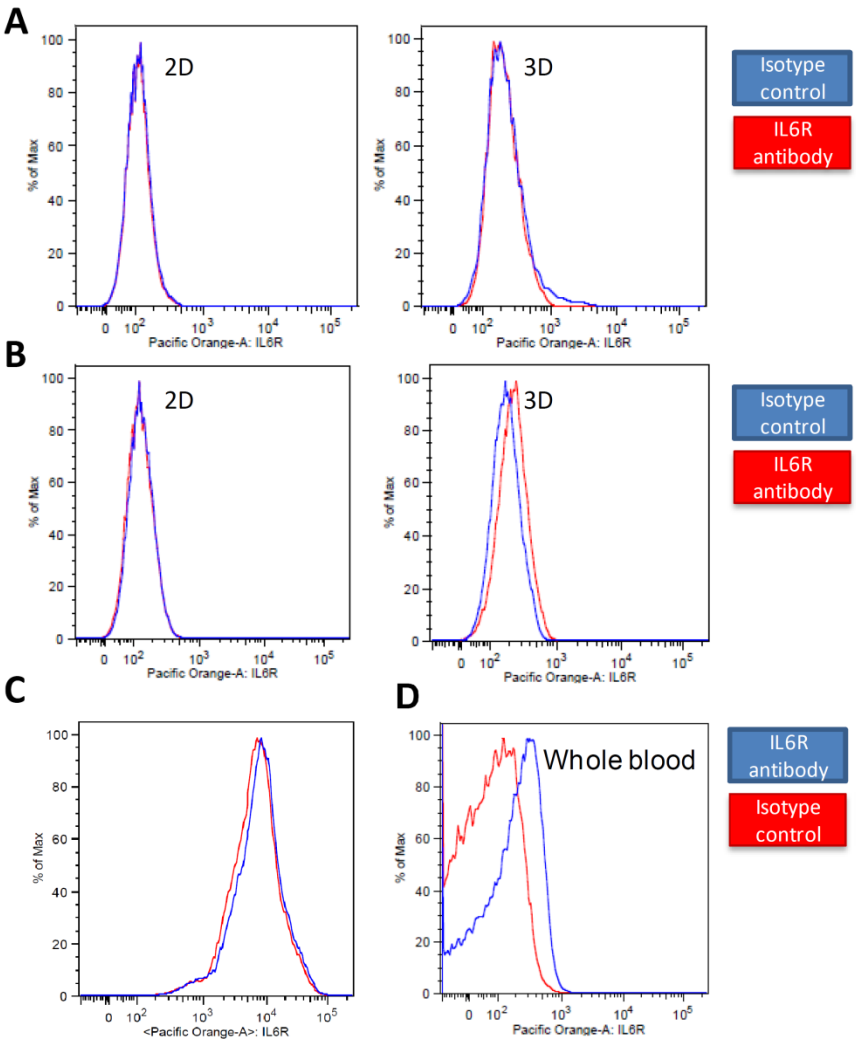

Figure 15. Mammary cell lines do not express membrane- bound IL6R. FACS analysis could not detect presence of membrane- bound IL6R on (A) MCF10A and (B) HME wt cell lines, neither on cell growth under 2D nor under 3D culture conditions; (C) Mammary fibroblasts do not express membrane-bound IL6R; (D) Blood donated by a healthy donor was used as a positive control. Biotinilated anti-IL6R antibody, UV-4 clone and mouse IgG1 κ, isotype control were used for FACS analysis. The experiment was performed 3 times (n=3).

To address how the IL6 signal is transmitted the next experiment tested whether IL6 trans-signaling could be utilized by mammary cells. Trans-signaling involves expression of the soluble form of IL6R (sIL6R). It was therefore tested whether the mRNA of *IL6* and *IL6R* is expressed by individual MCF10A and HME wt cells.

The mRNA of the single cells grown under 2D and 3D conditions were isolated and reversely transcribed into cDNA (Figure 16 a). In the case of MCF10A cells, the

results confirmed the presence of cells grown under 2D culture conditions expressing *IL6* and *IL6R*, but *IL6* expression could not be detected in cells grown under 3D culture conditions (Figure 16 b). Moreover, the analysis of *IL6* and *IL6R* co-expression in MCF10A cells showed that majority of cells do not co-express *IL6* and *IL6R* and thus the analysis suggested that IL6 trans-signaling could be achieved via paracrine stimulation where some cells express *IL6* while the other express *IL6R* (Figure 16 c).

Assessment of the *IL6* and *IL6R* expression in HME wt cells demonstrated increase in numbers of cells expressing *IL6* and *IL6R* when grown under 3D conditions (Figure 16 d). The analysis of the *IL6* and *IL6R* co-expression showed that majority of cells (87%) grown under 3D could trigger IL6 trans-signaling in autocrine way (Figure 16 e). Interestingly, all HME wt cells when grown under 3D culture conditions could contribute to IL6 trans-signaling.

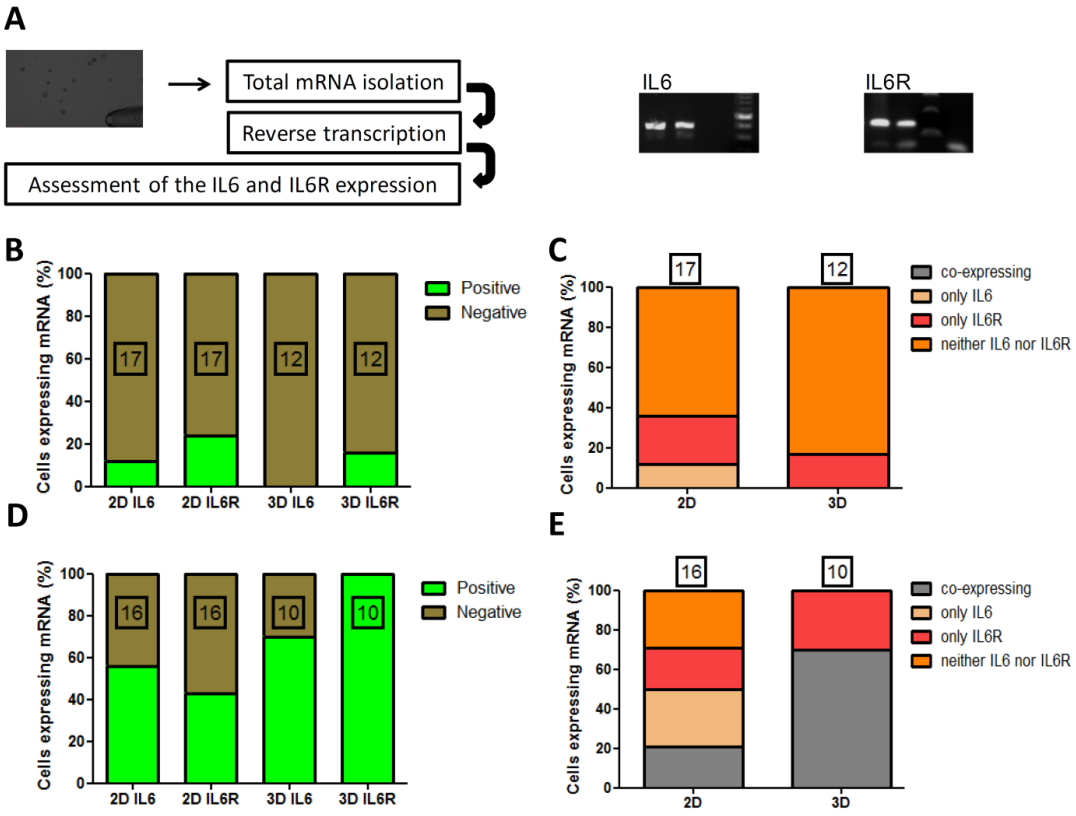

Figure 16. Expression of IL6 and IL6R in mammary cell lines. (A) Experimental design. Total mRNA of single 2D grown cells or 3D spheres were isolated and reverse transcribed. Expression of *IL6 and IL6R* in (B) MCF10A was assessed by PCR; (C) co-expression of *IL6 and IL6R* in MCF10A cells; (D) HME wt cells grown under 2D or 3D conditions express *IL6 and IL6R* (E) HME wt co-express *IL6 and IL6R*. The transcription assessment was performed by using multiple samples.

3.3.3. Mammary cell lines produce and secrete IL6 and sIL6R

Since the mRNA of *IL6* and *IL6R* could be detected in MCF10A and HME cells, the presence of the proteins was checked as a final verification of the ability of mammary cells to trigger IL6 trans-signaling. For this, the media of cells grown under 2D conditions were collected and used for measuring the IL6 and sIL6R protein. As control, the levels of the IL6 and sIL6R were assessed in fresh media.
It was found that both mammary cell lines are able to produce IL6 and sIL6R, indicating that trans-signaling underlines IL6 transmission in both cell lines (Figure 17 a). On average, HME wt cells showed a ten-fold higher IL6 protein production than MCF10A cells.
In addition, HME wt cells displayed a dose density- dependent secretion of IL6 and sIL6R, with the protein level of IL6 being inversely correlated to cell density (Figure 17 b).

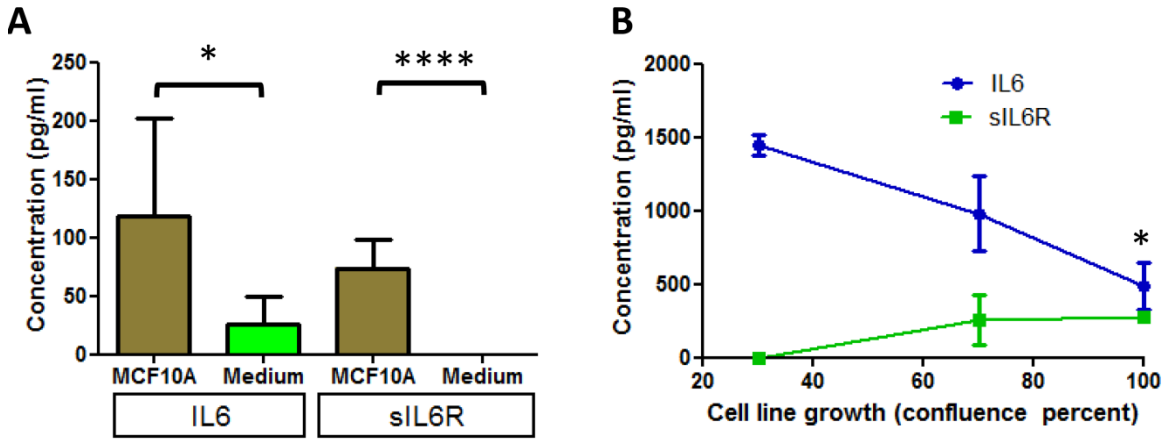

Figure 17. Mammary cell lines secrete IL6 and sIL6R. (A) MCF10A cell line produces soluble IL6R and IL6 (IL6 * p= 0.02; sIL6R ****p<0.0001, two- tailed unpaired t-test); (B) HME wt cells secrete IL6 and sIL6R in a cell density depending mode (IL6 level at 100% confluence vs. IL6 level at 30% confluence *p=0.016, two- tailed unpaired t-test). Results were confirmed in two independent experiments using technical replicates (n=2).

This phenomenon suggested a density control mechanism of IL6 signaling in HME wt cells. If true, than mammary cells, which contain activated IL6 signaling should regulate the expression of IL6 and IL6R as a part of observed feed-back loop.

3.4. The activation of the PI3K/Akt signaling pathway inhibits *IL6* and *IL6R* expression in mammary cells

The IL6 signals via activation of different pathways, the JAK/STAT3, SHP-2/Ras and PI3K/Akt pathways (Grivennikov and Karin, 2008). Therefore, the observed differences in mRNA and protein expression of *IL6 and IL6R* between MCF10A and HME wt cells may result from the activation of different downstream signaling pathways that may render some cells independent form the availability of IL6/IL6R. To test this IL6 and IL6R expression was assessed in HME cells in which PI3K/Akt signaling was over-activated.
HME PIK3CA ex20, carrying mutatation in exon 20, and HME shPTEN, displaying low PTEN down-regulated by short hairpin RNA, have constitutively activated PI3K/Akt signaling. From both cell lines single cells were isolated and their transcriptom was assessed for the expression of *IL6* and *IL6R*. Interestingly, the activation of PI3K/Akt signaling pathway resulted in reduced number of *IL6* and *IL6R* expressing cells (Figure 18 a-b), suggesting regulation of IL6 signaling/trans-signaling by the PI3K/Akt signaling network.

Since, activation of IL6 signaling had enhanced sphere forming ability (see 3.3.1), it was tested whether the activation of the downstream PI3K/Akt signaling in HME cells results in increased sphere forming ability of HME cells when propagated under anchorage independent conditions. Indeed, HME shPTEN and HME PIK3CA ex 20 cells formed considerably higher number of spheres compared to wt cells indicating that sphere forming ability induced by IL6 may be maintained via PI3K/Akt signaling pathway (Figure 18 c).

The reduced number of cells expressing *IL6* and *IL6R* in HME PIK3CA ex20 and HME PTEN cells compared to HME wt cells suggested that the activation of downstream effectors in IL6 signaling pathway reduces expression of *IL6 and IL6R* and induces propagation and survival of cells under anchorage independent conditions.

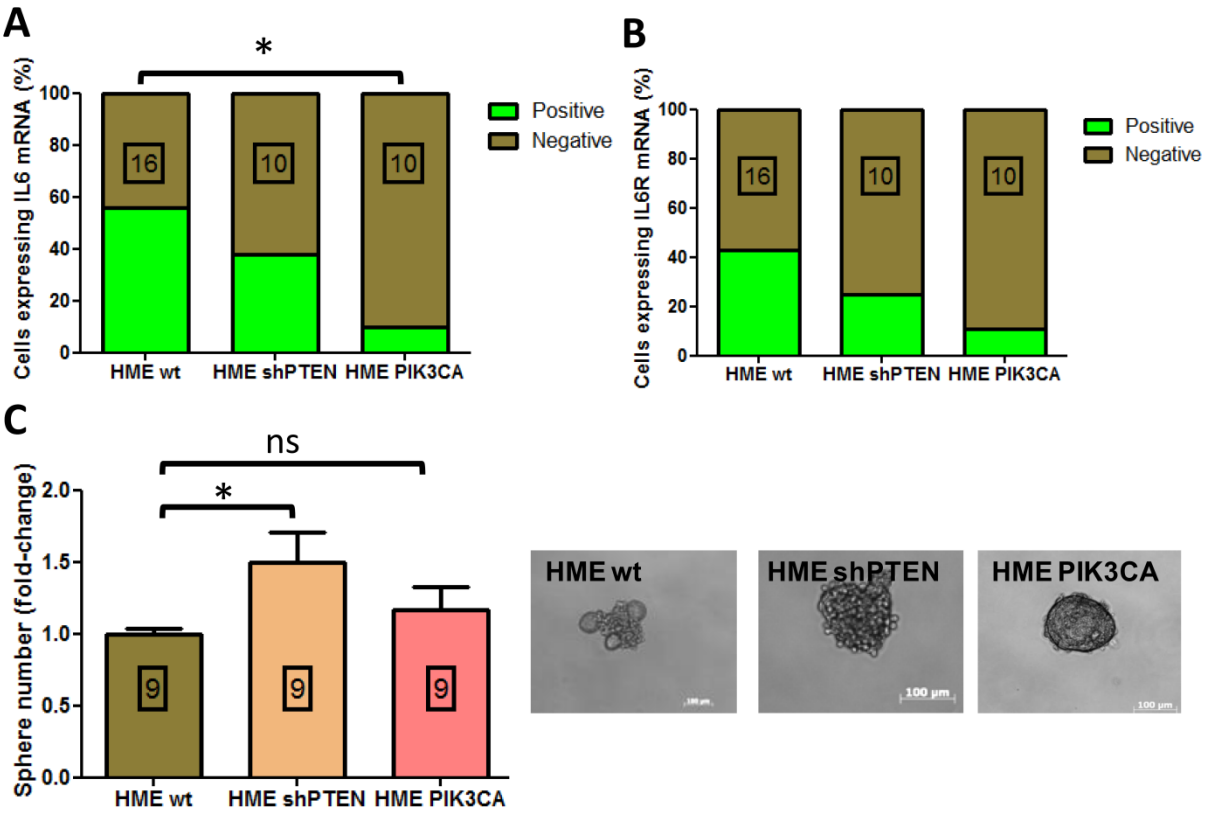

Figure 18. IL6 and IL6R expression in HME wt cells and cells with PIK3CA mutation and PTEN knockdown. Messenger RNA of single HME wt, HME PIK3CA ex.20 and HME PTEN cells were isolated and reversely transcribed. Assessment of (A) *IL6* and (B) *IL6R* expression was evaluated (p=0.016, Fisher's exact test); (C) Sphere forming ability of HME cells alternated for PI3K/Akt signaling (HME wt vs. HME shPTEN p=0.016, two- tailed unpaired t-test; HME wt vs. HME PI3KCA p=0.142, two-tailed unpaired t-test). Results represent mean of 3 independent experiments (n=3), each performed using technical replica (n=3).

The results obtained from analysis of mammary cell lines suggested that IL6 trans-signaling influences proliferation and survival of mammary stem and progenitor cells under anchorage independent conditions via PI3K/Akt signaling.

Obtained results suggested that IL6 trans-signaling is triggered in an autocrine and paracrine way in mammary cells. This finding raised a concern that utilization of epithelial cell lines may not reflect cellular complexity of the adult mammary gland and thus may not address contribution of various cells to IL6 trans-signaling activation. Therefore, the next experiments tried to address the influence of IL6 (trans-) signaling in normal mammary gland.

3.5. IL6 signaling in the adult human mammary gland

I tried to assess the effect of IL6 signaling in human adult mammary gland. The obtained results suggested that IL6 signals in mammary cell lines via trans-signaling. Therefore, I tried to address how IL6 signals in adult mammary gland and what is the contribution of various cells to IL6 trans-signaling.

3.5.1. Mammary gland does not contain cellular population with membrane bound IL6R

Mammary glands of the healthy donors undergoing breast reductions were used to investigate the effect of IL6 signaling in mammary stem and progenitor cells. It was first tested whether the IL6 signaling in the mammary gland is maintained trough membrane bound IL6R. Mammary tissue specimens cleared of fat tissue were mechanically and enzymatically digested after macroscopic exclusion of breast cancer by a pathologist (Figure 19 a). Cells from the digested tissue were stained with an antibody directed against membrane bound IL6R. FACS analysis demonstrated that cells which compose adult mammary glands do not express membrane bound IL6R (Figure 19 b).
To exclude that IL6R is expressed by a very small subpopulation that might escape detection in bulk tissue adult mammary stem and progenitor cells were enriched by mammosphere culture and grown for two passages. The secondary mammospheres were then dissociated and stained against membrane bound IL6R.
The FACS analysis suggested that the cells comprising secondary mammospheres do not express membrane bound IL6R (Figure 19 b).

Thus membrane bound IL6R could neither be detected on the surface of cells comprising the secondary mammospheres, nor on cells directly isolated from digested tissue specimen. The lack of IL6R surface expression in mammary cells suggested that the IL6 signaling in the adult mammary gland is maintained via trans-signaling.

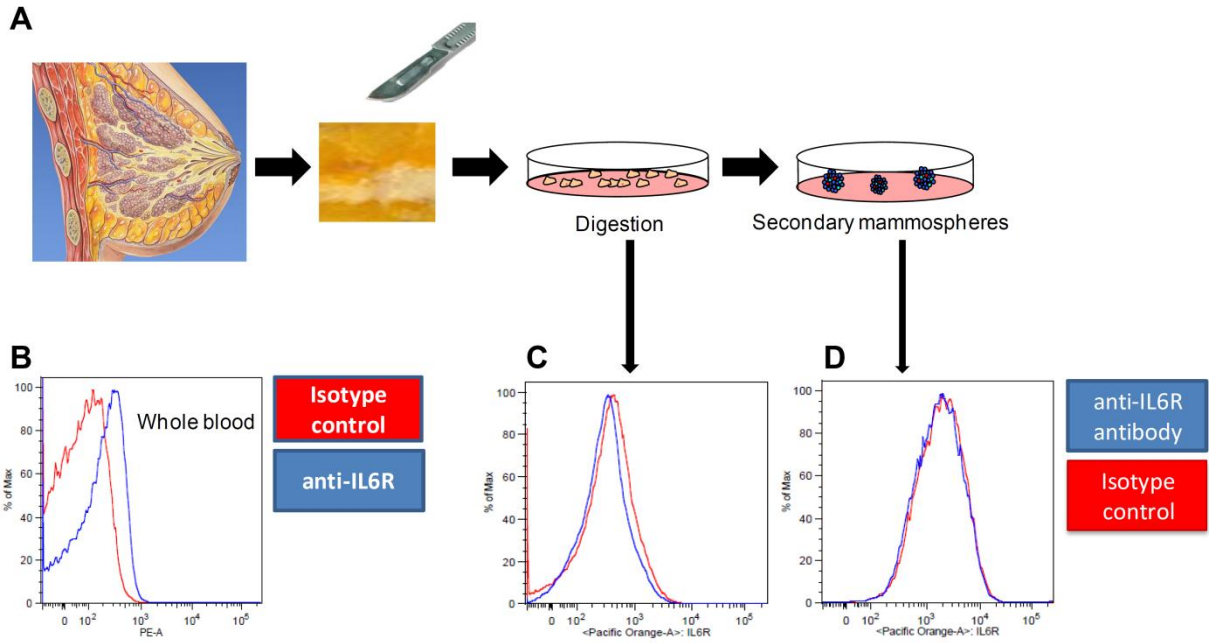

Figure 19. Evaluation of the IL6R expression in the adult mammary gland. (A) Mammary glands of healthy donors were digested and propagated under anchorage independent conditions; (B) Positive control- expression of the membrane bound IL6R in blood cells of a healthy donor; (C) Cells comprising the adult mammary gland do not express membrane bound IL6R; (D) Cells obtained after tissue digestion were under 3D conditions. Biotinilated anti-IL6R antibody, UV-4 clone and mouse IgG1 κ, isotype control were used for FACS analysis. Results were confirmed in 3 independent samples (n=3).

3.5.2. Mammary gland contains cellular populations which enable IL6 trans-signaling

IL6 trans- signaling in normal mammary gland is only possible if sIL6R and IL6 are expressed by any cellular population present in healthy organ.

Cells obtained after mammary gland digestion represent many different cell types in different differentiation stages. I therefore investigated which cells express *IL6 and IL6R* transcripts and thus enable IL6 trans-signaling.

First, the mRNA of laser-microdissected differentiated mammary ducts (DfMD) were globally amplified and *IL6* and *IL6R* mRNA expression was assessed by gene specific PCR. Interestingly, none of the analyzed donors (n=3) expressed *IL6* and *IL6R* (Figure 20 a-b), suggesting that these genes may be transcribed only by stroma or undifferentiated epithelial cells. Next, it was tested whether mammospheres

express *IL6* and *IL6R* (Figure 20 a-b). Interestingly, both messages were detected when cells were propagated under conditions selecting for stem and progenitor cells. Therefore, undifferentiated cells may enable IL6 trans-signaling in the adult mammary gland.

Moreover, as the adult mammary gland is consisted of developed stroma I tried to assess contribution of stroma in maintaining IL6 trans-signaling in adult human mammary gland. Therefore, mammary fibroblasts were isolated and propagated under defined culture conditions. The reversely transcribed mRNA isolated from single fibroblast was analyzed. The results indicated that 100% of analyzed cells express *IL6* mRNA while *IL6R* mRNA was found in 30% of cells (Figure 20 a-b). Testing for the presence of IL6 and IL6R protein in the media confirmed high levels of IL6 expression by propagated fibroblasts (Figure 20 c). In addition, sIL6R protein could not be detected by analysis of fibroblast media.

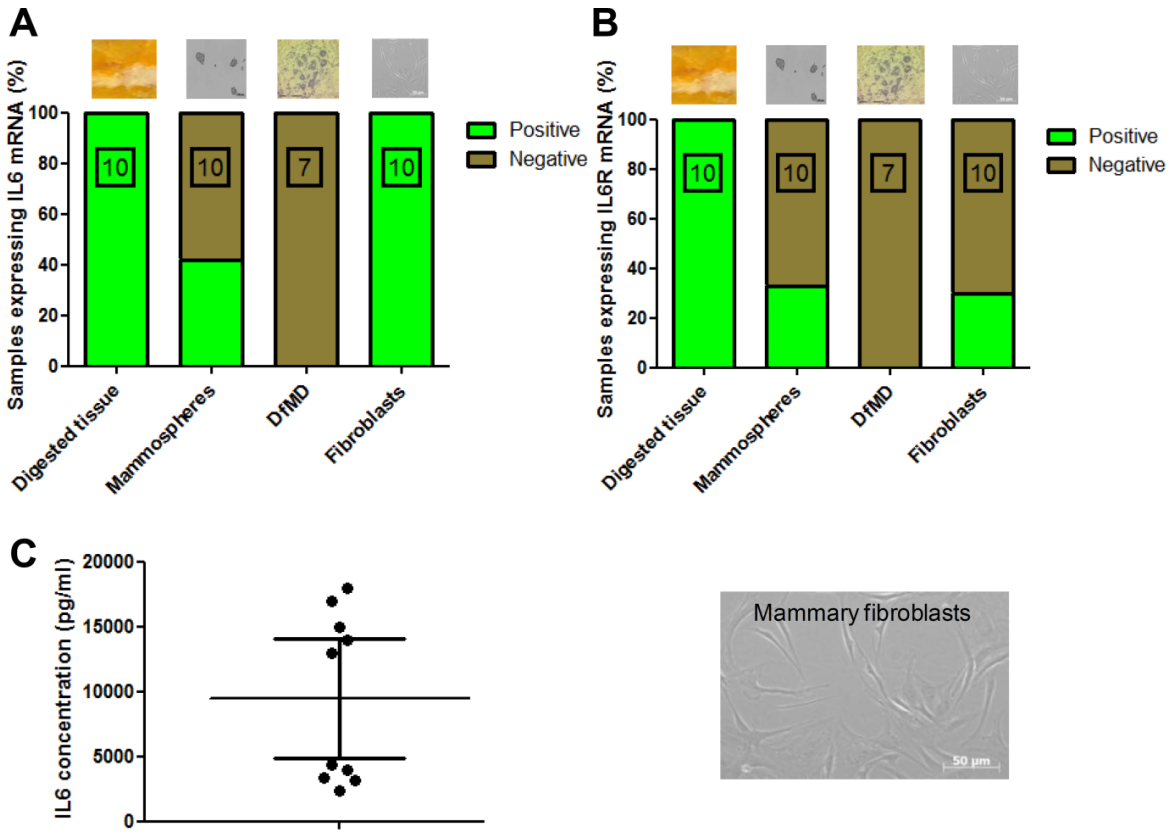

Figure 20. *IL6* and *IL6R* expression in the adult mammary gland. Digested mammary gland, mammospheres and terminally differentiated mammary ducts (DfMD) after laser- microdissection were examined for the expression of the (A) *IL6* and (B) *IL6R* expression; (C) IL6 production and secretion by mammary fibroblasts. Results obtained from 9 independent tissue specimens (n=9).

Taken together these data suggested that the IL6 signals via trans-signaling mechanism in the adult mammary gland. Moreover, the results suggested that IL6 trans-signaling is maintained by fibroblasts and adult mammary stem and progenitor cells.

In the following work I explored the role of IL6 trans-signaling in normal mammary cells.

3.5.3. IL6 trans-signaling in adult mammary stem and progenitor cells

IL6 signaling in the adult mammary gland is maintained via trans-signaling where mammary undifferentiated cells and mammary fibroblasts produce IL6 and sIL6R. The impact of the IL6 trans-signaling on the mammary gland was studied in regard to stem and progenitor cells.

3.5.3.1. IL6 signaling induces proliferation of adult mammary stem and progenitor cells

The expression of sIL6 by adult mammary stem and progenitor cells suggested that addition of external IL6 may trigger IL6 trans-signaling in adult mammary stem and progenitor cells. Therefore, the impact of IL6 trans-signaling on mammosphere formation was investigated.
For this, the mammary glands of healthy donors were dissociated and propagated under anchorage independent conditions. Briefly, after tissue digestion cells were propagated under anchorage independent conditions in mammosphere medium (MSM) or MSM supplemented with IL6. Primary mammospheres were passaged 7-10 days post tissue digestion and further propagated in MSM or in MSM supplemented with IL6. The influence of IL6 trans-signaling activation was assessed by comparing the number of observed mammospheres and the average mammosphere size (Figure 21 a).

The mammary cells supplemented with IL6 during the second passage formed 50% more mammospheres compared to cells grown in control medium. Interestingly, addition of IL6 over two passages did not increase total mammosphere numbers (Figure 21 b).

The proliferative capacity of single mammospheres was measured by assessing the change in sphere diameter. Mammospheres supplemented with IL6 during the second passage were on average 16% bigger compared to mammospheres propagated in the medium without IL6 (Figure 21 c). However, the diameter of the secondary mammospheres supplemented over two passages with IL6 could not be measured because many mammospheres appeared to have fused due to their large size.

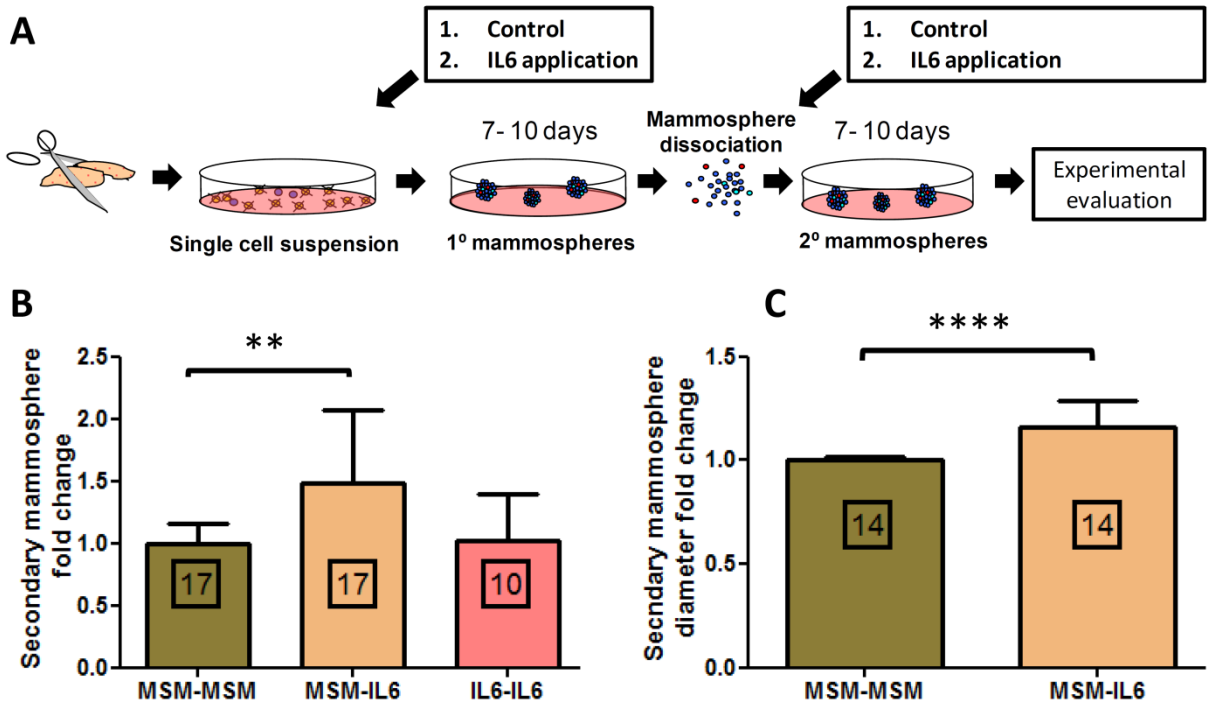

Figure 21. IL6 stimulates mammosphere propagation. (A) Experimental strategy. After tissue digestion, cells were propagated in mammosphere medium (MSM) or in MSM supplemented with IL6 (IL6). After primary mammospheres were formed, mammospheres were digested and further propagated in absence (MSM) or presence (IL6) of IL6. The overall number and size of the secondary mammosphere were evaluated; (B) The number of secondary mammospheres increased after application of IL6 during the second passage ($p= 0.002$, two- tailed unpaired t-test); (C) IL6 influenced proliferation of single mammosphere measured by the fold change of the mammosphere diameter ($p< 0.0001$, two- tailed unpaired t-test). Results are obtained from 7 independent tissue specimens ($n=7$).

Taken together, application of IL6 triggered IL6 trans-signaling what resulted in increased proliferation rate of the adult mammary stem and progenitor cells.

3.5.3.2. IL6 trans-signaling induces proliferation of adult mammary stem and progenitor cells

While the effect of externally added IL6 is most likely mediated via soluble IL6R and trans-signaling (see previous data on *IL6R* and *IL6* mRNA and protein expression), I directly tested whether mammary stem and progenitor cells are responsive to IL6 trans-signaling. For this I used Hyper-IL6 (HIL6), a fusion protein of IL6 and sIL6R.

The mammary tissue of healthy donors was dissociated to a single cell level and propagated under anchorage independent conditions over two passages. The cytokines (IL6 and HIL6) were applied on a day of mammary cell isolation or after the first passage. The influence of the IL6 trans-signaling in adult mammary stem cells was measured by the number of propagated secondary mammospheres, while the effect of IL6 trans-signaling on progenitor cells was measured by average fold-change in diameter of the secondary mammospheres (Figure 23 a). Untreated cells (MSM) were used as experimental control. Although, the equal numbers of cells were plated after tissue digestion, mammary cells supplemented with HIL6 over two passages showed the highest mammosphere number indicating the influence of IL6 trans-signaling in adult mammary stem cells (Figure 23 a). Moreover, IL6 trans-signaling induced higher proliferation of mammospheres compared to untreated cells measured by mammosphere diameter (Figure 23 c). The size of the secondary mammospheres supplemented with HIL6 over two passages could not be evaluated due to frequent fusion of large mammospheres. However, the profound HIL6 effect on mammosphere diameter suggested that HIL6 induced proliferation of progenitor cells (Figure 22 and Figure 23).

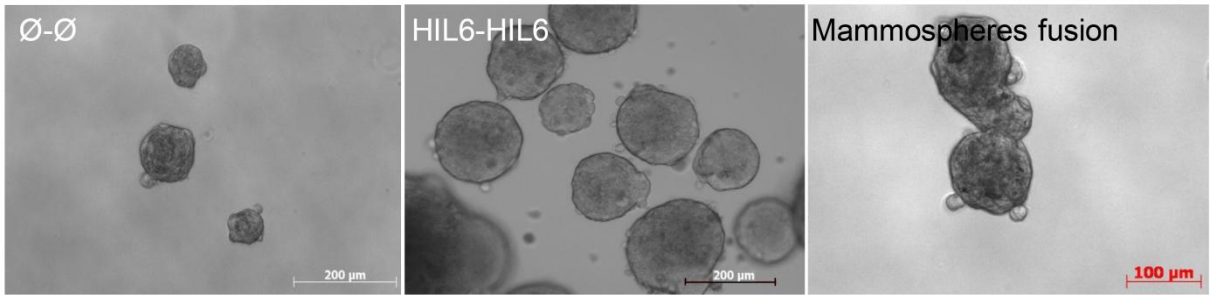

Figure 22. Activation of IL6 trans-signaling by HIL6 application induces increased mammosphere number and size.

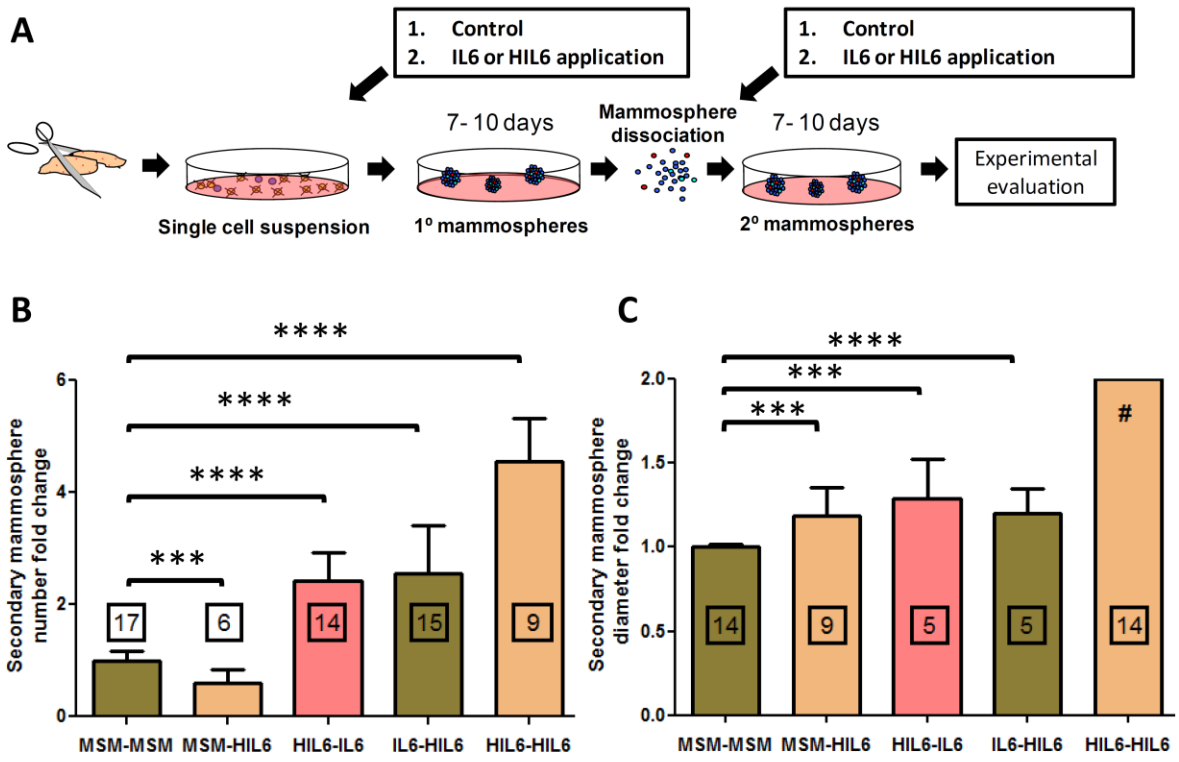

Figure 23. IL6 trans-signaling stimulates proliferation of mammary stem and progenitor cells. (A) Experimental strategy. After tissue digestion, cells were propagated in mammosphere medium (MSM) or in MSM supplemented with IL6 or HIL6. After primary mammospheres were formed, mammospheres were digested and further propagated in absence (MSM) or presence IL6 or HIL6. The overall number and size of the secondary mammosphere were evaluated; (B) HIL6 induced the outgrowth of the secondary mammospheres; (C) IL6 trans-signaling induced proliferation of the secondary mammospheres (**** $p < 0.0001$; *** $p = 0.0001$, two- tailed unpaired t-test). The # indicates that the average diameter was not measurable due to mammosphere fusions. Results are obtained from 7 independent tissue specimens (n=7).

Activation of IL6 trans-signaling induced proliferation of mammary stem and progenitor cell what raised a concern that IL6 trans-signaling might affect the basic biological features of mammary stem and progenitor cells, such as: differentiation ability, asymmetrical cell division and self-renewal.

3.6. IL6 trans-signaling preserves and promotes the functional phenotype of stem and progenitor cells

Since the data showed that activation of IL6 signaling affects survival and proliferation of human mammary stem and progenitor cells, the effect of the IL6 trans-signaling on stem and progenitor cell phenotype was further evaluated.

3.6.1. IL6 trans-signaling triggers mammospheres self-renewal

The enhanced proliferation of mammospheres activated for IL6 trans-signaling raised the question whether the stimulated proliferation of stem and progenitor cells might reduce the self-renewal capacity of the adult mammary stem cells.

Mammospheres were propagated under anchorage independent conditions either in mammosphere medium (MSM) or MSM supplemented with HIL6. The mammosphere self-renewal ability was measured by the ability of cells to form mammospheres of higher passages after mammosphere dissociation and re-plating. Mammospheres were passaged once a week. Mammospheres propagated in the presence of the HIL6 survived up to 6 passages after initial tissue dissociation, suggesting that IL6 trans-signaling preserves the self-renewal ability of human mammary stem and progenitor cells. Moreover, mammary cells propagated in absence of HIL6 could be maintained for 4 weeks. This finding suggests that IL6 trans-signaling promoted self-renewal in mammary stem cells.

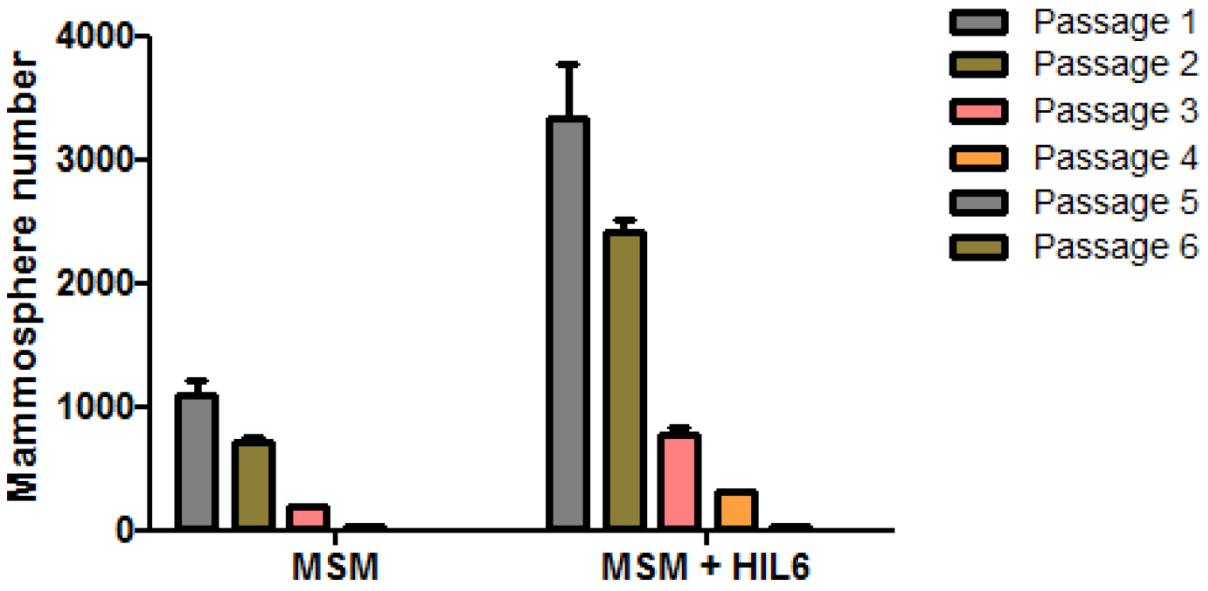

Figure 24. IL6 trans-signaling preserves and induces mammosphere self-renewal.
Mammospheres were propagated either in MSM or in MSM supplemented with HIL6**.** Obtained results were confirmed in 3 independent tissue specimens (n=3).

3.6.2. Activation of the IL6 trans-signaling does not reduce ability of the mammary stem and progenitor cells to differentiate

3.6.2.1. Ability of HIL6-treated cells to differentiate *in vitro*

The mammary stem and progenitor cells differentiate in Matrigel© into tubular-duct lobular units (TDLU) and in acinar structures. To test whether activation of IL6 trans-signaling affects *in vitro* differentiation ability, the secondary mammospheres propagated in MSM or in MSM supplemented with HIL6 were propagated under differentiation conditions in 3D Matrigel©. The secondary mammospheres were dissociated and plated in "sandwich" embedding model (described in chapter 3.2.4). The differentiation ability was evaluated three weeks post-plating by counting acinar and TDLU differentiation structures. No difference was observed for the cells propagated in the presence or absence of HIL6 in mammosphere medium. These results indicate that IL6 trans-signaling does not influence the *in vitro* differentiation ability of the secondary mammospheres (Figure 25).

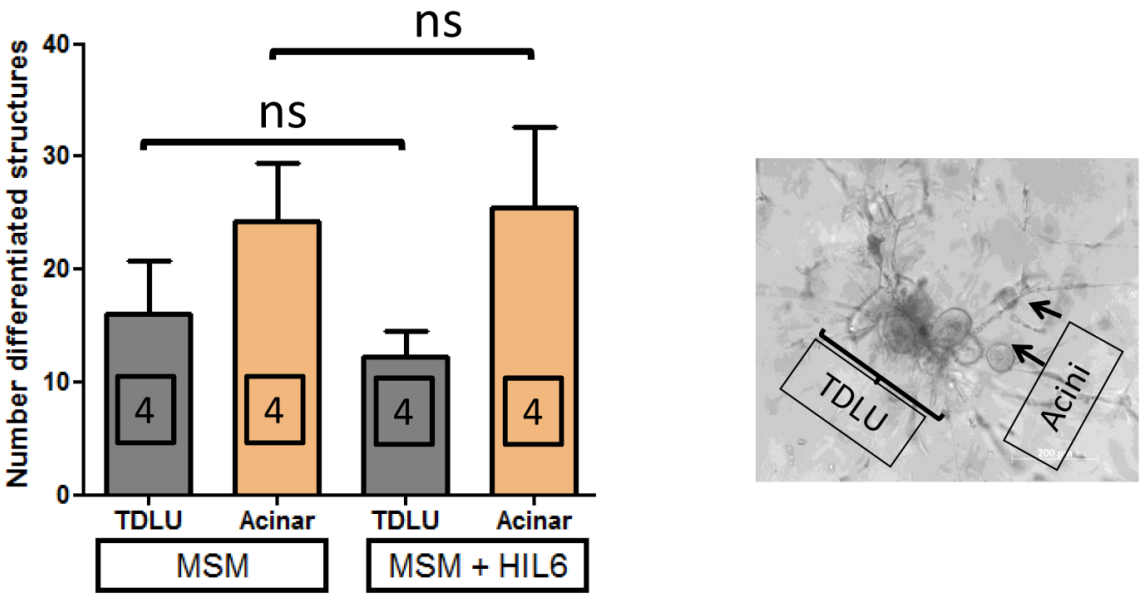

Figure 25. Mammosphere *in vitro* differentiation in 3D Matrigel©. The secondary mammospheres were embedded in Matrigel©. Differentiation ability was evaluated three weeks post embedding. Mammospheres were propagated either in mammosphere medium (MSM) or in MSM supplemented with HIL6 (p= 0.20 TDLU of MSM vs. TDLU MSM+HIL6; p= 0.78 Acinar structures MSM vs. MSM+HIL6; two- tailed unpaired t-test). Results were obtained using tissue specimens of 2 donors (n=2). Experiments were performed in technical duplicates.

3.6.2.2. Activation of IL6 trans-signaling in mammospheres does not influence their differentiation ability in animal hosts

To test the differentiation ability of the secondary mammospheres *in vivo*, the mammary cells isolated from human donors were first propagated in MSM supplemented with HIL6 and after generation of secondary mammospheres inoculated into NSG mice according to the previously established protocol (3.2.5.3). The mammary fat-pads of NSG mice were examined 8 weeks post-inoculation.

The analyzed mammary fat-pads contained differentiated epithelial structures resembling human mammary ducts (Figure 26 a). The human origin and the differentiated luminal phenotype of observed cells was confirmed by immunohistochemistry using a human specific antibody against CK18, an antigen expressed in differentiated mammary ducts (Figure 26 b).

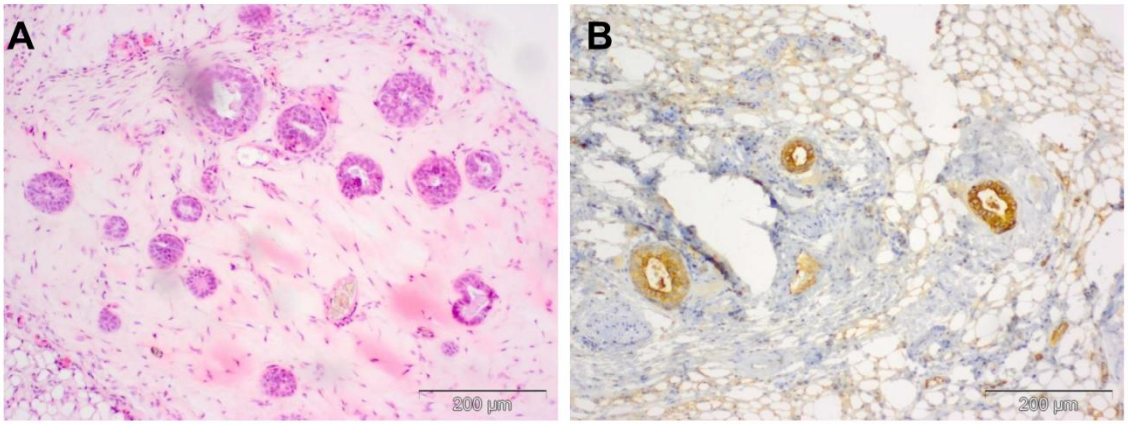

Figure 26. *In vivo* differentiation of mammospheres activated by IL6 trans-signaling. The secondary mammospheres co-mixed with C3H10T1/2 murine fibroblasts were injected into pre-cleared mammary fat-pad of NSG mice. Eight weeks later mammary fat-pads were analyzed for the presence of human mammary glandular structures. (A) Human mammary epithelial ductual structures in mouse mammary fat-pad; (B) observed epithelial cells expressed human CK18. The results were obtained using mammary tissue donated by two healthy donors (n=2). In total, six mice were included in the analysis.

The ductal structures which were shown to express CK18 were further tested for their human origin by assessing the human origin of isolated DNA. For this, laser micro-dissection of ductal structures was performed by P.A.L.M laser-microdissection microscope. Following DNA isolation by Mse PCR global genome amplification, a

PCR assay designed to amplify either unique human or mouse specific sequences was applied.
Micro-dissected ducts clearly contained human specific genomic sequences of P53 and pseudo cytokeratin 19 genes, while these sequences were not amplified in micro-dissected mouse tissue what further confirmed their human origin (Figure 27).

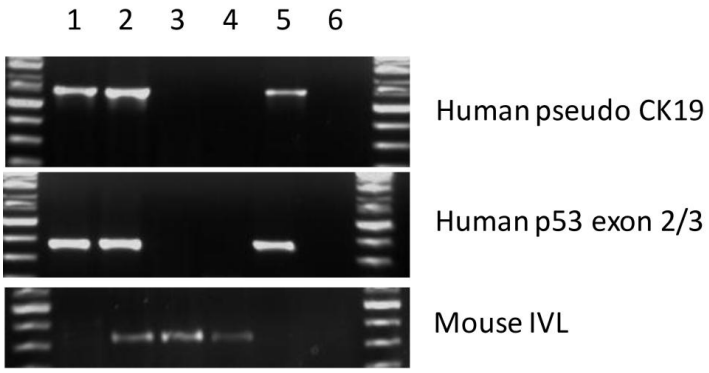

Figure 27. Micro-dissected CK18 expressing cells are of human origin. DNA were isolated from micro-dissected (1, 2) CK18 expressing cells and (3) CK18 non expressing cells. PCR amplification of CK18 positive cells resulted in amplification of human specific sequences. (4) Mouse positive control; (5) Human positive control; (6) Negative control.

Taken together, secondary mammospheres propagated in presence of HIL6 can differentiate *in vivo* demonstrating that IL6 trans-signaling does reduce the differentiation ability of mammary stem and progenitor cells.

3.6.3. IL6 trans-signaling does not influence asymmetric cell division

Adult mammary stem cells divide asymmetrically. The results of such cellular divisions are two daughter cells, one of which preserves the ability to self-renew, while the other cell differentiates into a faster dividing progenitor cell.
The cell membrane of the dividing cell is shared among the daughter cells. Thus, when the cell membrane of mammary stem cells is labeled by an unspecific dye, the marker molecule will be shared among daughter cells and diluted upon each cell division (Figure 28 a).

The mammary cells isolated from donated tissue specimens were labeled by fluorescent PKH26 marker. Anchorage independent environment enabled survival and propagation of undifferentiated cells. Two passages after labeling, it was

observed that mammospheres consisted of many unlabeled cells and rare, label retaining cells (LRC). The detection of LRC suggested that activation of IL6 trans-signaling did not abolish asymmetric cell divisions of mammary stem cells (Figure 28 b-c).

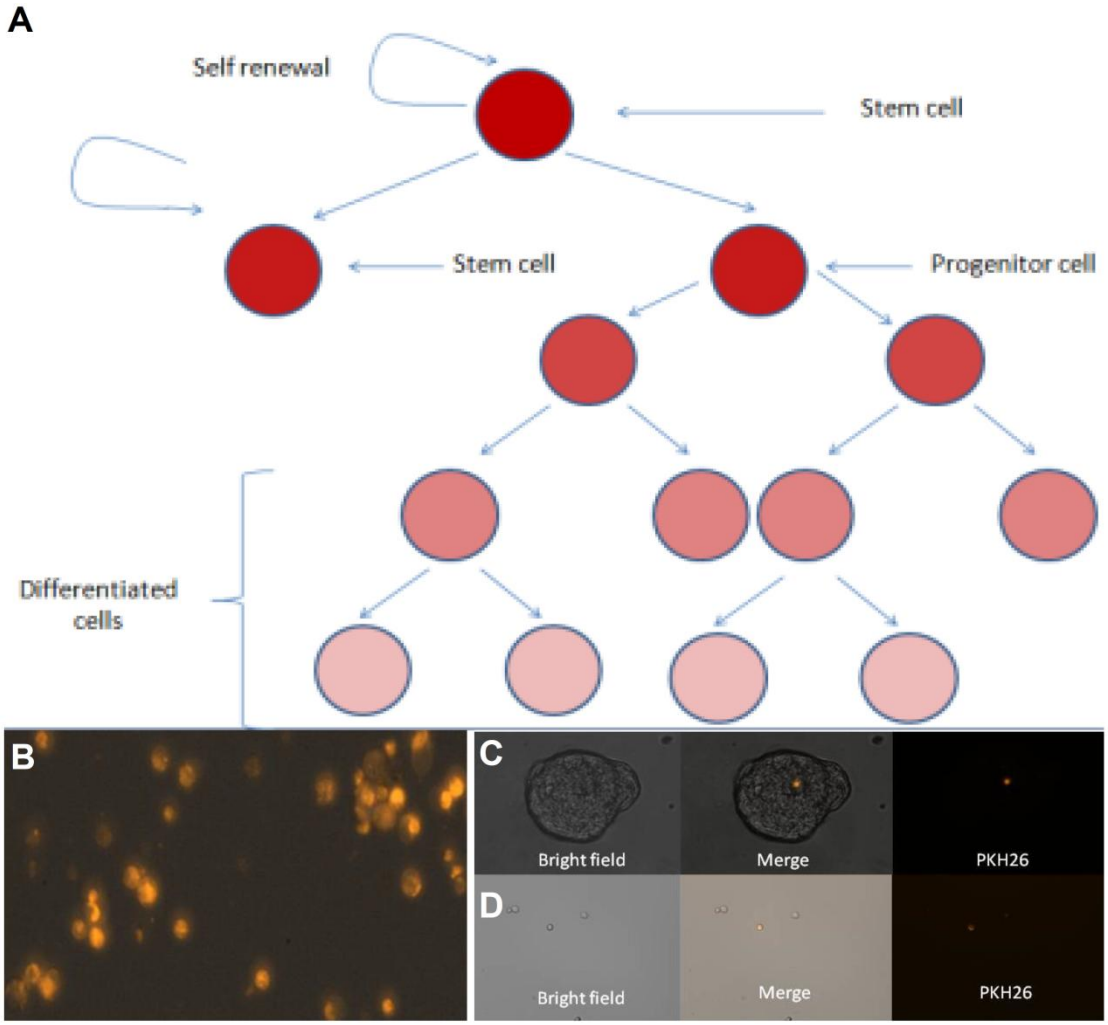

Figure 28. IL6 trans-signaling preserves the ability of stem cells to divide asymmetrically. (A) Mammary stem cells are slow cycling cells which divide into one slow cycling self-renewed stem cell and one faster dividing progenitor cell; (B) PKH26 labeling of cells isolated from the donor's tissue specimens; (C) Detection of the slow dividing, label retaining cells (LRC) and faster dividing non LRC (nLRC), PKH26-negative cells. nLRC eventually diluted the dye to undetectable levels. The results were confirmed by utilizing 10 tissue specimens.

Taken together, the activation of IL6 trans-signaling enhances self-renewal capacity and proliferation of normal mammary stem and progenitor cells, while doesn't influence their ability to differentiate and asymmetrically divide. Furthermore,

ability to identify stem and progenitor cells within single mammosphere by label retention provided an opportunity to assess the effect of IL6 trans-signaling on mammary stem and progenitor cells.

3.7. Activation of IL6 trans-signaling induces mammosphere forming ability of nLRC

Secondary mammospheres can differentiate into all epithelila lineages of a differentiated mammary gland. I used LRC and nLRC to narrow down the identity of mammary stem cells.

3.7.1. nLRC are not able to form mammospheres unless IL6 trans-signaling is activated

LRC are rare and slow dividing cells and thus represent good candidates for mammosphere founder cells. To test whether LRC are able to form mammospheres, single LRC and non-LRC (nLRC) were transferred to a 96 well plate and monitored for a period of two weeks for a single cell survival and mammosphere formation (Figure 29 a).

In total, 4 out of 97 plated single LRC proliferated and formed mammospheres indicating the ability of LRC to form mammospheres. However, nLRC of the mammospheres obtained from the same tissue donors (n=4) did not show the ability to form mammospheres (0/175) (Figure 29 b).

The ability of mammary cells to secrete soluble factors such as cytokines, which could in turn stimulate cell proliferation, proposed that nLRC propagation in condition medium (CM), may be beneficial for mammosphere formation. CM is mammosphere medium which was used for propagation of mammary cells. In prior to use, CM was filtered trough 0,45 µm filters to omit the cellular presence. However, nLRC propagated in condition medium (CM) did not trigger mammosphere formation as none of the 180 plated cells formed mammospheres (Figure 29 b).

Although nLRC cells were not able to form mammospheres, propagation of nLRC obtained from the same tissue specimens in mammosphere media supplemented with HIL6 resulted in mammosphere formation (5/179) suggesting important role of IL6 trans-signaling in mammosphere formation (Figure 29 b).

Obtained results suggested that mammosphere forming ability of LRC may be a result of an autocrine activated IL6 trans-signaling. Therefore, the co-expression of *IL6* and *IL6R* in LRC and nLRC was tested. *IL6* and *IL6R* expression was assessed in nLRC and LRC isolated from 9 tissue specimens. The percent of the cells expressing *IL6* or *IL6R* was higher in case of LRC compared to nLRC (Figure 29 c). Next, the co-expression of *IL6* and *IL6R* in nLRC and LRC was assessed. The result indicated a tendency of LRC to co-express *IL6* and *IL6R* more frequently compared to nLRC (LRC vs. nLRC=13% vs. 6%) (Figure 29 d).

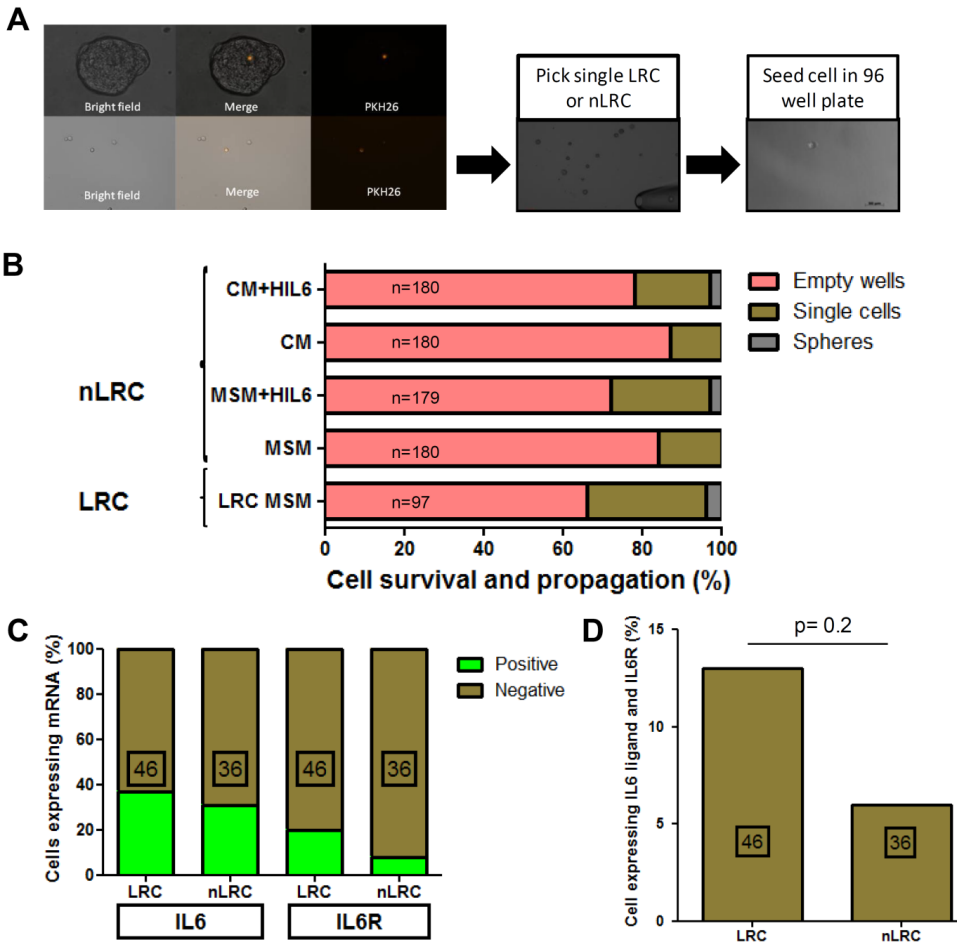

Figure 29. LRC and HIL6 treated nLRC encompass mammosphere forming ability. (A) Experimental strategy. LRC and nLRC were isolated from the secondary mammospheres, plated in a 96-well plate and observed for 2 weeks for a mammosphere formation or cell survival; (B) LRC and HIL6 treated nLRC formed mammospheres. nLRC maintained in condition medium without HIL6 did not develop mammospheres; (C) LRC and nLRC express *IL6* and *IL6R*; (D) LRC and nLRC co-express *IL6* and *IL6R* (p= 0.2 two-sided Fisher's exact test). The results were obtained using 15 tissue specimens (n=15).

The acquisition of the mammosphere forming ability, the characteristic of stem cells, by triggering IL6 trans-signaling in progenitor cells suggested the influence of IL6 signaling in mammary cell hierarchy. Cellular hierarchy is also in particular important for breast cancer and cancer stem cell concept and therefore, I tried to address the impact of IL6 trans-signaling in cancer stem and non stem cells.

3.8. IL6 trans-signaling in breast cancer

IL6 trans-signaling affects stem and progenitor cells proliferation and self-renewal, while it maintains stem cell characteristics such as, asymmetrical cell division and differentiation ability. Moreover, activation of the IL6 trans-signaling enables nLRC to acquire the mammosphere forming ability what is rather the characteristic of LRC. Therefore, IL6 trans-signaling may also have a role in propagation and proliferation of cancer stem cells (CSC) and thereby affect tumor growth.

3.8.1. Breast cancer cells do not contain membrane-bound IL6R

Breast cancer cell lines derived from primary tumor and metastasis (BT474, MCF7, SKBR3, T47D, MDA-MB-231) were used to test whether IL6 signals in cancer cells via membrane bound IL6R.

The cancer cells were propagated under conventional 2D culture conditions or under 3D mammosphere conditions. After cell detachment and disaggregation, cells were stained with antibodies against the IL6R. None of the examined cell lines was found to express the membrane bound form of the IL6R (Figure 30 a-e) suggesting that IL6 signaling might be maintained in breast cancer cell lines via trans-signaling.

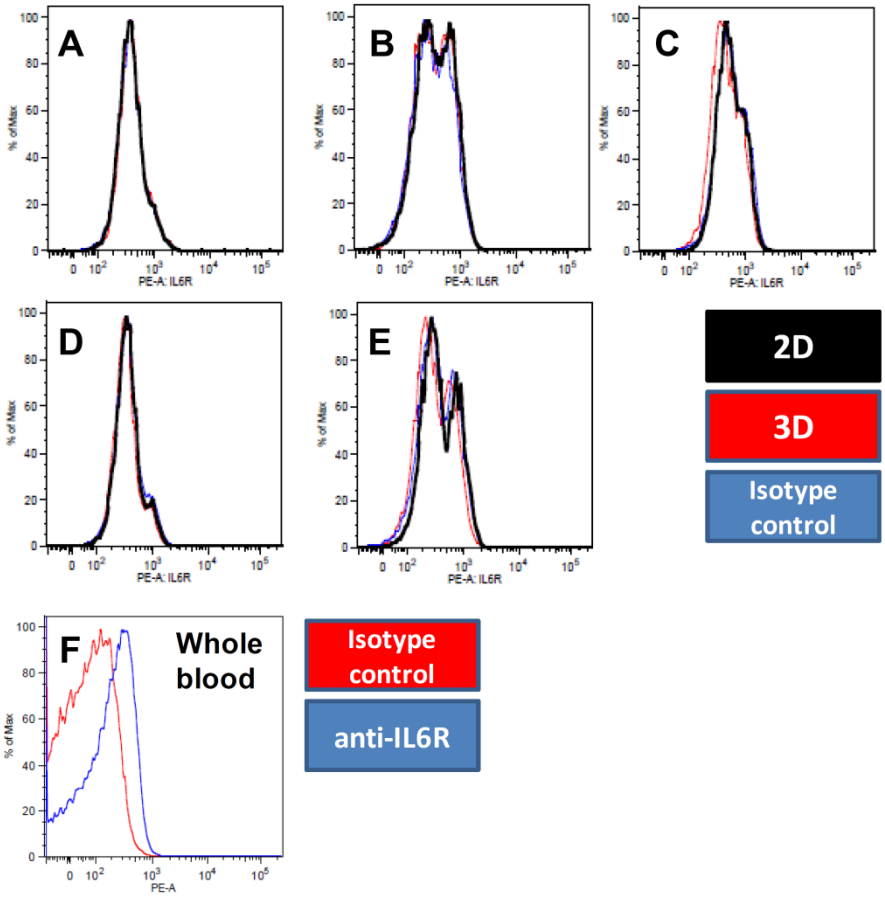

Figure 30. The expression of IL6R in breast cancer cell lines. The expression of membrane-bound IL6R was assayed by FACS. (A) BT474, (B) MCF7, (C) SKBR3, (D) T47D, (E) MDA-MB-231, (F) Whole blood of a healthy individual was used as a positive control. Biotinilated anti-IL6R antibody, UV-4 clone and mouse IgG1 κ, isotype control were used for FACS analysis. The results were confirmed by independent experiments (n=2).

3.8.2. MDA-MB-231 cells express IL6 and IL6R

The lack of the membrane bound IL6R in cancer cells raised a question whether breast cancer cells exploit IL6 trans-signaling. To test this hypothesis transcription of *IL6* and *IL6R* in breast cancer cells were assessed. MDA-MB-231 cells were propagated under 2D or 3D conditions and mRNA of single cancer cells were isolated and after reverse transcription tested for the presence of *IL6* or *IL6R* transcripts by gene specific PCR. Results showed that MDA-MB-231 cells propagated under the 3D conditions expressed in a higher level *IL6* and *IL6R* compared to cells propagated as a 2D monolayer (Figure 31 a).

Interestingly, the activation of IL6 signaling by the addition of external IL6

resulted in the higher number of obtained spheres indicating that observed cells secrete sIL6R. The effect in the sphere formation ability and cancer cell proliferation was even more striking if the trans-signaling was directly triggered by HIL6 application. On the other hand, blocking of the IL6 signaling resulted in reduced numbers of mammospheres and reduced proliferation shown by the mammosphere size (Figure 31 b-c).

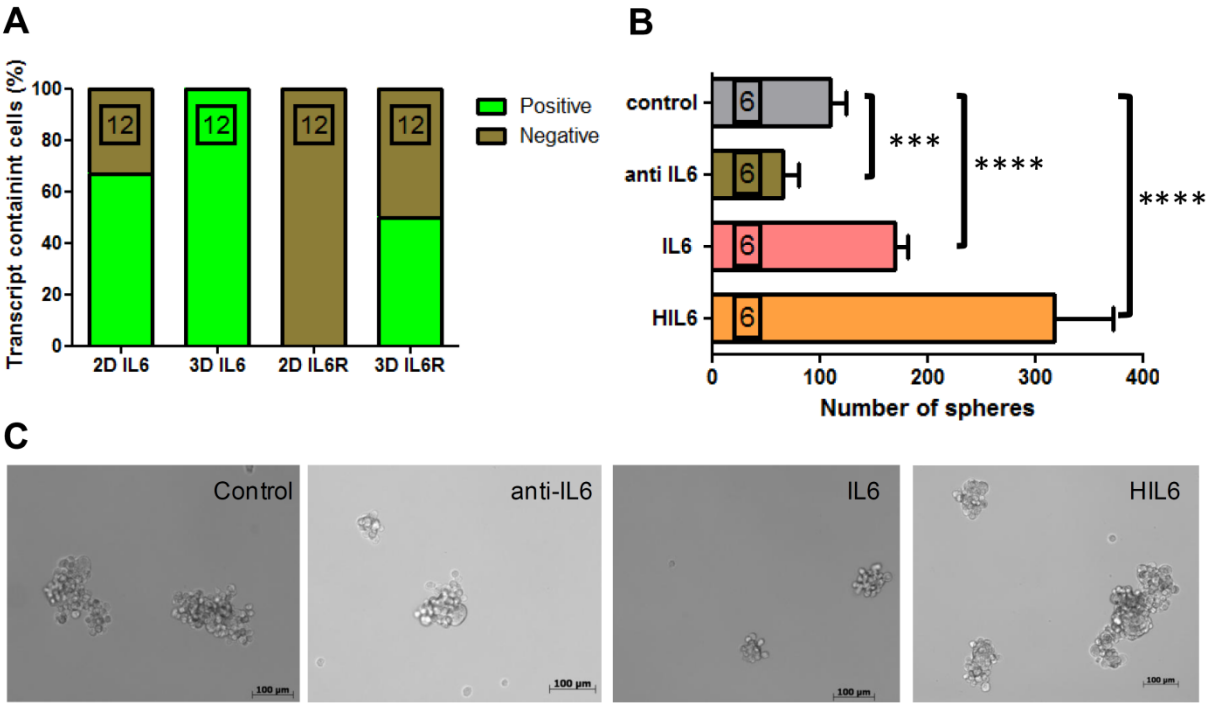

Figure 31. IL6 trans-signaling in MDA-MB-231 cells. (A) MDA-MB-231 cells express *IL6* and *IL6R* and thus enable IL6 trans-signaling; (B) IL6 trans-signaling induced sphere formation and (C) IL6 trans-signaling stimulated cell proliferation under 3D conditions. Results represent a mean of 3 experiments (n=3), each performed in technical replicates. (*** p= 0.0001, two- tailed unpaired t-test; **** p< 0.0001, two- tailed unpaired t-test).

The obtained results indicated that IL6 trans-signaling activates proliferation and survival of MDA-MB-231 cells under anchorage independent conditions and thus may affects their cancer stem cell phenotype.

3.8.3. IL6 trans-signaling stimulates tumor formation of MDA-MB-231 cells

Cancer stem cells are defined as cells able to grow tumors in animal hosts. Since IL6 trans-signaling promoted survival and proliferation of cancer cells under anchorage independent conditions the impact of activated IL6 signaling for MDA-MB-231 tumor formation *in vivo* was tested.

IL6 trans-signaling was activated by incubation of the cells with HIL6, while IL6 signaling was blocked by the application of blocking antibody. The influence of IL6 trans-signaling on tumor formation, tumor size and metastasis formation were analyzed by inoculation of cells pre-incubated with either HIL6 or blocking antibody (Figure 32 a).
The MDA-MB-231 cells were propagated under 2D conditions and and treated either with HIL6 or blocking antibody 4 hours before inoculation. The pre-treated MDA-MB-231 cell were inoculated into pre-cleared mammary fat-pad of NSG mice (Figure 32 a). The effect of IL6 trans-signaling was evaluated seven weeks post-inoculation. The tumors of mice inoculated with HIL6 pre-treated MDA-MB-231 cells were in average twice bigger compared to tumors of a control group (HIL6 vs. PBS = 425 mm^3 vs. 237 mm^3). Interestingly, despite the differences in a tumor growth, there were no evidences that IL6 trans-signaling influences metastasis formation.

The obtained results proposed that IL6 trans-signaling induces CSC propagation *in vivo* and influences tumor outgrowth.

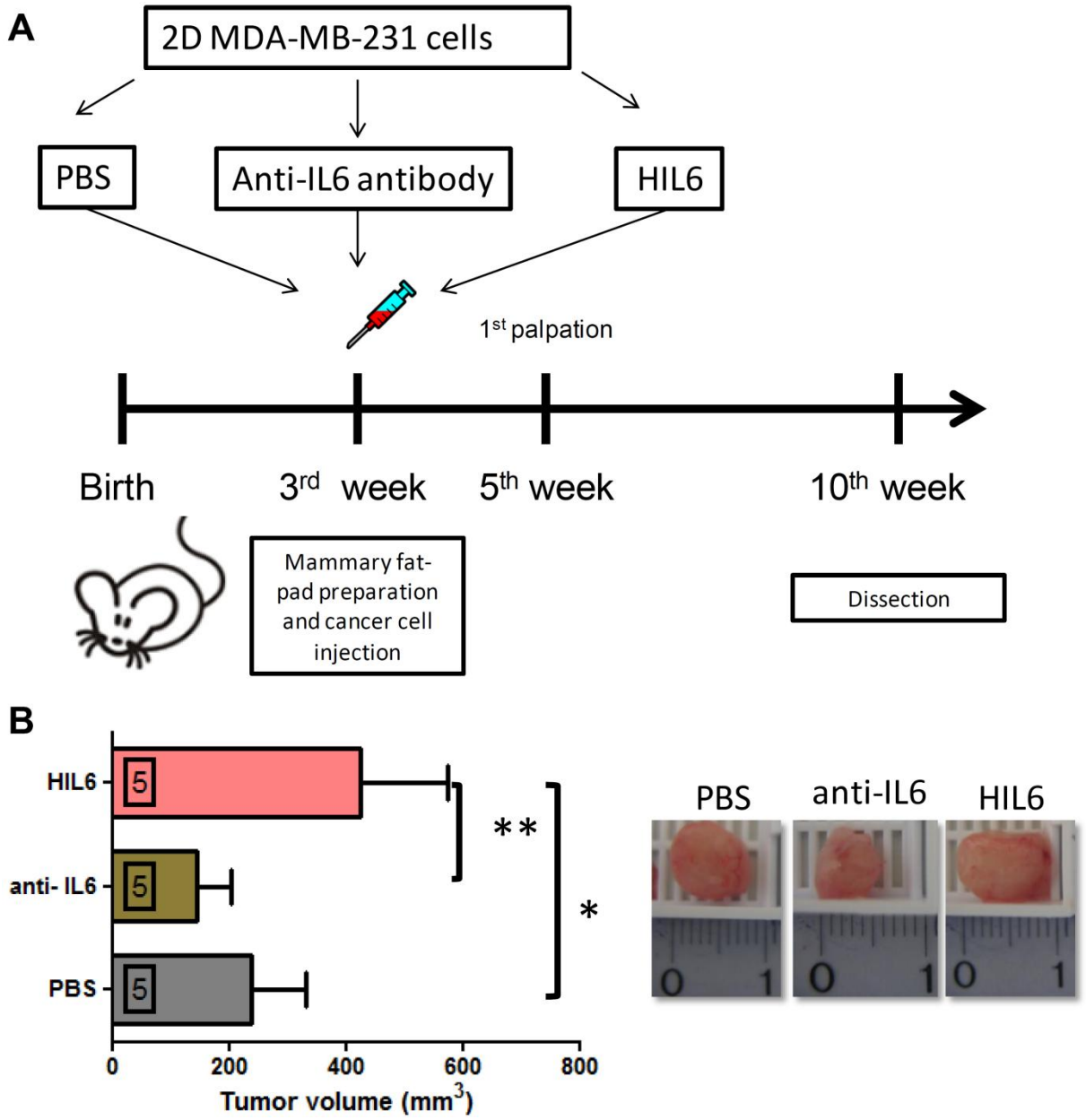

Figure 32. IL6 trans-signaling induces tumor formation *in vivo*. (A) Experimental strategy. MDA-MB-231 cells were treated for 3 hours with HIL6, IL6 singling blocking antibody or PBS. Mice were analyzed seven weeks post inoculation. (B) Activation of the IL6 trans-signaling in MDA-MB-231 cell line induced formation of tumors with higher volume compared to PBS control (PBS vs. HIL6 p= 0.04; anti-IL6 vs. HIL6 p=0.004; two- tailed unpaired t-test). Results were obtained from a group of 15 mice (n=15).

3.8.4. Activation of IL6 (trans)-signaling does not induce proliferation of MCF7 derived CSC

Since activation of PI3K/Akt signaling in HME cells resulted in higher sphere forming ability and decreased number of IL6 and IL6R expressing cells, I aimed to explore whether IL6 induces CSC phenotype as observed in MDA-MB-231 cells via downstream increase in PI3K/Akt signaling.

MCF7 cancer cells do not express membrane bound IL6R (Figure 33 a) and have constitutive increase in PI3K/Akt signaling due to the activated mutation in exon 9 of *PIK3CA* and thus represent a good model for testing whether IL6 induces CSC phenotype via increase in PI3K/Akt signaling.

Transcriptom of MCF7 cells propagated under 2D and 3D conditions were isolated and reversely transcribed. The *IL6* and *IL6R* expression assessment indicated that low number of MCF7 cells express *IL6* mRNA (1/22, 5% in 2D) while number of cells expressing *IL6R* was extensively increased when cells were propagated under 3D conditions (2D= 1/22 vs. 3D= 12/12) (Figure 33 b). Although assessment of transcription suggested that IL6 trans-signaling could be triggered by expressional activity of MCF7 cells, analysis of growth media showed that MCF7 cells secrete low levels, if any of IL6 (Figure 33 c). Interestingly, MCF7 cells grown under anchorage independent conditions expressed low levels of sIL6R what was in line with results obtained from transcriptom analysis (Figure 33 b c).

As MCF7 cells produce low levels of IL6 and sIL6R, I hypothesized that activation of IL6 trans-signaling by application of HIL6 may affect CSC phenotype as observed in MDA-MB-231 cells.

MCF7 cells were propagated 7 days under anchorage independent conditions in mammosphere medium supplemented by HIL6 or IL6. Interestingly, activation of IL6 trans-signaling by addition of HIL6 or IL6 did not resulted in increased number of observed spheres.

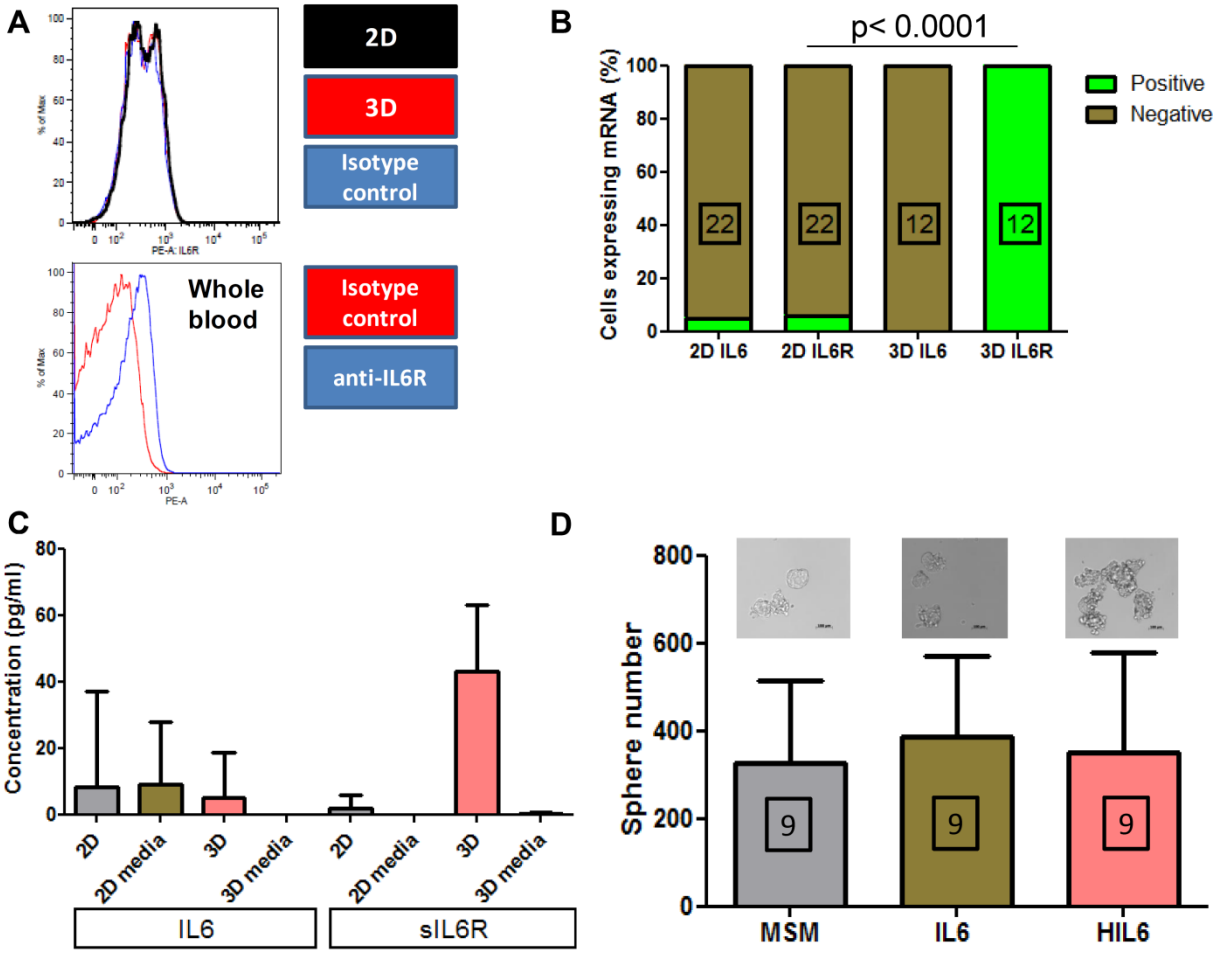

Figure 33. IL6 signaling in MCF7 cells. (A) MCF7 cells propagated under anchorage independent conditions (3D) or under 2D conditions do not express membrane bound IL6R as shown by flow cytometry; (B) Assessment of *IL6* and *IL6R* expression in single MCF7 cells propagated under 2D conditions or sphere propagated under 3D conditions (*IL6R* expression 2D vs. 3D p<0.0001, Fisher's exact test); (C) Assessment of IL6 and sIL6R protein in growth media of MCF7 cells propagated under 2D or 3D conditions (n=3, IL6 2D vs. 2D media p= 0.938, two- tailed unpaired t-test; n=3, sIL6R 3D vs 3D media p=0.002; two- tailed unpaired t-test); (D) IL6 trans-signaling does not influence sphere forming ability of MCF7 cells. MCF7 cells were propagated in mammosphere medium (MSM), MSM supplemented with IL6 or MSM supplemented with HIL6. (MSM vs IL6 p= 0.589; MSM vs. HIL6 p=0.836; IL6 vs. HIL6 p=0.777 two- tailed unpaired t-test). Results represent mean of 3 experiments (n=3), each experiment was performed in technical replicates.

Taken together these data suggest that activation of IL6 trans-signaling in MCF7 cells, breast cancer cells which have constitutively activated PIK3/Akt signaling, does not influence CSC phenotype.

4. Discussion

The adult mammary gland is a complex organ composed of epithelial derived ducts surrounded by connective tissue and adipose tissue lobes (Sheffield, 1988). The development of the human mammary gland is driven by mammary stem cells and occurs in three distinct and differentially regulated stages: embryonic, pubertal and adult (Anbazhagan et al., 1991; Gjorevski and Nelson, 2011; Howard and Gusterson, 2000). Although mammary gland development starts early during ontogeny, most of developmental processes occur postnatal. More precisely, mammary glands reach functional maturity at late pregnancy during a process known as lactation (Radisky and Hartmann, 2009). At this stage the mammary gland is mostly composed of secretory terminally differentiated epithelia (>90%) and low numbers (0,2-0,45%) of undifferentiated adult stem and progenitor cells (Alvi et al., 2002; Borellini and Oka, 1989). Adult mammary stem and progenitor cells enable cyclic bursts of proliferation and differentiation which take place at each pregnancy cycle (Van Keymeulen et al., 2011). However, these cell populations are also a source of various breast abnormalities. Deregulation of the both stromal and epithelial stem cells cause breast hypertrophy, which manifests as abnormal breast sizes, or cancer (Dancey et al., 2008; Dehner et al., 1999; Ginestier et al., 2007b).

Breast cancer accounts as the most frequent cancer type among women. Only in 2008, breast cancer caused 458 503 deaths worldwide (WHO, 2008). It has been proposed that breast cancer development is driven by a small population of cancer stem cells (CSC), rare tumor clones able to grow tumors in animal hosts which also can differentiate into non-CSC (Clarke et al., 2006). The current CSC concept suggests that disease relapse and later progression is largely due to the intrinsic therapy resistance of CSC (Gupta et al., 2009). Although the first experiments suggested that CSC are transformed normal stem cells, the CSC concept also suggests that the target cell of malignant transformation may be differentiated cells which acquire malignant and stem cells properties by the transformation process (Bjerkvig et al., 2005).

It was suggested that acquisition of CSC phenotype is facilitated trough activation of

epithelial to mesenchymal transition (EMT), a developmental process that enables epithelial cells to acquire a mesenchymal phenotype. This data suggest that EMT not only comprises the ability to migrate but also stem cell properties such as self-renewal and differentiation through activation of a set of transcription factors (Mani et al., 2008). The activation of EMT is a result of a complex interaction of normal and cancer cells with the micro-environment composed of stromal and infiltrating cells and adjacent extracellular matrix (Hanahan and Weinberg, 2011; Lee et al., 2007). Moreover, the extracellular matrix has been described as a functional unit of the mammary gland, which regulates mammary gland differentiation, development and proliferation (Schedin et al., 2004; Wicha et al., 1980). Extracellular matrix maintains paracrine and autocrine signaling networks by storing and supplying cells with soluble factors such as Interleukin 6 (Bonafe et al., 2012; Maller et al., 2010).

IL6 signals in mammary cells via soluble IL6 receptor

Despite considerable knowledge about the development and the regulation of mammary gland function under physiological and pathophysiological conditions, the effect of Interleukin 6 (IL6) in normal and cancer stem cells is largely unknown. IL6 is a multifunctional cytokine which has a role in many diseases (Kishimoto, 2005). IL6 signaling is activated through IL6 binding to specific membrane-bound IL6 receptor (IL6R) while the subsequent interaction of IL6-IL6R complex with gp130 leads to signal initiation (Kishimoto, 2005; Korkaya et al., 2011; Scheller et al., 2006). Sansone and colleagues demonstrated that activation of IL6 signaling induces an autocrine loop which triggers self renewal of normal mammary stem and progenitor cells in mammary glands (Sansone et al., 2007). Therefore, I tried to assess whether mammary stem and progenitor cells regulate their phenotype via higher expression of membrane-bound IL6R compared to more differentiated cells. Stem and progenitor cells were enriched by propagation of cells under 3D, anchorage independent growth conditions (Dontu et al., 2003a; Sansone et al., 2007) and compared to cells propagated under conventional 2D growth condition. Surprisingly, assessment of membrane bound IL6R expression by flow cytometry suggested that neither MCF10A nor HME wt cells express membrane bound IL6R. Moreover, enrichment of stem and progenitor cells did not result in detectable membrane-bound IL6R expression in both cell lines. This finding challenged my observation that application of IL6 induces

sphere-forming ability of HME wt and MCF10A and thus stimulates stem and progenitor phenotype. Moreover, lack of membrane bound IL6R on MCF10A and HME wt cells challenged the current view on IL6 signal transduction in mammary cells as it has been suggested that IL6 signals in mammary cells via membrane bound IL6R (Grivennikov and Karin, 2008).

An alternative mechanism to activate IL6 signaling involves trans-signaling. Expression of IL6R is not restricted only to a membrane bound form, analysis of human sera confirmed presence of soluble form of IL6R (sIL6R) (Montero-Julian, 2001) which can trigger mechanism known as IL6 trans-signaling (Scheller et al., 2006). I therefore investigated whether mammary cells express IL6 and sIL6R and thus utilize IL6 trans-signaling. The assessment of *IL6R* transcription showed that normal mammary cells, MCF10A and HME wt cells, express *IL6R* and *IL6* mRNA. Subsequently, both proteins could be detected in media of the cells indicating that all the pre-requisites for trans-signaling are available. The assessment of *IL6* and *sIL6R* mRNA co-expression suggested that due to the low frequency of cells able to co-express *IL6* and *sIL6R,* IL6 trans-signaling in mammary cells is rather maintained in a paracrine way or rarely in an autocrine manner by co-expressing cells.
For these analysis, it cannot be excluded that sensitivity of flow cytometry was insufficient to detect low surface receptor expression (Kishimoto, 2005). However, even in such a scenario IL6 trans-signalling should be considered as a mechanism of an autocrine/paracrine regulation in mammary cells. Indeed, activation of IL6 trans-signalling by addition of IL6 or Hyper-IL6 (HIL6), a fusion protein of IL6 and sIL6R, had an effect on mammary cell propagation under anchorage independent conditions. These findings pointed to a direct impact of IL6 trans-signalling on mammary stem and progenitor cells.

IL6 trans-signaling activates propagation of normal mammary stem cells

IL6 can activate stem cell signalling pathways such as Notch signalling pathway in cancer cells. This pathway is particularly involved in the formation of mammospheres (Sansone et al., 2007). The mammosphere assay enables propagation of mammary stem and progenitor cells (Dontu et al., 2003a) in form of spherical colonies, which arise from a single stem cell (Liu et al., 2008). It is assumed that the number of

mammospheres represents the initial number of stem cells, while the mammosphere size represents the proliferative capacity of stem and progenitor cells contained within the single colony.

The data presented here suggest that IL6 trans-signalling has a broader effect. It activates propagation of the non cancer stem cells and enables them to form mammospheres, since activation of IL6 trans-signalling increased total mammosphere numbers and average mammosphere sizes. Inactivation of the IL6 signalling pathway by IL6R blocking antibody affected the outgrowth of mammospheres, but did not result in total ablation of the mammospheres, suggesting that IL6 signalling is supportive, but not the only determining factor for the establishment of stem and progenitor phenotype.

IL6 signals via activation of JAK/STAT, SHP2/Ras and PI3K/Akt signaling pathways (Kishimoto, 2005). Therefore, blocking an upstream effector of these pathways such as IL6 may not be sufficient for ablation of the stem cell phenotype. Interestingly, I found that up-regulation of the PI3K/Act signalling by activating mutations resulted in higher numbers of observed mammospheres, while *IL6* and *IL6R* transcription was down-regulated. These experiments were performed using isogenic cell lines where the transformed normal mammary cell line HME had been modified by knocking in a mutated exon 20 of *PIK3CA*. In these cells I could not detect cells co-expressing *IL6* and *IL6R*. The cross-regulation of the PI3K/Act signalling pathway and the IL6 signalling pathway in cancer cells might be of particular importance for breast cancers with deregulated PI3K pathway or higher IL6 levels (Bachelot et al., 2003), as *PIK3CA* is one of the most frequently mutated genes in breast cancer (Adams et al., 2011). On the other hand, it could well be that mutations of *PIK3CA* enable cancer cells to become independent of IL6 trans-signalling. Therefore, it was important to assess whether trans-signalling has a physiological role in mammary glands.

Since the adult mammary gland is composed of both epithelial and mesenchymal derived cells, IL6 trans-signalling may be triggered as a result of the secretory activity of different cell types. Indeed, it has been proposed that fibroblasts are the major source of IL6 in various organs and in cancer (Bonafe et al., 2012) and thus may

contribute to IL6 trans-signaling. I therefore explored the mechanism of IL6 trans-signaling activation in normal adult mammary glands.
Digested mammary glands were analyzed by FACS for the expression of membrane bound IL6R. The results indicated that normal adult mammary gland does not contain a cell population that expresses membrane bound IL6R. Therefore, I explored whether mammary gland is able to utilize IL6 trans-signaling. Transcriptom analysis of cells isolated from the adult mammary gland indicated presence of cells expressing *IL6* and *IL6R* suggesting that IL6 signaling is maintained in adult mammary glands via trans-signaling. Next, it was explored which of the cellular populations within adult mammary gland expresses *IL6* and *IL6R.* Therefore transcriptoms of (1) terminally differentiated mammary cells; (2) adult mammary stem and progenitor cells and (3) normal mammary fibroblasts were analyzed for the expression of *IL6* and *IL6R.* Surprisingly, although terminally differentiated mammary epithelial cells represent more than 90% of all epithelial cells within adult mammary glands (Stingl et al., 2005) they fail to express *IL6* or *IL6R*. However, the same analysis suggested that IL6 trans-signaling is enabled in adult mammary gland due to expression of *IL6* and *IL6R* by mammary fibroblasts, stem and progenitor cells. Moreover, mammary fibroblasts expressed high levels of IL6 as assessed by analysis of protein secreted in growth media. Mammary fibroblasts showed over 10 fold higher expression of IL6 compared to HME wt cells confirming that fibroblasts are one of the major sources of IL6 (Bonafe et al., 2012). Thus, it is suggested that IL6 trans-signalling in adult mammary gland is maintained via trans-signaling.

IL6 trans-signaling triggers a stem cell phenotype in mammary cells

Activation of IL6 trans-signaling in fresh ex-vivo isolated mammary glands by addition of IL6 increased the number of mammospheres and induced their proliferative ability as measured by the mammosphere size. These data indicated that IL6 induces normal mammary stem/progenitor cell proliferation. However, IL6 trans-signaling in adult mammary gland could be generated with the help of mammary fibroblasts. Therefore, I aimed to assess the responsiveness of mammary stem and progenitor cells to IL6 trans-signaling via application of HIL6. Propagation of mammary stem and progenitor cells in presence of HIL6 substantially increased mammosphere formation and proliferation as measured by number of obtained mammospheres and

their size. Thus, mammary stem and progenitor cells readily respond to IL6 trans-signaling.

In the next step, I tried to address whether IL6 trans-signaling influences stem cells characteristics such as self-renew ability, differentiation capacity and ability to divide asymmetrically (Pece et al., 2010; Smalley and Ashworth, 2003).
Self-renewal was measured by the ability of mammospheres to be serially passaged (Aceto et al., 2012). The normal adult mammary stem and progenitor cells can be maintained over several weeks under anchorage independent conditions until they ultimately stop propagating and undergo cellular senescence (Dontu et al., 2003a). HIL6 treated mammospheres were propagated up to 6 passages while non-activated cells were propagated for up to 4 passages. This result indicated that activation of IL6 trans-signaling triggers self-renewal capacity of the adult mammary stem and progenitor cells. Furthermore, it specifies the findings of Sansone and colleagues who attributed similar effects in breast cancer cells to conventional signaling (Sansone et al., 2007).
The differentiation ability of stem and progenitor cells was investigated *in vitro* by cell propagation in 3D Matrigel© and by differentiation of mammary stem and progenitor cells in immunodeficient mice (Lee et al., 2007; Proia and Kuperwasser, 2006). Quantification of the *in vitro* differentiation ability indicated that activation of IL6 trans-signaling in adult mammary stem and progenitor cells preserves differentiation ability as shown by the formation of acini and TDLU structures. The small insignificant differences in overall numbers of the TDLU structures between HIL6 treated and untreated cells may be interpreted as a result of the experimental setting rather than reflects biology. Ultimately, human mammospheres propagated in presence of HIL6 showed differentiation ability *in vivo* by forming complex structure resembling human adult mammary gland when inoculated in pre-cleared mammary fat-pad of NSG mice. Together, this data showed that IL6 trans-signaling does not negatively influence the differentiation ability of mammary stem cells.
As an aside, the *in vivo* experiments led to a novel *in vivo* differentiation assay, which overcomes substantial experimental hurdles. Co-injection of murine fibroblasts instead of human hTERT immortalized fibroblasts led to significantly higher engraftment of normal human mammary stem cells and abolished the need for a two-

step surgical transplantation protocol. The resulting protocol is fairly simple and might be used as an efficient and reproducible orthotopic xenotransplantation model in mammary gland biology.

During asymmetrical stem cell divisions, stem cells give rise to two daughter cells of different phenotype. One cell is a stem cell with self-renewal ability, while the other daughter cell is a progenitor cell (Smalley and Ashworth, 2003). Based on the assumption that stem cells are rarely and slow dividing cells, I exploited a method introduced by Pece and colleagues to mammary stem cell biology (Pece et al., 2010). The protocol uses the ability of unspecific membrane dyes to mark cells which, upon division, provide each progeny with half of the dye. Thus, the marker molecule is diluted upon each cell division. Since stem cells (sphere forming cells) are slow dividing cells, asymmetrical division of mammary stem cells can be monitored by dilution of unspecific dye during mammosphere outgrowth in the majority of rapidly dividing progenitor cells (Pece et al., 2010), whereas rarely dividing stem cells would stay labeled (so called “label retaining cells”) over several culture passages. In these experiments, surgical specimen were digested, the epithelial cell fraction labeled with the unspecific fluorescent membrane dye PKH26 and propagated in mammosphere medium containing HIL6 or in control medium. Two weeks post labeling, HIL6 treated and untreated secondary mammospheres showed presence of rare label retaining cells (LRC) indicating that asymmetrical cell division is not affected by IL6 trans-signaling. Therefore, it seems unlikely that the increase of mammospheres by HIL6 is caused via the generation of symmetrically dividing cells.

IL6 trans-signaling induces stem cell phenotype in progenitor cells

Consequently, I aimed to directly address role of IL6 trans-signaling in stem and in progenitor cells. Using the assay mentioned above, stem cells were identified as label retaining cells (LRC), while the label non-retaining cells (nLRC) were identified with progenitor cells. The functional difference between LRC and nLRC was assessed by the ability of single stem cells (LRC) to form mammospheres. While single LRC were able to form mammospheres, single nLRC were able to grow as mammospheres only when supplemented by HIL6. Obviously, IL6 trans-signaling modified the functional phenotype of progenitor cells by inducing stem-like

characteristics. Thus, the increased number of the secondary mammospheres observed upon activation of IL6 trans-signaling is a result of acquisition of mammosphere forming ability of progenitor cells rather than influence of IL6 trans-signaling on mammary stem cells. Of interest, assessment of *IL6* and *IL6R* expression revealed a tendency of LRC to co-express *IL6* and *IL6R,* suggesting that physiological IL6 trans-signaling is involved in stem cell-renewal in an autocrine way.

IL6 trans-signaling enables CnCS-CSC conversion in breast cancer

Increased levels of IL6 in sera of breast cancer patients correlate with poor disease prognosis (Bachelot et al., 2003) what suggested that IL6 signaling plays an important role in shaping aggressive phenotype of breast cancer. This finding was supported by observations observation that malignant transformation may trigger IL6 signaling (Iliopoulos et al., 2011). On the background of the CSC concept the results presented here suggested that IL6 trans-signaling acts upon progenitor cells and might affect the expansion of the CSC pool in breast cancer. Particularly, it may help non- stem cancer cells (CnSC) to acquire a CSC phenotype.
I explored this hypothesis in MDA-MB-231 cell line, a metastatic cell line derived from pleural effusion of a donor diagnosed with breast cancer. MDA-MB-231 shows highly aggressive phenotype as shown by *in vivo* propagation in immunodeficient mice (Minn et al., 2005). The measurement of *IL6* and *IL6R* expression in MDA-MB-231 cells suggested that propagation of MDA-MB-231 cells under anchorage independent conditions triggers *IL6* and *IL6R* expression. Thus, IL6 trans-signaling may be linked to the cancer stem cell phenotype in MDA-MB-231 cells. Moreover, activation of IL6 trans-signaling by application of HIL6 resulted in considerable increased proliferation of MDA-MB-231 cells under anchorage independent conditions. When MDA-MB-231 cells were bathed in HIL6 containing medium and subsequently transplanted into NSG mice, tumors grow much faster, while block of IL6 signaling by single shot treatment with blocking antibody resulted in decreased tumor volume. Interestingly, blocking IL6 signaling pathway reduced proliferation of CSC *in vitro* and *in vivo* but did not resulted in complete ablation of CSC indicating that IL6 signaling is an important but not the only determinant of the CSC phenotype. On the other hand, outgrowth of tumors from cells blocked for IL6 signaling might be a consequence of re-establishment of IL6 signaling pathway due to the long lasting *in vivo* experiment.

The results obtained from transformed normal mammary HME cells (see above) suggested that the deregulation of PI3K/Akt signaling effects expression of *IL6* and *IL6R.* PI3K/Akt signaling is frequently deregulated in breast cancer (Adams et al., 2011). Therefore, I tried to explore the effect of IL6 trans-signaling in MCF7 cells, which have constitutive active PI3K/Akt signaling due to a mutation in exon 9 of *PIK3CA* gene (Sanger-Institute, 2013). The assessment of *IL6* and *IL6R* expression indicated low frequency of MCF7 cells expressing *IL6* and *IL6R* and subsequent low protein expression. Surprisingly, activation of IL6 trans-signaling by HIL6 did not result in increased number of observed mammospheres suggesting IL6 trans-signaling cannot add any significant stimulus in addition to the over-activation of PI3K/Akt pathway. Taken together, these data suggested that IL6 induced CSC phenotype via PI3K/Akt signaling.

Recent data suggested the existence of a “equilibrium force” which coverts CnSC to CSC and *vice versa* (Gupta et al., 2009). Others argued that such conversion might be facilitated in cancer cells by induction of IL6 signaling (Iliopoulos et al., 2011). The results presented in this work suggested that the underlying mechanism of the CSC to CnSC conversion and *vice versa* reflects the biology of normal adult mammary stem and progenitor cells where the stem cell phenotype might be influenced via autocrine/paracrine signals. The data are in line with a model where stromal cells may influence hierarchy of epithelial cells of an adult mammary gland via IL6 trans-signaling. This is of obvious relevance for the therapeutic implications of the CSC concept. The CSC proposes that only CSC can give rise to the disease relapse and metastasis and thus represent the only important therapy target which we currently miss. If however the CSC-CnSC hierarchy is not fixed, sole therapeutic eradication of CSC is unlikely to cure patients.

Taken together, the presented data in this work suggest that IL6 signals in mammary cancer and normal cells via utilization of sIL6R employing IL6 trans-signaling. Normal and cancer mammary cells are able to express IL6 and sIL6R and therefore may utilize IL6 trans-signaling in an autocrine or paracrine way.
In breast cancer cells IL6 trans-signaling resulted in increased proliferation of CSC. The results further indicated that IL6 trans-signaling induces stem cell characteristics via PI3K/Akt signaling pathway.

5. Summary

The mammary gland is a paired, tubuloalveolar, exocrine gland which produces milk in females. The mammary gland is an inhomogeneous organ composed of epithelial derived ductal- alveolar structures responsible for milk production surrounded by connective tissue immersed in the lobes of adipose tissue. Mammary glands reach functional maturity at late pregnancy during a process known as lactation. During this process extensive proliferation and differentiation is enabled by adult mammary stem cells. Regulation of mammary cell phenotype and function is regulated by various signaling pathways which are activated as a result of the dynamic interaction between mammary cells and micro-environment. Deregulation of stem cell signaling pathways has been suggested to drive breast cancer by maintaining cancer stem cells (CSC), cells that give rise to all other cancer cell types detected within the tumor and contribute to an invasive phenotype observed in metastatic breast tumors. As normal stem cells, CSC interact with micro-environment and these interactions involve inflammatory cytokines such as Interleukin 6 (IL6).

The aim of this work was to explore the effect of IL6 signaling in normal and malignant mammary stem and progenitor cells. Results indicated that activation of IL6 promotes proliferation of the normal and malignant stem and progenitor cells via mechanism know as IL6 trans-signaling. This mechanism is mainly activated via PI3K/Akt signaling. The obtained results suggested that the IL6 trans-signaling in normal mammary gland is activated in rather paracrine than autocrine way suggesting the role of mammary stromal cells in modulating hierarchy of epithelial cells. Indeed, the analysis of normal mammary gland indicated that fibroblasts, stem and progenitor cells but not terminally differentiated cells are able to trigger IL6 trans-signaling and thus may prompt self-renewal and proliferation of adult mammary stem and progenitor cells. Moreover, the results indicated that cancer cells utilize IL6 trans-signaling and via paracrine signaling induce CSC phenotype of observed cells.

Importantly, activation of IL6 trans-signaling resulted in acquisition of stem-like properties by normal progenitor cells. This is of obvious relevance for the therapeutic implications of the CSC concept. The CSC proposes that only CSC can give rise to

the disease relapse and metastasis and thus represent the only important therapy target which we currently miss. If however the CSC-CnSC hierarchy is not fixed, sole therapeutic eradication of CSC is unlikely to cure patients.

Altogether, IL6 signals in normal and malignant mammary cells via process known as trans-signaling. Paracrine and autocrine induced IL6 trans-signaling stimulates normal and malignant stem and progenitor cells and enables progenitor and CnSC to acquire stem-like cell phenotype.

6. Literature

Aceto, N., Sausgruber, N., Brinkhaus, H., Gaidatzis, D., Martiny-Baron, G., Mazzarol, G., Confalonieri, S., Quarto, M., Hu, G., Balwierz, P.J., *et al.* (2012). Tyrosine phosphatase SHP2 promotes breast cancer progression and maintains tumor-initiating cells via activation of key transcription factors and a positive feedback signaling loop. Nat Med *18*, 529-537.

Adams, J.R., Schachter, N.F., Liu, J.C., Zacksenhaus, E., and Egan, S.E. (2011). Elevated PI3K signaling drives multiple breast cancer subtypes. Oncotarget *2*, 435-447.

Alvi, A.J., Clayton, H., Joshi, C., Enver, T., Ashworth, A., Vivanco, M., Dale, T.C., and Smalley, M.J. (2002). Functional and molecular characterisation of mammary side population cells. Breast Cancer Res *5*, R1-8.

Anbazhagan, R., Bartek, J., Monaghan, P., and Gusterson, B.A. (1991). Growth and development of the human infant breast. Am J Anat *192*, 407-417.

Bachelot, T., Ray-Coquard, I., Menetrier-Caux, C., Rastkha, M., Duc, A., and Blay, J.Y. (2003). Prognostic value of serum levels of interleukin 6 and of serum and plasma levels of vascular endothelial growth factor in hormone-refractory metastatic breast cancer patients. Br J Cancer *88*, 1721-1726.

Bartek, J., Bartkova, J., and Taylor-Papadimitriou, J. (1990). Keratin 19 expression in the adult and developing human mammary gland. Histochem J *22*, 537-544.

Ben-Porath, I., Thomson, M.W., Carey, V.J., Ge, R., Bell, G.W., Regev, A., and Weinberg, R.A. (2008). An embryonic stem cell-like gene expression signature in poorly differentiated aggressive human tumors. Nat Genet *40*, 499-507.

Bjerkvig, R., Tysnes, B.B., Aboody, K.S., Najbauer, J., and Terzis, A.J. (2005). Opinion: the origin of the cancer stem cell: current controversies and new insights. Nat Rev Cancer *5*, 899-904.

Bonafe, M., Storci, G., and Franceschi, C. (2012). Inflamm-aging of the stem cell niche: breast cancer as a paradigmatic example: breakdown of the multi-shell cytokine network fuels cancer in aged people. Bioessays *34*, 40-49.

Borellini, F., and Oka, T. (1989). Growth control and differentiation in mammary epithelial cells. Environ Health Perspect *80*, 85-99.

Bundred, N.J. (2001). Prognostic and predictive factors in breast cancer. Cancer Treat Rev *27*, 137-142.

Campbell, J.J., Davidenko, N., Caffarel, M.M., Cameron, R.E., and Watson, C.J. (2011). A multifunctional 3D co-culture system for studies of mammary tissue morphogenesis and stem cell biology. PLoS One *6*, e25661.

CellsignalingTechnology (2012). IL6 signaling pathway.

Charafe-Jauffret, E., Ginestier, C., and Birnbaum, D. (2009). Breast cancer stem cells: tools and models to rely on. BMC Cancer *9*, 202.

Chepko, G., and Smith, G.H. (1997). Three division-competent, structurally-distinct cell populations contribute to murine mammary epithelial renewal. Tissue Cell *29*, 239-253.

Cianfrocca, M., and Goldstein, L.J. (2004). Prognostic and predictive factors in early-stage breast cancer. Oncologist *9*, 606-616.

Ciftci, K., and Levy, R.J. (2001). Enhanced plasmid DNA transfection with lysosomotropic agents in cultured fibroblasts. Int J Pharm *218*, 81-92.

Cirri, P., and Chiarugi, P. (2012). Cancer-associated-fibroblasts and tumour cells: a diabolic liaison driving cancer progression. Cancer Metastasis Rev *31*, 195-208.

Clarke, M.F., Dick, J.E., Dirks, P.B., Eaves, C.J., Jamieson, C.H., Jones, D.L., Visvader, J., Weissman, I.L., and Wahl, G.M. (2006). Cancer stem cells--perspectives on current status and future directions: AACR Workshop on cancer stem cells. Cancer Res *66*, 9339-9344.

Dancey, A., Khan, M., Dawson, J., and Peart, F. (2008). Gigantomastia--a classification and review of the literature. J Plast Reconstr Aesthet Surg *61*, 493-502.
Daniel, C.W., Young, L.J., Medina, D., and DeOme, K.B. (1971). The influence of mammogenic hormones on serially transplanted mouse mammary gland. Exp Gerontol *6*, 95-101.
Dehner, L.P., Hill, D.A., and Deschryver, K. (1999). Pathology of the breast in children, adolescents, and young adults. Semin Diagn Pathol *16*, 235-247.
Deome, K.B., Faulkin, L.J., Jr., Bern, H.A., and Blair, P.B. (1959). Development of mammary tumors from hyperplastic alveolar nodules transplanted into gland-free mammary fat pads of female C3H mice. Cancer Res *19*, 515-520.
Dontu, G., Abdallah, W.M., Foley, J.M., Jackson, K.W., Clarke, M.F., Kawamura, M.J., and Wicha, M.S. (2003a). In vitro propagation and transcriptional profiling of human mammary stem/progenitor cells. Genes Dev *17*, 1253-1270.
Dontu, G., Al-Hajj, M., Abdallah, W.M., Clarke, M.F., and Wicha, M.S. (2003b). Stem cells in normal breast development and breast cancer. Cell Prolif *36 Suppl 1*, 59-72.
Dontu, G., Liu, S., and Wicha, M.S. (2005). Stem cells in mammary development and carcinogenesis: implications for prevention and treatment. Stem Cell Rev *1*, 207-213.
Dontu, G., and Wicha, M.S. (2005). Survival of mammary stem cells in suspension culture: implications for stem cell biology and neoplasia. J Mammary Gland Biol Neoplasia *10*, 75-86.
Downs-Holmes, C., and Silverman, P. (2012). Breast cancer: Overview & updates. The Nurse Practitioner *36*.
Eirew, P., Stingl, J., Raouf, A., Turashvili, G., Aparicio, S., Emerman, J.T., and Eaves, C.J. (2008). A method for quantifying normal human mammary epithelial stem cells with in vivo regenerative ability. Nat Med *14*, 1384-1389.
Elston, C.W., and Ellis, I.O. (1991). Pathological prognostic factors in breast cancer. I. The value of histological grade in breast cancer: experience from a large study with long-term follow-up. Histopathology *19*, 403-410.
Elston, E.W., and Ellis, I.O. (1993). Method for grading breast cancer. J Clin Pathol *46*, 189-190.
Erbacher, P., Roche, A.C., Monsigny, M., and Midoux, P. (1996). Putative role of chloroquine in gene transfer into a human hepatoma cell line by DNA/lactosylated polylysine complexes. Exp Cell Res *225*, 186-194.
Ginestier, C., Hur, M.H., Charafe-Jauffret, E., Monville, F., Dutcher, J., Brown, M., Jacquemier, J., Viens, P., Kleer, C.G., Liu, S.*, et al.* (2007a). ALDH1 is a marker of normal and malignant human mammary stem cells and a predictor of poor clinical outcome. Cell Stem Cell *1*, 555-567.
Ginestier, C., Korkaya, H., Dontu, G., Birnbaum, D., Wicha, M.S., and Charafe-Jauffret, E. (2007b). [The cancer stem cell: the breast cancer driver]. Med Sci (Paris) *23*, 1133-1139.
Gjorevski, N., and Nelson, C.M. (2011). Integrated morphodynamic signalling of the mammary gland. Nat Rev Mol Cell Biol *12*, 581-593.
Gotze, K.S., Keller, U., Rose-John, S., and Peschel, C. (2001). gp130-stimulating designer cytokine Hyper-interleukin-6 synergizes with murine stroma for long-term survival of primitive human hematopoietic progenitor cells. Exp Hematol *29*, 822-832.
Grivennikov, S., and Karin, M. (2008). Autocrine IL-6 signaling: a key event in tumorigenesis? Cancer Cell *13*, 7-9.
Gupta, P.B., Chaffer, C.L., and Weinberg, R.A. (2009). Cancer stem cells: mirage or reality? Nat Med *15*, 1010-1012.
Gusterson, B.A., and Stein, T. (2012). Human breast development. Semin Cell Dev Biol *23*, 567-573.
Hanahan, D., and Weinberg, R.A. (2011). Hallmarks of cancer: the next generation. Cell *144*, 646-674.
Harmes, D.C., and DiRenzo, J. (2009). Cellular quiescence in mammary stem cells and breast tumor stem cells: got testable hypotheses? J Mammary Gland Biol Neoplasia *14*, 19-27.
Hartmann, C.H., and Klein, C.A. (2006). Gene expression profiling of single cells on large-scale oligonucleotide arrays. Nucleic Acids Res *34*, e143.

Henrikson, R.C., Kaye, G.I., and Mazurkiewicz, J.E. (1997). Histology.
Hens, J.R., and Wysolmerski, J.J. (2005). Key stages of mammary gland development: molecular mechanisms involved in the formation of the embryonic mammary gland. Breast Cancer Res *7*, 220-224.
Howard, B.A., and Gusterson, B.A. (2000). Human breast development. J Mammary Gland Biol Neoplasia *5*, 119-137.
Iliopoulos, D., Hirsch, H.A., Wang, G., and Struhl, K. (2011). Inducible formation of breast cancer stem cells and their dynamic equilibrium with non-stem cancer cells via IL6 secretion. Proc Natl Acad Sci U S A *108*, 1397-1402.
Jemal, A., Siegel, R., Ward, E., Hao, Y., Xu, J., Murray, T., and Thun, M.J. (2008). Cancer statistics, 2008. CA Cancer J Clin *58*, 71-96.
Keller, P.J., Arendt, L.M., Skibinski, A., Logvinenko, T., Klebba, I., Dong, S., Smith, A.E., Prat, A., Perou, C.M., Gilmore, H.*, et al.* (2011). Defining the cellular precursors to human breast cancer. Proc Natl Acad Sci U S A *109*, 2772-2777.
Keller, U., Gotze, K.S., Duyster, J., Schmidt, B., Rose-John, S., and Peschel, C. (2002). Murine stromal cells producing hyper-interleukin-6 and Flt3 ligand support expansion of early human hematopoietic progenitor cells without need of exogenous growth factors. Leukemia *16*, 2122-2128.
Kishimoto, T. (2005). Interleukin-6: from basic science to medicine--40 years in immunology. Annu Rev Immunol *23*, 1-21.
Korkaya, H., Kim, G.I., Davis, A., Malik, F., Henry, N.L., Ithimakin, S., Quraishi, A.A., Tawakkol, N., D'Angelo, R., Paulson, A.K.*, et al.* (2012). Activation of an IL6 inflammatory loop mediates trastuzumab resistance in HER2+ breast cancer by expanding the cancer stem cell population. Mol Cell *47*, 570-584.
Korkaya, H., Liu, S., and Wicha, M.S. (2011). Breast cancer stem cells, cytokine networks, and the tumor microenvironment. J Clin Invest *121*, 3804-3809.
Kuperwasser, C., Chavarria, T., Wu, M., Magrane, G., Gray, J.W., Carey, L., Richardson, A., and Weinberg, R.A. (2004). Reconstruction of functionally normal and malignant human breast tissues in mice. Proc Natl Acad Sci U S A *101*, 4966-4971.
Lanzkron, S.M., Collector, M.I., and Sharkis, S.J. (1999). Hematopoietic stem cell tracking in vivo: a comparison of short-term and long-term repopulating cells. Blood *93*, 1916-1921.
Lee, G.Y., Kenny, P.A., Lee, E.H., and Bissell, M.J. (2007). Three-dimensional culture models of normal and malignant breast epithelial cells. Nat Methods *4*, 359-365.
Linzell, J.L., and Peaker, M. (1971). Mechanism of milk secretion. Physiol Rev *51*, 564-597.
Liu, S., Dontu, G., Mantle, I.D., Patel, S., Ahn, N.S., Jackson, K.W., Suri, P., and Wicha, M.S. (2006). Hedgehog signaling and Bmi-1 regulate self-renewal of normal and malignant human mammary stem cells. Cancer Res *66*, 6063-6071.
Liu, S., Ginestier, C., Charafe-Jauffret, E., Foco, H., Kleer, C.G., Merajver, S.D., Dontu, G., and Wicha, M.S. (2008). BRCA1 regulates human mammary stem/progenitor cell fate. Proc Natl Acad Sci U S A *105*, 1680-1685.
Luo, J., Yin, X., Ma, T., and Lu, J. (2010). Stem cells in normal mammary gland and breast cancer. Am J Med Sci *339*, 366-370.
Maller, O., Martinson, H., and Schedin, P. (2010). Extracellular matrix composition reveals complex and dynamic stromal-epithelial interactions in the mammary gland. J Mammary Gland Biol Neoplasia *15*, 301-318.
Mani, S.A., Guo, W., Liao, M.J., Eaton, E.N., Ayyanan, A., Zhou, A.Y., Brooks, M., Reinhard, F., Zhang, C.C., Shipitsin, M.*, et al.* (2008). The epithelial-mesenchymal transition generates cells with properties of stem cells. Cell *133*, 704-715.
Minn, A.J., Gupta, G.P., Siegel, P.M., Bos, P.D., Shu, W.P., Giri, D.D., Viale, A., Olshen, A.B., Gerald, W.L., and Massague, J. (2005). Genes that mediate breast cancer metastasis to lung. Nature *436*, 518-524.

Montanaro, F., Liadaki, K., Schienda, J., Flint, A., Gussoni, E., and Kunkel, L.M. (2004). Demystifying SP cell purification: viability, yield, and phenotype are defined by isolation parameters. Exp Cell Res *298*, 144-154.
Montero-Julian, F.A. (2001). The soluble IL-6 receptors: serum levels and biological function. Cell Mol Biol (Noisy-le-grand) *47*, 583-597.
Nelson, C.M., and Bissell, M.J. (2006). Of extracellular matrix, scaffolds, and signaling: tissue architecture regulates development, homeostasis, and cancer. Annu Rev Cell Dev Biol *22*, 287-309.
Nguyen, J.T., Wheatley, M.J., Schnur, P.L., Nguyen, T.A., and Winn, S.R. (2008). Reduction mammaplasty: a review of managed care medical policy coverage criteria. Plast Reconstr Surg *121*, 1092-1100.
Oftedal, O.T. (2002). The mammary gland and its origin during synapsid evolution. J Mammary Gland Biol Neoplasia *7*, 225-252.
Outzen, H.C., and Custer, R.P. (1975). Growth of human normal and neoplastic mammary tissues in the cleared mammary fat pad of the nude mouse. J Natl Cancer Inst *55*, 1461-1466.
Palmer, N.P., Schmid, P.R., Berger, B., and Kohane, I.S. (2012). A gene expression profile of stem cell pluripotentiality and differentiation is conserved across diverse solid and hematopoietic cancers. Genome Biol *13*, R71.
Parham, D.M., Hagen, N., and Brown, R.A. (1992). Simplified method of grading primary carcinomas of the breast. J Clin Pathol *45*, 517-520.
Parmar, H., and Cunha, G.R. (2004). Epithelial-stromal interactions in the mouse and human mammary gland in vivo. Endocr Relat Cancer *11*, 437-458.
Parmar, H., Young, P., Emerman, J.T., Neve, R.M., Dairkee, S., and Cunha, G.R. (2002). A novel method for growing human breast epithelium in vivo using mouse and human mammary fibroblasts. Endocrinology *143*, 4886-4896.
Pece, S., Tosoni, D., Confalonieri, S., Mazzarol, G., Vecchi, M., Ronzoni, S., Bernard, L., Viale, G., Pelicci, P.G., and Di Fiore, P.P. (2010). Biological and molecular heterogeneity of breast cancers correlates with their cancer stem cell content. Cell *140*, 62-73.
Peters, M., Blinn, G., Solem, F., Fischer, M., Meyer zum Buschenfelde, K.H., and Rose-John, S. (1998a). In vivo and in vitro activities of the gp130-stimulating designer cytokine Hyper-IL-6. J Immunol *161*, 3575-3581.
Peters, M., Muller, A.M., and Rose-John, S. (1998b). Interleukin-6 and soluble interleukin-6 receptor: direct stimulation of gp130 and hematopoiesis. Blood *92*, 3495-3504.
Proia, D.A., and Kuperwasser, C. (2006). Reconstruction of human mammary tissues in a mouse model. Nat Protoc *1*, 206-214.
Radisky, D.C., and Hartmann, L.C. (2009). Mammary involution and breast cancer risk: transgenic models and clinical studies. J Mammary Gland Biol Neoplasia *14*, 181-191.
Rudland, P.S. (1987). Stem cells and the development of mammary cancers in experimental rats and in humans. Cancer Metastasis Rev *6*, 55-83.
Russo, J., and Russo, I.H. (2004). Development of the human breast. Maturitas *49*, 2-15.
Sanger-Institute (2013).
Sansone, P., Storci, G., Tavolari, S., Guarnieri, T., Giovannini, C., Taffurelli, M., Ceccarelli, C., Santini, D., Paterini, P., Marcu, K.B.*, et al.* (2007). IL-6 triggers malignant features in mammospheres from human ductal breast carcinoma and normal mammary gland. J Clin Invest *117*, 3988-4002.
Schedin, P., Mitrenga, T., McDaniel, S., and Kaeck, M. (2004). Mammary ECM composition and function are altered by reproductive state. Mol Carcinog *41*, 207-220.
Scheller, J., Ohnesorge, N., and Rose-John, S. (2006). Interleukin-6 trans-signalling in chronic inflammation and cancer. Scand J Immunol *63*, 321-329.
Shackleton, M., Vaillant, F., Simpson, K.J., Stingl, J., Smyth, G.K., Asselin-Labat, M.L., Wu, L., Lindeman, G.J., and Visvader, J.E. (2006). Generation of a functional mammary gland from a single stem cell. Nature *439*, 84-88.

Sheffield, L.G. (1988). Organization and growth of mammary epithelia in the mammary gland fat pad. J Dairy Sci *71*, 2855-2874.
Sheridan, C., Kishimoto, H., Fuchs, R.K., Mehrotra, S., Bhat-Nakshatri, P., Turner, C.H., Goulet, R., Jr., Badve, S., and Nakshatri, H. (2006). CD44+/CD24- breast cancer cells exhibit enhanced invasive properties: an early step necessary for metastasis. Breast Cancer Res *8*, R59.
Smalley, M., and Ashworth, A. (2003). Stem cells and breast cancer: A field in transit. Nat Rev Cancer *3*, 832-844.
Snedeker, S.M., Brown, C.F., and DiAugustine, R.P. (1991). Expression and functional properties of transforming growth factor alpha and epidermal growth factor during mouse mammary gland ductal morphogenesis. Proc Natl Acad Sci U S A *88*, 276-280.
Sotiriou, C., Wirapati, P., Loi, S., Harris, A., Fox, S., Smeds, J., Nordgren, H., Farmer, P., Praz, V., Haibe-Kains, B., *et al.* (2006). Gene expression profiling in breast cancer: understanding the molecular basis of histologic grade to improve prognosis. J Natl Cancer Inst *98*, 262-272.
Sternlicht, M.D., Kouros-Mehr, H., Lu, P., and Werb, Z. (2006). Hormonal and local control of mammary branching morphogenesis. Differentiation *74*, 365-381.
Stingl, J. (2011). Estrogen and progesterone in normal mammary gland development and in cancer. Horm Cancer *2*, 85-90.
Stingl, J., Eaves, C.J., Kuusk, U., and Emerman, J.T. (1998). Phenotypic and functional characterization in vitro of a multipotent epithelial cell present in the normal adult human breast. Differentiation *63*, 201-213.
Stingl, J., Eaves, C.J., Zandieh, I., and Emerman, J.T. (2001). Characterization of bipotent mammary epithelial progenitor cells in normal adult human breast tissue. Breast Cancer Res Treat *67*, 93-109.
Stingl, J., Raouf, A., Eirew, P., and Eaves, C.J. (2006). Deciphering the mammary epithelial cell hierarchy. Cell Cycle *5*, 1519-1522.
Stingl, J., Raouf, A., Emerman, J.T., and Eaves, C.J. (2005). Epithelial progenitors in the normal human mammary gland. J Mammary Gland Biol Neoplasia *10*, 49-59.
Taga, T., Hibi, M., Hirata, Y., Yamasaki, K., Yasukawa, K., Matsuda, T., Hirano, T., and Kishimoto, T. (1989). Interleukin-6 triggers the association of its receptor with a possible signal transducer, gp130. Cell *58*, 573-581.
Tiede, B., and Kang, Y. (2011). From milk to malignancy: the role of mammary stem cells in development, pregnancy and breast cancer. Cell Res *21*, 245-257.
Van Keymeulen, A., Rocha, A.S., Ousset, M., Beck, B., Bouvencourt, G., Rock, J., Sharma, N., Dekoninck, S., and Blanpain, C. (2011). Distinct stem cells contribute to mammary gland development and maintenance. Nature *479*, 189-193.
Visvader, J.E., and Lindeman, G.J. (2011). The unmasking of novel unipotent stem cells in the mammary gland. EMBO J *30*, 4858-4859.
Weaver, V.M., and Bissell, M.J. (1999). Functional culture models to study mechanisms governing apoptosis in normal and malignant mammary epithelial cells. J Mammary Gland Biol Neoplasia *4*, 193-201.
WHO (2008). Globocon.
Wicha, M.S., Liotta, L.A., Vonderhaar, B.K., and Kidwell, W.R. (1980). Effects of inhibition of basement membrane collagen deposition on rat mammary gland development. Dev Biol *80*, 253-256.
Wikipedia (2012). Breast.

7. List of abbreviations

1	**AB- serum**	Human serum AB blood type
2	**ATCC**	American Type Culture Collection
3	**BCIP/NBT**	5-bromo-4-chloro-3-indolyl-phosphate/nitro blue tetrazolium
4	**bFGF**	Basic fibroblast growth factor
5	**bio-dUTP**	Biotin bound to deoxyuridine triphosphate
6	**BSA**	Bovine serum albumin
7	**cDNA**	Complementary DNA
8	**CK**	Cytokeratin
9	**CM**	Condition medium
10	**CSC**	Cancer stem cells
11	**DAPI**	4',6-diamidino-2-phenylindole
12	**dATP**	2'-deoxyadenosine 5'-triphosphate
13	**dCTP**	2'-deoxycytidine 5'-triphosphate
14	**DfMD**	Differentiated mammary ducts
15	**dGTP**	2'-deoxyguanosine 5'-triphosphate
16	**DMEM**	Dulbecco's Modified Eagle's Medium
17	**DMEM/F12**	Dulbecco's Modified Eagle's Medium (DMEM) and Ham's F-12
18	**dNTP**	Deoxyribonucleotides
19	**DSL peptide**	Delta/Serrate/Lag-2 peptide
20	**dTTP**	2′-deoxythymidine 5'-triphosphate
21	**EB buffer**	Elution buffer
22	**EDTA**	Ethylenediaminetetraacetic acid
23	**EF1-α**	Elongation factor 1 alpha
24	**EGF**	Epidermal growth factor
25	**EGFR**	Epidermal growth factor receptor
26	**EpCAM**	Epithelial cell adhesion molecule

27	**FACS**	Fluorescence-activated cell sorting
28	**FCS**	Fetal calf serum
29	**g**	Gramm
30	**GFP**	Green fluorescent protein
31	**Gy**	Gray (SI unit for absorbed dose of ionizing radiation)
32	**H&E**	Hematoxylin and eosin
33	**HEPES**	4-(2-hydroxyethyl)-1-piperazineethanesulfonic acid
34	**HIF**	Human immortalized fibroblasts
35	**HIL6**	Hyper interleukin 6
36	**HME**	Human mammary epithelial
37	**IHC**	Immunohistochemistry
38	**IL6**	Interleukin 6
39	**IL6R**	Interleukin 6 receptor
40	**LB medium**	Liquid broth medium
41	**LRC**	Label retaining cells
42	**m-DIO**	Mouse iodothyronine deiodinase
43	**MEBM**	Mammary Epithelial Cell Growth Medium
44	**MFC**	Mammosphere forming capacity
45	**mg**	milligramme
46	**m-IVL**	Mouse involucrin
47	**ml**	milliliter
48	**MOI**	Multiplicity of infection
49	**MSM**	Basic mammosphere medium
50	**MUC1**	Mucin 1
51	**nLRC**	Non label retaining cells
52	**non-CSC**	Non cancer stem cells
53	**NSG**	NOD.Cg-*Prkdc*^{scid} *Il2rg*^{tm1Wjl}/SzJ
54	**PBS**	Phosphate Buffer Saline
55	**PCR**	Polymerase chain reaction
56	**PFA**	Paraformaldehyde
57	**PIK3CA**	p110α protein

58	**Polybrene**	Hexadimethrine bromide
59	**poly-HEMA**	Poly(2-hydroxyethyl methacrylate)
60	**PTEN**	Phosphatase and tensin homolog
61	**RPMI 1640**	Roswell Park Memorial Institute medium
62	**RT**	Room temperature
63	**shPTEN**	short hairpin PTEN RNA
64	**sIL6R**	soluble interleukin 6 receptor
65	**SMA**	Smooth muscle actin
66	**TDLU**	Terminal duct lobular units
67	**TE buffer**	Tris/EDTA buffer
68	**THY1**	**Thy**mocyte differentiation antigen 1
69	**TNS**	Trypsin neutralizing solution
70	**tRNA**	Transfer ribonucleic acid
71	**µl**	Microliter

8. Acknowledgments

"Life is not a walk across a field" – Boris Pasternak
"PhD is not a walk across a field"- Milan

I met wonderful people, I learned from and with them, I had fun with them, I mourned with them, I did some great and some crazy things together with them and that's why I want to acknowledge their artistic souls which put a lot of colors during my PhD work.

The list of acknowledgments is long because many people helped in various ways shaping this work. Despite my great fear that I will not be able to express adequate gratitude for all the support, motivation, mentorship, ideas, group work, I will mention some people which were significant for shaping this PhD thesis.

I am grateful to Prof. Dr. Christoph A. Klein for his mentorship, work and trust during my PhD thesis work. I am thankful for the possibility to work and study interesting and attractive topics which occupy many amazing people around the globe which I met due to the kindness of Prof. Dr. Christoph A. Klein. The obtained knowledge I will try to use as a basis for my future scientific interests.

I am grateful to Prof. Dr. Ralph Witzgall for mentorship and advices during work.

My work at the beginning was hampered due to my lack of knowledge about mammary stem cells and related methodology. However, Dr. Claus Lattrich helped me to overcome these problems and supported my work in collaboration with Dr. Norbert Heine with precious tissue specimens. I am thankful for their support.

I am grateful to Dr. Fabian Eder and Frank van Rey for their immense help with immunohistochemistry.
Dr. Melanie Werner-Klein helped me with analysis of the IL6R expression by FACS and I am grateful for the great job and her help.

I am grateful to Zbigniew Czyz, Miodrag Gužvić and Bernhard Polzer for useful comments, advices and discussions during work on my PhD thesis.

I am grateful to all members of AG Klein for provided help, useful comments and advices, support and group work. Therefore, I am grateful to: Zbigi, Nina, Miodrag, Felix, Gundula, Lahiri, Heda, Gianni, Sebasitan, Steffi R., Stefi P., Bernhard P., Bernhard B., Sophi, Yves, Carolin, Mani, Tom, Katharina, Sandra, Hans, mama Irene, Irina, Davide and Lorenzo…

The work on PhD thesis knows to be stressful, but in such moments many friends helped with their positive attitude. I am grateful for provided motivation and encourages in the moments of doubts to: kum Vlada Jovanović, Jelena Milošević, Milica Komnenić, Rumlica, Zbigniew Czyz, Peter Pröls, Miriam, Tanja, Claudia and Amauri, Florian Schmidt, Heiner Paulus, Ana Živaljević, kum Dusan Basalo, Nikola Jovanović, club Alte Film Bühne, and many other friends which I do not mention here but are in my heart.

I am also proud to acknowledge help of all the positive thinking people of Regensburg. Guys, you are rare do not give up.

I would like to express all my gratitude to my family, but I not aware of any appropriate words to acknowledge their love and support. Thus, I would let these lines to be only a small sign of my endless love and gratitude. Thank you for all the love, support and motivation.